Interaction of bacterial homoserine lactones (HSLs) with Amoebae

Masters by Research Thesis

Rebecca Louise McStay BSc (Hons)
Lancaster University

June 2022

Declaration

I, Rebecca Louise McStay, confirm that the work presented in this thesis is my own and has not been submitted in substantially the same form for the award of a higher degree elsewhere. Where information has been derived from other sources, I confirm this has been indicated in the thesis.

Signed
Rebecca McStay

Submitted in part fulfilment of the requirements for the degree of Masters by Research.

Table of Contents

Abbreviations

AI	Autoinducers
AC	Adenylyl Cyclase
ADP	Adenosine diphosphate
AHL	Acyl Homoserine Lactone (see HSL)
ATP	Adenosine triphosphate
C4	*N*-butyryl-homoserine lactone
C6	*N*-Hexanoyl-homoserine lactone
C8	*N*-Octanoyl-homoserine lactone
C10	*N*-Decanoyl-homoserine lactone
C12	*N*-Dodecanoyl-homoserine lactone
Cap	Capsazepine, Transient Vanilloid receptor antagonist
cAR1	Cyclic AMP Receptor 1
cAMP	3',5'-cyclic adenosine monophosphate
CBD	Cannabidiol
CDK	Cyclin-dependent kinases
CMC	Critical Micelle Concentration
DMSO	Dimethyl sulfoxide
EMD	EMD 281014 hydrochloride, Serotonin 5-HT2A receptor antagonist
fAR1	Folic Acid Receptor 1
Gal	Gallien, GPCR antagonist
GDP	Guanine diphosphate
GPCR	G-Protein Coupled Receptor
GTP	Guanine triphosphate
GW	GW9662, PPAR antagonist
Halo	Haloperidol hydrochloride, Serotonin and Dopamine Receptor antagonist
HC6	*N*-(3-Hydroxyhexanoyl)-homoserine lactone
HC12	*N*-(3-Hydroxydodecanoyl)-homoserine lactone
HSL	Acyl-Homoserine Lactone
IC50	Half-maximal inhibitory concentration A.K.A, Inhibitory concertation at 50%
IQGAP1	IQ-motif containing GTPase-activating proteins
LD	Lethal Dose

Ln	Natural Log
MAPK	Mitogen-activated protein kinase
Mel	Melittin, G_s GPCR antagonist
MIC	Minimum Inhibitory Concentration
NNA	Non-nutrient agar
NNAg	Non-nutrient agarose
OC6	*N*-(3-Oxohexanoyl)-homoserine lactone
OC8	*N*-(3-Oxooctanoyl)-homoserine lactone
OC10	*N*-(3-Oxodecanoyl)-homoserine lactone
OC12	*N*-(3-Oxododecanoyl)-homoserine lactone
PAR	Protease-Activated Receptor
PC	Phosphatidylcholine
PCD	Programmed Cell Death
PKA	Protein kinase A
PON-2	Paraoxonase 2
PPAR	Peroxisome Proliferator Activated Receptor
PPRE	Peroxisome Proliferators Response Elements
PQS	*Pseudomonas* Quinolone Signal, 2-heptyl-3-hydroxy-4-quinolone
PTX	Pertussis Toxin, $G_{i/o}$ and G_t GPCR antagonist
QS	Quorum Sensing
RXR	Retinoid X Receptor
SCH	SCH 23390 hydrochloride, Dopamine D1 receptor antagonist
THC	Delta-9-tetrahydrocannabinol
TM	Transmembrane
TRP	Transient Receptor Potential Channels
TRPA1	Transient Receptor Potential Channel, Subfamily A, member 1
TRPV1	Transient Receptor Potential Channel, Subfamily V, member 1
ZM	ZM241385, Adenosine A2 receptor antagonist

1. Abstract

Bacteria produce signal molecules (Acyl-Homoserine Lactones, HSLs) that have been shown to impact not only bacterial behaviour, but also the behaviour of eukaryotic cells. This study examined the impact of HSLs on multiple species of amoebae. Amoebae were grown in the presence and absence of HSLs, with and without putative HSL-receptor antagonists, and population growth rate was examined. Calculated parameters included the Minimum Inhibitory Concentration, Inhibitory Concentration at 50%, Lethal Dose and growth rates, as well as the data providing indications of potential receptors involved in the amoeba-HSL interaction. This study found that five out of 17 amoebae strains tested were susceptible to at least one HSL, *N*-Dodecanoyl-homoserine lactone; *Naegleria gruberi*, *Vermamoeba vermiformis* (two strains), *Echinamoeba silvestris* and *Flamella arnhemensis*, with one *V. vermiformis* strain, and *E. silvestris* being dually sensitive to *N*-Decanoyl-homoserine lactone and *N*-Hexanoyl-homoserine lactone, respectively. There appeared to be no correlation between sensitivity and phylogeny. *N*-Dodecanoyl-homoserine lactone impacted on amoebic growth rate at lower concentrations, suggesting apoptosis/lack of proliferation was occurring, whilst at high concentrations, *N*-Dodecanoyl-homoserine lactone was instantly lethal to amoebae, suggesting necrosis. This study also found that *N*-Dodecanoyl-homoserine lactone executed more of a negative effect on amoeba population growth than *N*-(3-Oxododecanoyl)-homoserine lactone. It also proposes that a G_s G-Protein Coupled Receptor as a potential HSL-receptor in amoebae. This study therefore supports the hypothesis that HSLs interact via a membrane bound receptor. G_s GPCRs are involved in growth and apoptosis, further supporting the role of HSLs as important interkingdom signalling molecules in therapeutic treatments, including cancer treatments.

2. Literature Review

2.1 Signalling and Cellular communication

2.1.1 The role of signalling

Signalling and cellular communication are crucial for the proper functioning and survival of multicellular organisms. They control many important functions including cell differentiation, growth and apoptosis, and can have immense impacts on, for example, animal movement (via neuronal signalling) (Sullivan, 2017), foetal development (Basson, 2012) and the immune response to infections (Janeway et al., 2001). Issues can arise when signalling goes wrong. For example, in type 2 diabetes mellitus, defective insulin secretion by dysfunctional pancreatic β-cells, and insulin resistance caused by insulin receptors being unresponsive to insulin, leads to fatal levels of hyperglycaemia unless properly treated (DeFronzo et al., 2015; Galicia-Garcia et al., 2020). Cellular communication is not only important in multicellular organisms. In prokaryotes, it is important in regulating changes to cell division and morphology (Patzelt et al., 2013), and in the activation of protective mechanisms such as biofilm formation (Williams et al., 2007), the production of virulence factors (Rutherford and Bassler, 2012), and in helping cells evade the immune system of its host (Liu et al., 2018).

The main steps of cellular communication involve, (i) Reception, (ii) Transduction and, (iii) Response, which together facilitate a coordinated cellular behaviour in response to a certain stimulus, i.e., a ligand (signal molecule) (Radhakrishnan et al., 2010). (i) 'Reception' is the connection of a ligand to its appropriate receptor, causing a conformational change in the receptor which either allows the molecule to pass through the membrane or causes the receptor to bind with another receptor, for example, to form a dimer. (ii) 'Transduction' is the process by which the signal at the cell surface is converted into a specific cellular response. This is a multi-step process and involves multiple levels of amplification. (iii) 'Response' is the step in which the cell appropriately responds to the ligand signal, for example, via gene regulation and protein expression (Radhakrishnan et al., 2010).

2.1.2 Lipid signalling

There are many types of cell to cell signalling; autocrine ('self-signalling'), endocrine (long distance; hormonal, multicellular only), paracrine (local signalling, e.g. neuronal signalling) and juxtacrine (direct cell to cell), all with the use of different ligands (Gilbert, 2000; Hancock,

2017). Lipid signals are common in both eukaryotes and prokaryotes and act as both extracellular and intracellular signals to control cellular outcomes (Wymann and Schneiter, 2008). Imbalances in lipid signalling pathways can contribute to diseases such as cancers, inflammation, cardiovascular disease and more (Wymann and Schneiter, 2008). In prokaryotes, lipid signalling has been established as highly important in many aspects of microbial life, most of which are population density dependent such as, cell motility, bioluminescence, biofilm formation and virulence factor production (Soto et al., 2019).

2.2 Bacterial Signalling

2.2.1 Quorum Sensing

The cell signalling used by bacteria is known as Quorum sensing (QS) because it is density-dependent (Eickhoff and Bassler, 2018). It involves the continuous production of signal molecules (autoinducers, AIs) which can freely diffuse across the bacterial cell membrane, and/or bind to a membrane bound receptor (Kaplan and Greenberg, 1985; Papenfort and Bassler, 2016). As the cell-population density increases, the concentration of the autoinducer increases both intra- and extracellularly (Miller and Bassler, 2001). When a threshold or 'quorum' of signal molecules is reached, the molecules complex with their complimentary receptor proteins. These autoinducer-sensing receptors are either cytoplasmic transcription factors, known as 'LuxR-type' (see 2.2.1.1.-2), or membrane-bound histidine sensor kinases, known as 'LuxN-type' (Papenfort and Bassler, 2016). This binding to the cognate receptor causes a signal transduction pathway that ultimately results in the initiation or upregulation of expression of certain genes (Miller and Bassler, 2001; Eickhoff and Bassler, 2018).

QS commonly results in alterations to cell motility and the production of biofilms (Williams et al., 2007; Castillo-Juárez et al., 2015), virulence factors such as pigments, toxins and hydrolases (Rutherford and Bassler, 2012) and bioluminescence (Nealson et al., 1970; Bassler et al., 1993). Gram-negative and Gram-positive bacteria use different molecules in QS, Gram-negative bacteria primarily use lipid molecules known as Acyl-Homoserine Lactones (HSLs, also known as AHLs), whereas Gram-positive bacteria primarily use protein-based molecules known as Oligopeptide AIs (Camilli and Bassler, 2006). However other signal molecules can be produced and used in QS, such as generic autoinducers (autoinducer 2 and 3, [AI-2 and 3]), quinolones, cyclodipeptides, partially cyclic peptides and other small signalling molecules (Shrestha and Schikora, 2020). QS was first fully described in the bioluminescent bacterium

Vibrio fischeri which is Gram-negative and as such, signals primarily with HSLs (Miller and Bassler, 2001).

2.2.1.1 Vibrio fischeri LuxI/R system

The *V. fischeri* QS system contains the Lux operon (*luxICDABE*) (**Figure 2.1**), whereby LuxI is the protein responsible for the synthesis of the HSL (*N*-[3-Oxohexanoyl]-L-homoserine lactone, OC6), while LuxR is the protein that the LuxI HSL binds to (Miller and Bassler, 2001). When a quorum has been reached, this HSL/LuxR complex binds to the Lux operon to activate the transcription of the luciferase structural genes (*luxICDABE*). This results in an exponential increase in HSL synthesis due to increased *luxI* transcription as well as an exponential increase in light production (bioluminescence) via the increased transcription of *luxCDABE*. The *luxAB* encodes the α and β subunits of the luciferase enzyme which oxidises aldehyde into fatty acids (Danilov et al., 2008), and in so doing, the luciferase enzyme becomes excited and emits a light wavelength, at 490 nm.

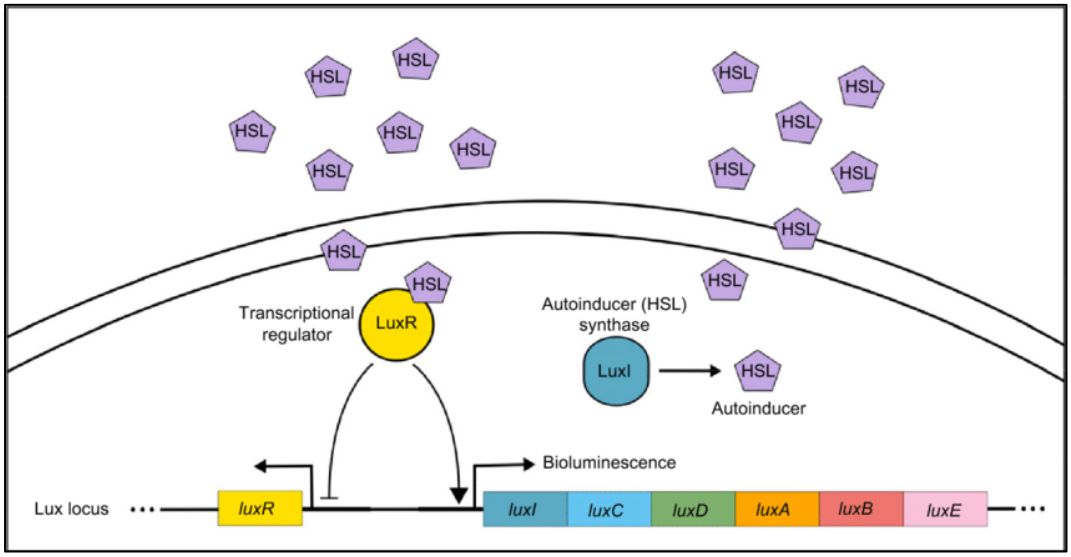

Figure 2.1. The *Vibrio fischeri* LuxI/LuxR HSL quorum sensing circuit. The LuxI protein is responsible for synthesis of *N*-(3-oxohexanoyl)-homoserine lactone (OC6, Pentagon). Taken from Reuter et al., (2016). Pathway described in text.

luxCDE encodes for the components that make up the components of a fatty acid reductase enzyme; fatty acid reductase, transferase and synthetase, are produced by *luxC*, *luxD* and *luxE*, respectively. The fatty acid reductase enzyme reduces fatty acids to aldehyde, to ensure that the substrate for bioluminescence is continuously present (Danilov et al., 2008). The LuxR-HSL complex also binds at the *luxR* promoter and represses the transcription of *luxR*. This acts

to repress the expression of *luxICDABE* in response to compensate the positive action that HSL detection has on the *luxICDABE* promoter (Miller and Bassler, 2001).

2.2.1.2 Pseudomonas aeruginosa LasI/R and RhlI/R systems

Many Gram-negative bacteria that have HSL-dependent QS ability have been shown to have homologues of the LuxI/LuxR system (Miller and Bassler, 2001). The QS system of *P. aeruginosa* has been well studied as it has a hierarchical nature, in which the activation of the first system results in the activation of others. The 2 HSL systems involve 2 LuxI and 2 LuxR homologues, known as LasI and LasR, respectively in the first system, and RhlI and RhlR, respectively, in the second system (Miller and Bassler, 2001). The first system to be activated is the Las system. The LasI protein produces a HSL (*N*-[3-Oxododecanoyl]-L-homoserine lactone, OC12) which binds to the LasR protein when a quorum has been achieved. This HSL/LasR complex binds to virulence factor promoters and initiates their transcription. This complex also initiates the transcription of *rhlR* to initiate the second QS system (Miller and Bassler, 2001) (**Figure 2.2**).

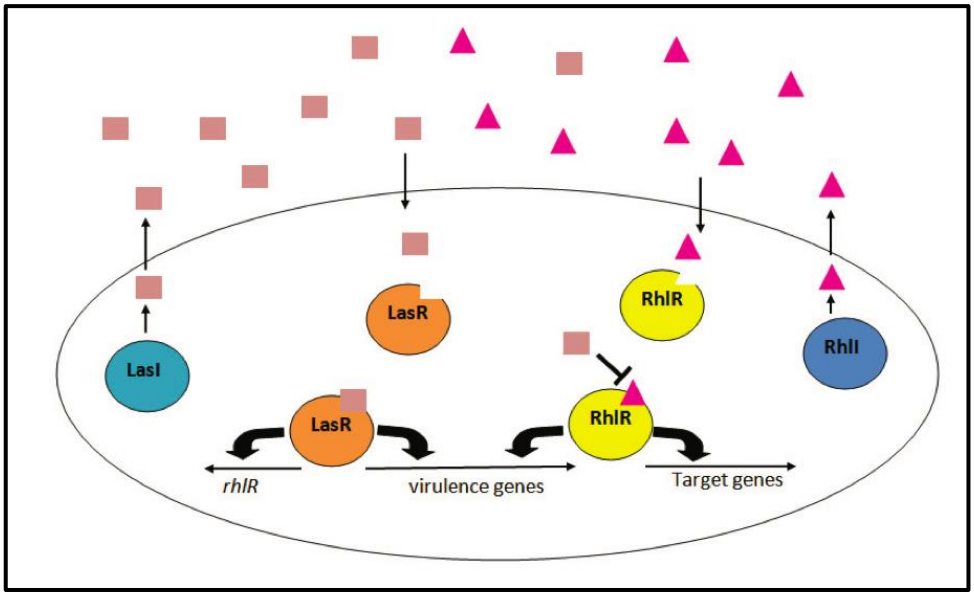

Figure 2.2. The *Pseudomonas aeruginosa* LasI/LasR and RhlI/RhlR quorum sensing system. The LasI protein is responsible for the synthesis of *N*-(3-Oxododecanoyl)-L-homoserine lactone (OC12, Square), whilst the RhlI protein is responsible for the synthesis of *N*-Butyryl-DL-homoserine Lactone (C4, Triangle) Taken from Alfiniyah et al. (2019). Pathway described in text.

As part of the second system the RhlI protein produces another HSL (*N*-Butyryl-DL-homoserine Lactone, C4) which binds to the RhlR protein. This complex activates the

transcription of a subset of the LasR-activated virulence genes as well as several target genes that are not regulated by LasR. The LasI HSL interferes with binding of the RhlI HSL to RhlR, with the assumption that the LasI/LasR circuit is fully established prior to the commencement of the RhlI/RhlR circuit. In total, the genes targeted by both the Las and Rhl systems account for approximately 10% of the *P. aeruginosa* genome (Schuster and Greenberg, 2006).

P. aeruginosa also utilises another QS molecule that is chemically distinct from the HSLs of the Las and Rhl systems (Pesci et al., 1999). This signal molecule is an alkylquinolone; 2-heptyl-3-hydroxy-4-quinolone, also known as the *Pseudomonas* Quinolone Signal (PQS) (Lee and Zhang, 2015) (**Figure 2.3**). PQS is detected by PqsR, a LysR-type transcriptional regulator, and is synthesized by the products of *pqsABCDEH* genes (Castillo-Juárez et al., 2015). PQS can control the production of *P. aeruginosa* virulence factors. For example, PQS influences expression of the *lasB* virulence gene which encodes LasB elastase (Pesci et al., 1999). PQS is also known to control the production of another virulence factor, the pigment Pyocyanin (Das et al., 2022). PQS is not involved in sensing cell density like the HSL systems previously described, it is instead an intracellular signal molecule that helps to coordinate the cellular processes, including virulence factor production, in response to the density-sensing HSL systems (McKnight et al., 2000).

2.2.2 Signal molecules

Figure 2.3 shows a range of signal molecules that are produced by Gram-negative and Gram-positive bacteria, i.e., HSLs and oligopeptides, respectively. HSLs are lipid molecules which have a core subunit which is a homoserine lactone ring and an acyl chain, which is also referred to as the 'carbon backbone' (Churchill and Chen, 2011) (**Figure 2.3**). HSLs primarily differ in the length of the carbon backbone. For example, the RhlI protein produced by *P. aeruginosa* synthesizes *N*-(butyryl)-homoserine lactone, which is also referred to as C4 because the backbone contains 4 carbons. Likewise, the LasI protein produces the HSL *N*-(3-oxododecanoyl)-homoserine lactone, also referred to as OC12 because the backbone contains 12 carbons (**Figure 2.3**).

HSLs can also differ by having additional groups added to the third carbon (C3 position) such as ketone and hydroxyl groups. For example, OC12 has an additional alteration to include a ketone (oxo, O) group attached to the third carbon while addition of a hydroxyl group (OH) yields HC12 (Vesty et al., 2020) (**Figure 2.4**).

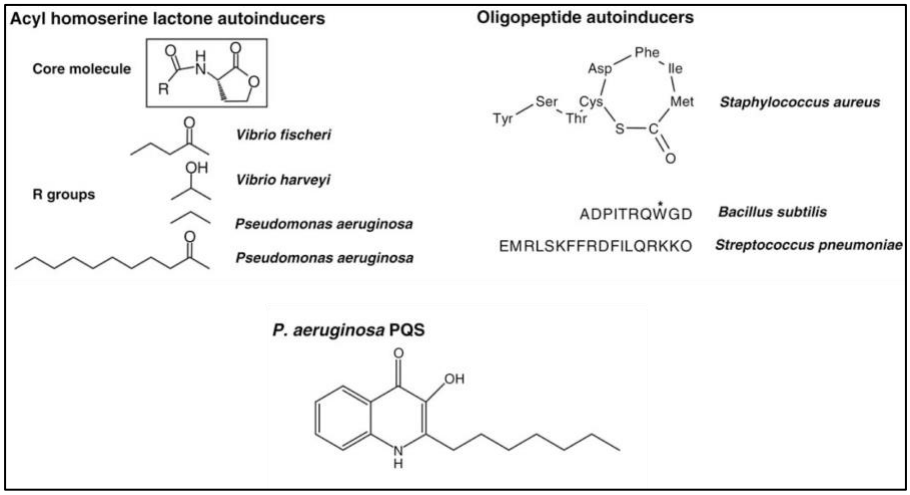

Figure 2.3. Small-molecule bacterial signals. Representative structures of autoinducer molecules used in bacterial cell-cell communication. Modified from Camilli and Bassler, (2006).

Although there is high specificity for the correct HSL molecule to bind to the correct cognate receptor, it has been reported that some receptors are "promiscuous" (Hawver et al., 2016) and that similarly shaped molecules can bind to the same receptor with a reduced affinity than the cognate HSL (Nasser and Reverchon, 2007; Prescott and Decho, 2020). It has been shown that "promiscuous" LuxR-type receptors have a more "relaxed specificity" than non-promiscuous LuxR-type receptors (Hawver et al., 2016). This is because the amino acid residues that bind the core subunit present on every HSL, (the homoserine lactone ring moiety), are highly conserved among LuxR-type receptors, however the amino acid residues that bind to the HSL side chain (carbon backbone) are less conserved (Li and Nair, 2012). As such, some HSL molecules may be able to bind with reduced affinity to a non-cognate LuxR-type receptor.

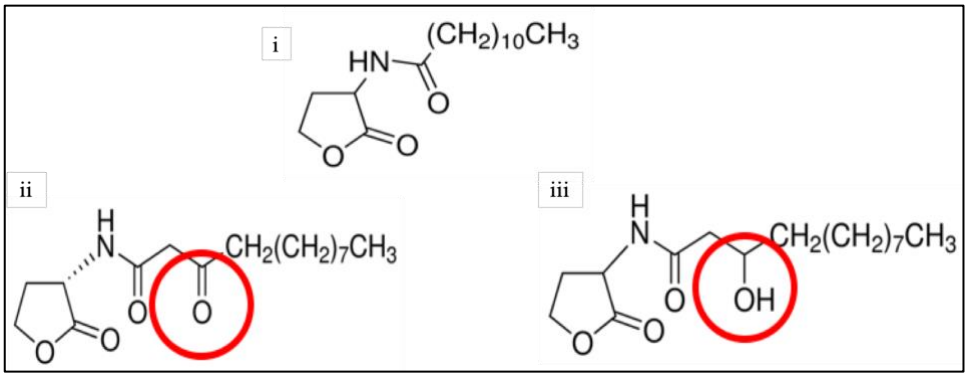

Figure 2.4. (i) *N*-Dodecanoyl-DL-homoserine lactone (C12), (ii) *N*-(3-Oxododecanoyl)-L-homoserine lactone (OC12) and (iii) *N*-(3-Hydroxydodecanoyl)-DL-homoserine lactone (HC12) with the additional ketone (O) and hydroxyl (OH) groups attached to the C3 position on OC12 and HC12, respectively, highlighted with red rings. Images of HSL molecules obtained from Sigma-Aldrich.

Therefore, OC12 and HC12 could have the ability to bind to the same receptor as C12 (and vice versa). This is believed to be because the chain length is the same in all 3 HSLs and thus could fit (albeit not perfectly) in the HSL binding pocket of the same LuxR-type receptor.

2.2.2.1 Bacterial cross talk

Bacterial populations often live in biofilm communities with populations of various other species, which produce QS molecules including HSLs, and sometimes the same HSLs (and the Oxo + Hydroxy variants). These can be detected by other bacterial species giving rise to 'bacterial cross-talk' or 'interspecies communication' (Federle and Bassler, 2003). Interspecies communication is important as it allows bacteria within these biofilms to communicate not only within their own species but also communicate between genera and species by use of their HSLs and a signal molecule known as Auto-Inducer 2 (AI-2). AI-2 can be produced and detected by a wide-variety of bacterial species (Xavier and Bassler, 2005), including both Gram-positive and Gram-negative bacteria, therefore it is often considered as a 'universal' bacterial signalling molecule (Elgaml et al., 2014; Lamin et al., 2022). AI-2, along with species specific HSL-based interaction, allows bacteria to determine the local species population density, as well as distinguishing between self and non-self; improving the possibility of synchronisation of population behaviour (Pereira et al., 2013). This interspecies communication allows bacterial species to synchronise their behaviour when it is the most opportune time for a coordinated response in relation to its own population density, and the densities of other surrounding species. This is important as it ensures that costly processes such as gene expression, biofilm formation and production of virulence factors are not wasted and only produced when most advantageous to the population.

Not only have HSLs been shown to alter the behaviour of bacterial cells of the same and different species, they have also been shown to communicate with eukaryotic cells and alter their behaviour; a feature known as 'Interkingdom Signalling' (Hughes and Sperandio, 2008).

2.3 Interkingdom Signalling

Interkingdom Signalling is a form of communication which involves the interaction of signal molecules between different 'kingdoms' of organisms, i.e. between Prokaryotes and Eukaryotes. This involves the production of signal molecules from one or both parties, which are then detected by a member of the other party to cause specific and direct effects, such as apoptosis (Li et al., 2004). Interkingdom signalling can be uni-directional (where only one

party produces signals to alter the others behaviour), or it can be bi-directional (where both parties produce signals that alter the behaviour of the other party) (Kendall and Sperandio, 2016). For example, signal molecules produced by bacteria can be detected by eukaryotes and alter their behaviour, as demonstrated in **Table 2.1**.

Most of the work on interkingdom signalling revolves around the longer chain lipid signal molecules, such as OC12 (**Table 2.1**). It is believed that long chained lipid signalling molecules can freely diffuse across the membranes of eukaryotic cells without the need for a receptor because of their hydrophobicity and their known ability to diffuse across bacterial cell membranes (Kaplan and Greenberg, 1985; Shiner et al., 2005). This is similar to the mode of uptake of steroid hormones, that are also long-chained lipids, which then bind to intracellular receptors (Hughes and Sperandio, 2008). Some researchers however, believe that a second pathway for uptake exists, whereby the HSL binds to a receptor that is bound to, or resides close to the intracellular portion of, the lipid membrane of the eukaryotic cell (Shiner et al., 2006; Davis et al., 2010) This is because some HSLs bind to bacterial sensor kinases (LuxN-type) at the cell membrane, rather than diffusing across the membrane and binding intracellularly to a LuxR-type receptor (Papenfort and Bassler, 2016). Whatever the mechanism, interkingdom signalling appears to play an important role in the interaction of bacteria with eukaryotes with regards to disease and environmental interactions.

2.3.1 Disease and host interaction

Interkingdom signalling is extremely important when understanding disease and pathogen-host responses. For example, cystic fibrosis (CF) is a lung disease which involves large inflammatory responses resulting in compromised lungs (Pacheco and Sperandio, 2009). *P. aeruginosa* is a common opportunistic pathogen which colonises and forms biofilms in the lungs of CF patients, from which it can produce mass concentrations (up to 600 μM) of OC12 (Charlton et al., 2000; Pacheco and Sperandio, 2009). The concentrations of OC12 are so high that it can be detected in the CF patient's sputum (Singh et al., 2000).

Evidence suggests that OC12 induces pro-inflammatory responses in macrophages and bronchial epithelial cells at low concentrations of 50-100 μM (Bedi et al., 2016; Bedi et al., 2017), by triggering the induction of transcription of NF-kB and AP-2, thereby causing the production of IL-8, a pro-inflammatory chemokine (Pacheco and Sperandio, 2009; Qazi et al., 2011). Although *P. aeruginosa* induces inflammation of the lungs in CF, worsening the symptoms, it can also reduce the virulence of other harmful pathogens in CF patients. For

example, *Candida albicans* has the ability to convert from a budding yeast (non-virulent) to a filamentous yeast (virulent), however in the presence of C12 and OC12, *C. albicans* reverts to its non-virulent budding state (Hogan et al., 2004).

Eukaryotic cells themselves can also influence bacteria signalling, virulence and biofilm formation via bi-directional interkingdom signalling. *C. albicans* produces a signal molecule which is a long-chain alcohol, known as Farnesol (Polke et al., 2018). Farnesol is able to inhibit the synthesis of *Pseudomonas* quinolone signal (PQS), a QS molecule important in biofilm formation (Bandara et al., 2016). Thus, Farnesol can help to reduce and eliminate *P. aeruginosa* biofilms (Ramage et al., 2002). By inhibiting PQS, Farnesol also inhibits the production of a PQS controlled virulence factor; Pyocyanin (Cugini et al., 2007; McAlester et al., 2008). It is believed that Farnesol is able to do this by binding to, and blocking, the PQS receptor in *P. aeruginosa* (PqsR), thus preventing the transcription of the *pqs* operon (Cugini et al., 2007). Therefore, Farnesol has the potential to be clinically relevant as an anti-*Pseudomonas* drug in CF. However, there has been a suggestion of an additional effect of Farnesol on other eukaryotic cells which is immunomodulatory (Leonhardt et al., 2015; Polke et al., 2018) and so it could be problematic for use in immunocompromised patients, such as a CF patient.

Table 2.1. Overview of the effects of HSLs on different types of eukaryotic cells.

HSL	Eukaryotic Cell Type (Cell lines)	Effect(s)	Reference
OC12	Neutrophils and monocytic cells (U-937 and P388D1)	Induction of apoptosis	(Tateda et al., 2003)
	Human breast cancer cells (BR293, MCF-7 and MDA-MB-468)	Proliferation prevention and apoptosis induction	(Li et al., 2004)
	Candida albicans	Cell reverts from virulent to non-virulent state	(Hogan et al., 2004)
	Murine fibroblast (NIH3T3)	Increases in intracellular calcium levels and induces apoptosis, and modulation of the inflammatory response	(Shiner et al., 2006)
	Ulva zoospores	Calcium channel opening and calcium influx in response to OC12	(Joint et al., 2007)
	Murine fibroblast (NIH3T3)	Affect PPARγ DNA binding and transcriptional activity	(Jahoor et al., 2008)
	Human colon cancer cells (Caco-2)	OC12 binds to IQGAP1, 200 μM gradually decreased IQGAP1 levels and rapidly dropped phosphorylation of Rac1 and Cdc42, as well as modulating IQGAP1 distribution	(Karlsson et al., 2012)
	Human colon cancer cells (Caco-2)	Reduced viability and induced apoptosis	(Taguchi et al., 2014)
	Macrophages (RAW264.7) and Macrophage-like monocytic cells (THP-1)	Downregulation of PPARγ and paraoxonase-2 (PON-2)	(Bedi et al., 2016)
	Normal human bronchial epithelial cells (BEAS-2B)	Inactivation of enzyme paraoxonase 2 (PON-2) and disruption to tight junctions	(Bedi et al., 2017)
	Prostate adenocarcinoma cells (DU145 and LNCaP) and prostate small cell neuroendocrine carcinoma (PC3) cells	Induced apoptosis and altered viability of both cell types	(Kumar et al., 2018)
	Mouse colonic epithelial cell line (CT-26)	Reduction in cell viability	(Tao et al., 2021)
OC10	*Ulva* zoospores	Settlement of cells on substratum. Increased settlement with longer chains (>6) but still little settlement with C6 and HC6.	(Tait et al., 2005)

C4	*Arabidopsis thaliana*	Increase in cytosolic calcium	(Song et al., 2011)
C6	*Triticum aestivum* (Yatran 60)	Cell wall and cuticle layer increased, significant increases in photosynthetic pigments chlorophyll a and b	(Kosakivska et al., 2020)
OC6	*Arabidopsis thaliana*	Increase in cytosolic calcium and upregulation of calmodulin genes resulting in increases in calmodulin	(Zhao et al., 2015b)
	Arabidopsis thaliana and Wheat (*Triticum aestivum*)	Enhanced salt tolerance and upregulation of salt-responsive genes	(Zhao et al., 2020)
OC12 and OC10	*Ulva* zoospores	OC12 and OC10 were effective at altering swimming behaviour of *Ulva* zoospores.	(Wheeler et al., 2006)
OC6 and OC8	*Arabidopsis thaliana*	Root elongation through interaction with G-protein-coupled receptors (GPCRs)	(Liu et al., 2012)
C4 and OC12	Sino-nasal epithelial cells from C57BL/6 mice	Stimulation of calcium increase, leading to nitric oxide production to increase mucociliary clearance	(Lee et al., 2014)
C4 and C6	*Gracilaria dura*	Stimulate release of carpospores	(Singh et al., 2015)
C4, C6 and C10	*Arabidopsis thaliana*	C4 and C6 promoted root elongation whilst C8, C10 and C12 did not. C10 decreased root growth C6 induced gene expression led to an increase in auxins and a decrease in cytokinin.	(von Rad et al., 2008)
C2, C4, C8, C9, C10 and OC12	Human embryonic kidney (293T)	C2 and C4 activated TRPA1 OC12 activated TRPV1 C8, C9 and C10 all activated TRPA1 and TRPV1	(Tobita et al., 2022)

2.3.2 Environmental interaction

Bacterial populations in the environment exists alongside other microorganisms, these communities are often known as polymicrobial communities (Peters et al., 2012). Other common microorganisms/entities in these communities include protists, fungi, and viruses (Peters et al., 2012). Within these vast microbial populations, bi-directional interkingdom signalling occurs with the use of HSLs and other signal molecules. For example, signal molecules called furanones, produced by marine macroalga, mimic HSLs and can displace the HSL from a LuxR receptor, meaning furanones can effectively 'block' the HSL binding site of the regulatory proteins in bacteria (Manefield et al., 1999). Halogenated furanones produced by marine macroalga *Delisea pulchra* have been shown to inhibit the swarming ability of the bacterium *Serratia liquefaciens* (Rasmussen et al., 2000). Specifically, furanone C56 has been shown to affect the virulence and biofilm architecture of *P. aeruginosa*, which allows for increased antibiotic susceptibility (Hentzer et al., 2002). Bacterial HSLs have also been shown to affect the marine macroalga *Gracilaria dura* (Singh et al., 2015). A positive correlation was found between increases in C4 and C6 concentrations (up to 10 μM) and the enhaced liberation of *G. dura* carpospores; non-motile diploid spores produced after fertilisation of the carpogonium, i.e., HSLs enhance the reproduction ability of *G. dura* (Singh et al., 2015).

However, the most widely known example of environmental interkingdom signalling is the uni-directional signalling between the marine bacterium *Vibrio anguillarum* and the macroalga *Ulva*, previously known as *Enteromorpha* (reviewed in Joint et al. [2007]). *V. anguillarum* has 4 QS systems, 2 of which (VanI/R and VanM/N) are HSL based and result in the production of 3 different HSLs; OC10 (VanI/R), C6 and HC6 (VanM/N) (Frans et al., 2011). Joint et al. (2002) found a positive correlation between the numbers of zoospores attaching to the surface and the cell density of *V. anguillarum.* Tait et al. (2005) then showed that disrupting the *V. anguillarum* QS within its biofilm prevented the settling of *Ulva* zoospores on a surface and, by using GFP-tagged *V. anguillarum,* they revealed the *Ulva* zoospores settled directly onto sites of higher HSL concentration. Specifically, Tait et al. (2005) found that *Ulva* zoospores has a stronger response to OC10 than the two smaller chain HSLs; C6 and HC6. Further investigation, with the use of synthetic HC6, OC10 and OC12, found that the most effective signalling molecule for altering zoospore swimming behaviour was OC12, followed by OC10 (Wheeler et al., 2006; Joint et al., 2007). This supports the argument that long chain HSLs are more likely to have an effect on eukaryotic cells, due to the diffusion ability across the cell membrane.

Ulva zoospores resemble single-celled flagellates or protists. Other types of protists include ciliates and amoebae. Many ciliates and flagellates exist in the plankton and if any bacterial cells are producing HSLs in the plankton they would probably be too dilute to detect. However, within attached communities, where there is a high concentration of mixed bacterial species with high amounts of QS, protist detection of HSLs is more feasible. The primary grazers of attached bacteria are amoebae (Smirnov, 2012), thus out of flagellates, ciliates and amoebae, it is highly likely that if any protist is going to detect, and be affected by, HSLs it would be amoebae.

2.4 Amoebae

Amoebae are single celled eukaryotic protists. They are most commonly found in soil and water, in both fresh and marine environments (Fouque et al., 2012). As stated previously, amoebae are the primary grazers of bacterial biofilms (Smirnov, 2012), which in theory should be rife with HSLs. Therefore, they are a good model to test for Interkingdom Signalling.

Currently, the slime mould, *Dictyostelium discoideum*, has been widely studied as a 'model amoeba', as it possesses an amoeba stage in its complex life-cycle. But this is not a 'true amoeba', as many aspects of its life cycle are unique. For example, *D. discoideum* aggregates into a migrating slug when food is depleted (Bozzaro, 2013), whereas true amoebae form cysts (Smirnov, 2012). Based on this, the use of *D. discoideum* to infer behaviour of other amoebae can be called into question. Thus, other amoebae species, recognised as 'true amoeba', should be studied more widely, such as other commonly researched genera and species, e.g., *Acanthamoeba* spp. and *Amoeba proteus*.

2.4.1 Morphology and movement

Amoebae move via the breakdown and construction of components of the cytoskeleton, allowing the amoebae to move in the direction of their prey for feeding purposes (Smirnov, 2008). In the absence of a chemoattractant gradient, an amoeba cell migrates spontaneously, producing pseudopodia in multiple directions in order to 'probe' for food; in a similar manner to macrophages (Levin et al., 2016; Alonso et al., 2018). Polarised amoeba movement occurs in response to a chemoattractant gradient and can be described by 4 stages: (i) Cellular polarisation in the amoeba cell is thought to be similar to that of neutrophils, in which the cell rearranges to create an anterior 'leading' edge at the site closest to the chemoattractant and a posterior 'following' edge at the other end of the cell (Servant et al., 2000). (ii) Pseudopodia

extension to form the anterior ‘leading’ edge occurs by way of polymerization of G-actin into F-actin, an ATP-dependent process (Alsam et al., 2005). (iii) The attachment of the pseudopodia to the substratum is associated with the aggregation of F-actin and the Arp2/3 complex, an F-actin crosslinking protein complex, in the ‘leading’ edge (Dayel et al., 2001; Alonso et al., 2018). (iv) Detachment of the posterior myosin II rich uroid ‘following’ edge (Alonso et al., 2018). The detachment of the cell from the substratum is due to myosin-actin interaction causing contraction of cytoplasm and organelles towards the leading edge (Kaneshiro, 1995) (**Figure 2.5**).

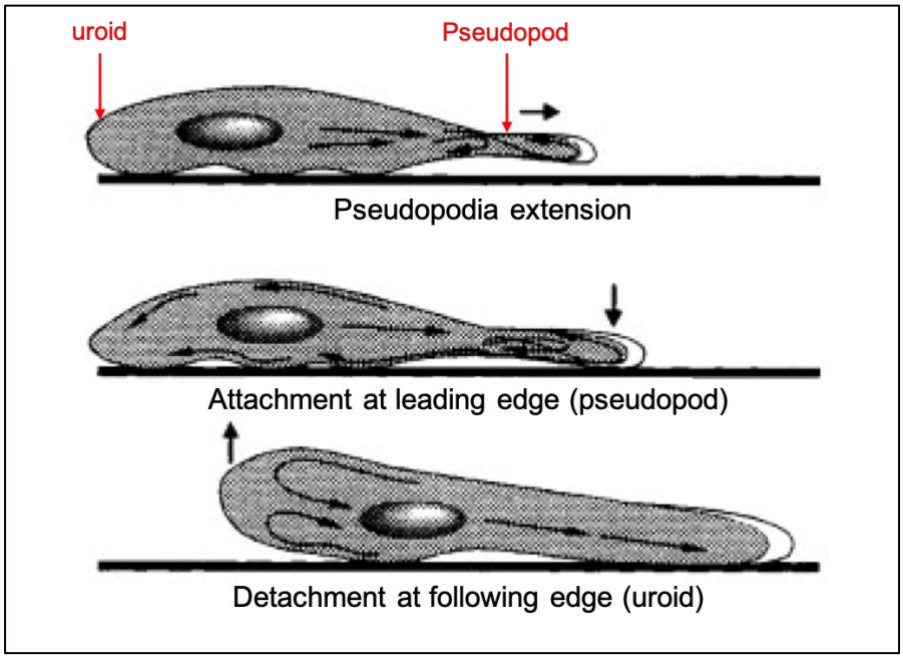

Figure 2.5. Locomotion of a polarised amoeba cell along a substrate. Process explained in text. Adapted from Kaneshiro (1995)

Due to the frequent rearrangement of the cytoskeleton for movement and feeding, amoebae do not have a definitive shape. They exist primarily in 2 states; active and dormant. In the active state amoebae can be within 2 forms known as locomotive trophozoites (feeding form) or a floating form (non-feeding form). The dormant state (cyst) is from the transformation of the trophozoite (not the floating form) (Smirnov, 2008) (**Figure 2.6**).

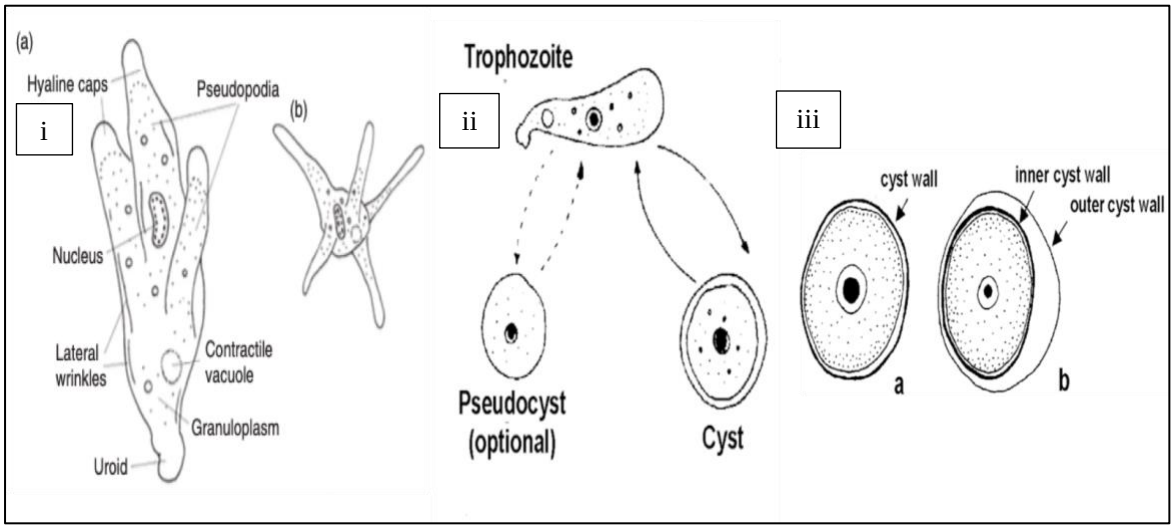

Figure 2.6. Morphology of amoebae forms. (i) Locomotive trophozoite (a) and floating form (b) of *Amoeba proteus*. (ii) Lifecycle change from active trophozoite to dormant states; cysts and pseudocysts. (iii) Cyst structures, (a) singled wall cyst, (b) double walled cyst. (i) Taken from (Smirnov, 2008), (ii) and (iii) taken from Smirnov and Brown, (2004).

The amoeboid shape can reflect the environment and conditions. For example, the floating form occurs when the amoebae have detached from the substrate and begin to float in suspension (Smirnov and Brown, 2004; Smirnov, 2008). This stage involves a morphological change to a 'stiff' morphology, as it has stiffened pseudopodia due to cytoskeletal alterations (Smirnov, 2002). Due to the stiff morphology, the floating stage does not allow for feeding or growth and is used solely for amoeba dispersal (Pickup et al., 2007). As such, it is sometimes considered a 'resting' state (Smirnov, 2008). One genus of amoebae (*Naegleria*) has an additional life stage for dispersal, known as the flagellate stage (Sanders, 2021).

The locomotive trophozoite stage occurs when the amoebae are living on a surface and are continuously moving, adopting a dynamically stable shape (Smirnov, 2008). This is the only stage in which amoeba are able to feed via phagocytosis (**see 2.4.3**) and replicate (**see 2.4.2**) (Pickup et al., 2007). The processes of movement, phagocytosis and pinocytosis (liquid uptake) all require cytoskeleton rearrangements. Due to the demand of the cytoskeleton components (actin and myosin), and ATP, in the process of locomotion and feeding, cell movement cannot occur whilst the amoeba is feeding, thus amoeba cannot eat and move at the same time (Kaneshiro, 1995).

The cyst stage can occur when unsuitable conditions arise. Cysts are unable to feed, move and replicate (Weisman and Moore, 1969). During encystment there is reorganisation of the

subcellular structures to become circular in shape (Griffiths, 1969). There is also the secretion of a cyst wall (or walls), which ruptures when conditions become favourable again, releasing the trophozoite via excystment (Smirnov, 2008). Some amoebae in culture form pseudocysts or 'round bodies' instead of 'true' cysts (**Figure 2.6**) (Smirnov and Brown, 2004; Pickup et al., 2007). A pseudocyst occurs when a trophozoite becomes rounded and has no evidence of activity, however it has no cyst wall and a reduced survival ability (compared to a 'true' cyst), and is thus considered a distinct life-cycle stage (Smirnov and Brown, 2004).

2.4.2 Reproduction

Amoebae reproduce asexually by binary fission (Byers, 1986). However, 'genetic exchanges', that occur as part of sexual reproduction, have been reported in 2 amoeba species, *Entamoeba histolytica* and *Naegleria lovaniensis* (Pernin et al., 1992). Further, Khan and Siddiqui (2015) identified meiosis genes in *Acanthamoeba* spp., indicating the possibility of sexual reproduction in this genus too. However, this theory is contradicted by Maciver et al. (2019) who suggest that these meiotic genes are instead "involved in the related process of homologous recombination in this amoeba".

2.4.3 Feeding

Amoebae can only feed when they are in the trophozoite form (Pickup et al., 2007). Amoeba feeding is reliant on a process known as phagocytosis. The full mechanism of phagocytosis in amoebae is poorly described in the literature. It is thought to be similar to that carried out by other eukaryotic cells such as macrophages. Broadly speaking, it occurs in the following stages.

2.4.3.1 Recognition

The first step of amoeba feeding is prey recognition, in which receptors on the cell surface recognise and bind to the prey ligands. This involves certain cell-surface proteins/receptors, specifically, polysaccharide binding proteins or C-type lectins (Declerck et al., 2007; Medina et al., 2014). 'Sugar blocking' experiments carried out with *Acanthamoeba* spp., whereby sugars were used to 'block' polysaccharide binding proteins, have shown that the mannose receptor is important in prey recognition and phagocytosis (Allen and Dawidowicz, 1990; Alsam et al., 2005; Declerck et al., 2007). The mannose receptor uses carbohydrate recognition domains to bind to mannose residues on the bacterial surface in order to recognise prey (Cutler and Davies, 1998). Allen and Dawidowicz (1990) also used sugar blocking experiments on *Acanthamoeba castellanii* to demonstrate that the mannose receptor was important for the recognition of yeast (*Saccharomyces cerevisiae*), whilst Alsam et al. (2005) showed that it is

important in *A. castellanii* recognition of bacterial prey; *Escherichia coli*. Another C-type lectin, the galactose and N-acetylgalactosamine (Gal/GalNAc) receptor, has also been identified in amoebic bacterial recognition. Specifically, this receptor has been associated with the recognition of Gal/GalNAc-rich *Escherichia coli* serotype O55 by *E. histolytica* (Bär et al., 2015).

2.4.3.2 Cytoskeleton rearrangement

As a response to prey recognition at the amoeba cell surface, a signalling cascade occurs resulting in cytoskeleton rearrangement (Smirnova and Segall, 2007). Polymerisation of monomeric G-actin to polymeric F-actin is crucial for phagocytosis (Alsam et al., 2005). This polymerisation allows the extension of two pseudopodia which begin to surround the prey. Myosin is also activated and facilitates pseudopod extension and pseudopod sealing around the phagocytotic target to form the phagosome (Levin et al., 2016). The detachment of the phagosome from the membrane into the cytoplasm occurs as a result of dynamin recruitment to the pseudopodal ends (Levin et al., 2016).

2.4.3.3. Phagosome maturation and resolution

The new phagosome then goes through a period of 'phagosomal maturation' in which the phagosome must become a hostile environment to promote the death and degradation of its cargo. It does this by fusion and fission with endosomes in the new, early and late stages of phagosome maturation. Then, in the late stage of phagosome maturation, the phagosome fuses with lysosomes to create a 'phagolysosome'. The phagolysosome is "the ultimate degradative compartment" as it is highly acidic and contains hydrolases and antimicrobial peptides to aid in the degradation of its contents (Levin et al., 2016; Pauwels et al., 2017).

Once the degradation of the phagolysosome cargo has taken place, 'phagosome resolution' occurs whereby the amino acid, proteins and lipid contents of the phagosome are transported into the cytosol through various receptors, and waste material is excreted ('exocytosis'/'egestion') by phagosome membrane fusion with cell membrane. Then, this membrane is endocytosed and recycled to form new phagosomes (Gotthardt et al., 2002; Levin et al., 2016; Lancaster et al., 2021).

2.4.4 Amoeba and interkingdom signalling

In the wider literature there is a lack of evidence of the role of amoebae in interkingdom signalling. It was shown that the growth of the slime mould *D. discoideum* was reduced in the

presence of wild-type *P. aeruginosa*, but increased in the presence of *las* and *rhl* mutants, more so in the latter, suggesting HSL QS was required for *P. aeruginosa*-mediated growth inhibition of *D. discoideum* (Cosson et al., 2002). In addition, some free-living amoebae have been shown to respond to HSLs (Parry, Personal communication). However, this requires deeper examination to establish if this is genera- or species-specific, or if this is a widespread response within amoebae. In addition, the identification of any receptor(s) that may be responsible for the interaction should also be conducted.

2.5 Possible eukaryotic receptors for HSLs

Some eukaryotic receptors and proteins have been identified to interact with HSLs (**Figure 2.7**). Research conducted by Tobita et al. (2022) showed that two Transient Receptor Potential (TRPs) channels were activated by HSLs. TRPV1 and TRPA1 were both activated by C8, C9 and C10, and OC12 activated TRPV1 while C2 and C4 activated TRPA1. However, to date, this effect has not been reported elsewhere and thus more research needs to be conducted into the role of TRP channels in HSL-based interkingdom signalling.

Karlsson et al. (2012) is the only study to date that has identified the interaction of HSLs and IQ-motif containing GTPase-activating proteins (IQGAP). They showed that OC12 interacts, and colocalises, with IQGAP1 and induced changes in the phosphorylation status of Rac1 and Cdc42 and the localization of IQGAP1 within Human Cell line Caco-2. IQGAP1 has also been shown to associate with other receptors that can themselves interact with HSLs, namely T2R38 (a G-protein Coupled Receptor, GPCR) in which IQGAP1 is thought to act as a scaffolding protein in the signal molecule cascades (Gaida et al., 2016).

To date, there are two main families of receptors that have been widely identified in the interaction between HSLs and eukaryotic cells; Peroxisome Proliferator Activator Receptors (PPARs) and GPCRs (Shrestha and Schikora, 2020).

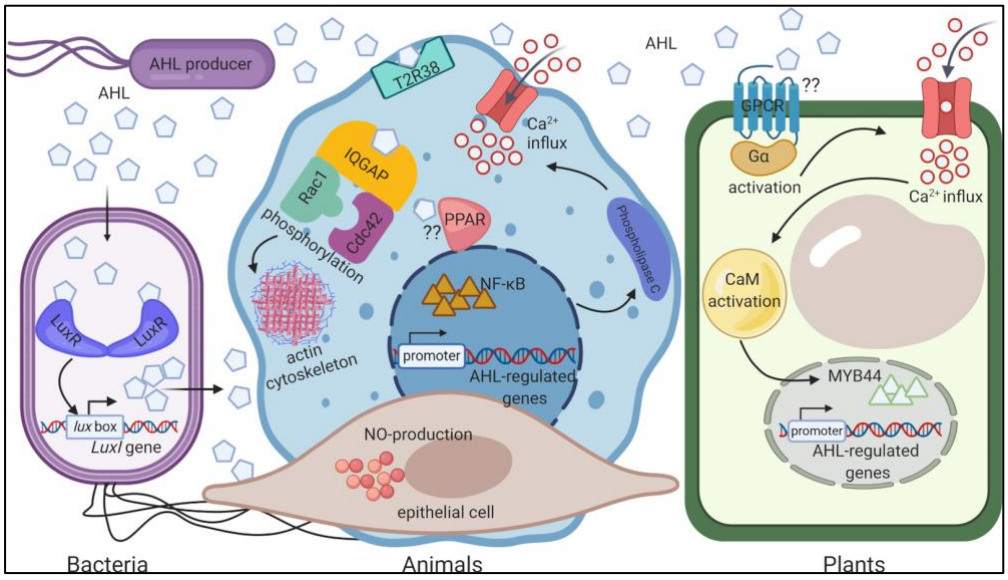

Figure 2.7. AHL-perception among different kingdoms. Perception of OC12 in animal cells can occur via three different proteins: IQ-motif containing GTPase-activating protein (IQGAP1), nuclear Peroxisome proliferator-activated receptors (PPAR) and T2R38 (G-Protein Coupled Receptor, GPCR). Additionally, AHLs induce nitric oxide (NO)-production in epithelial cells. AHL perception mechanism in plants is not yet known, however, OC6 and OC8 are suggested to interact with a GPCR and thus activate Gα ultimately inducing AHL-regulated gene expression. Taken from Shrestha and Schikora (2020).

2.5.1. Peroxisome Proliferator-Activated Receptors

2.5.1.1. Structure and function

Peroxisome proliferator-activated receptors (PPARs) are ligand-activated transcription factors, which belong to the superfamily of nuclear receptors (Tyagi et al., 2011). The PPAR structure consists of a DNA binding domain in the N-terminus and a ligand binding domain in the C-terminus (Grygiel-Górniak, 2014). PPARs are similar in structure to steroid or thyroid hormone receptors and their natural activating ligands are lipid-derived substrates, also known as Fatty acid (FA) derived compounds (Tyagi et al., 2011). Therefore, PPARs can be described as "lipid-sensing" receptors (Evans et al., 2004).

PPARs comprise three subtypes named PPARα, PPARβ/δ and PPARγ (Tyagi et al., 2011), also referred to in the literature as NR1C1, NR1C2 and NR1C3, respectively (Luquet et al., 2005). All subtypes are crucial in energy metabolism; however, these subtypes differ in their activity and their main areas of expression (Tyagi et al., 2011). PPARα is expressed predominantly in the liver, and also in muscle, the heart, kidneys and in bone (Chinetti et al., 2000; Gervois et al., 2000). PPARβ/δ is expressed ubiquitously across the whole body to regulate energy expenditure (Tyagi et al., 2011). PPARγ is expressed in multiple tissues including; adipose

tissue, the large intestine, immune system, and vascular smooth muscle cells (Gervois et al., 2000; Zoete et al., 2007; Tyagi et al., 2011), and is induced in monocyte to macrophage differentiation (Heming et al., 2018). PPARγ is primarily involved with adipocyte differentiation and lipid storage (Chinetti et al., 2000; Zoete et al., 2007).

PPARs are predominantly in the nucleus, however can be found in the cytoplasm (Umemoto and Fujiki, 2012). When they bind to a ligand/agonist in the cytoplasm they translocate to the nucleus where they form a complex with the retinoid X receptor (RXR) (Tyagi et al., 2011). The PPAR/RXR dimer, in association with a co- activator, enables the PPAR/RXR complex to bind to DNA sequences termed Peroxisome Proliferators Response Elements (PPREs) (**Figure 2.8**) (Tyagi et al., 2011; Grygiel-Górniak, 2014). PPREs are present in the promoter region of target genes, and so the activation of these genes leads to changes in the expression levels of mRNAs encoded by the PPAR target genes. These processes are termed transactivation and transrepression (Willson et al., 2000; Tyagi et al., 2011) which lead to an increase, or decrease, in the mRNA expression, respectively.

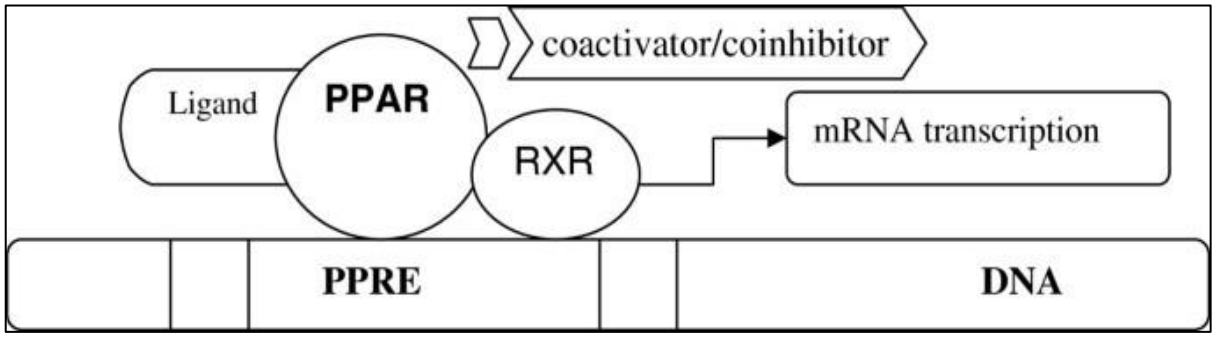

Figure 2.8. Mechanism of gene transcription by PPARs. Taken from Grygiel-Górniak (2014). Process described in text.

PPAR targeted genes are primarily involved in the regulation of glucose and lipid metabolism, and energy homeostasis, as well as cell differentiation, inflammation, proliferation and apoptosis (Tyagi et al., 2011). All 3 isoforms of PPARs play different roles in lipid metabolism and the immune response. However, only PPARγ and PPARβ/δ have been identified in HSL-perception, with opposing outcomes (Jahoor et al., 2008)

2.5.1.2. Evidence for interaction between HSLs and PPARs

Multiple eukaryotic cell types have been shown to be affected by OC12, as a direct result of PPAR binding (**Table 2.2**). OC12 can act as an antagonist and agonist, depending on the

receptor, i.e., an antagonist to PPARγ and an agonist to PPARβ/δ (Cooley et al., 2008; Jahoor et al., 2008). No interaction of HSLs with PPARα could be found in the literature. With PPARβ/δ, Jahoor et al. (2008) showed that OC12 enhanced the transcriptional activity of PPARβ/δ in a dose dependent manner. However, this effect has not been confirmed with other studies.

PPARγ activation has been shown to increase the levels of the enzyme paraoxonase 2 (PON-2) (**Figure 2.9**) and PON-2 has been shown to inactivate and degrade *P. aeruginosa* QS molecules, including OC12, via lactonase activity (Bedi et al., 2016). However, OC12 acts as an antagonist to PPARγ, leading to PPARγ inactivation. The inactivation of PPARγ by its antagonists (OC12 and GW9662), results in an inactivation of PON-2 as well as reduced expression of tight junction proteins, causing an increase in the host susceptibility to *P. aeruginosa* infection (Bedi et al., 2016). Conversely, PPARγ agonists such as pioglitazone (PIO) activate PPARγ and increase levels of tight junction proteins and PON-2, which ultimately results in degradation of OC12 and an enhanced host defence system (Bedi et al., 2016; Bedi et al., 2017).

Table 2.2. The effects of OC12 on PPARs in eukaryotic cells

Cell type	PPAR isoform	Effect(s)	Reference
Murine fibroblast (NIH 3T3) and human alveolar epithelial cells (A549)	PPARγ	200-400 μM OC12 acts as an antagonist of transcriptional activity and 100 μM inhibited DNA binding ability. 25 μM OC12 had a pro-inflammatory effect on A549 cells which was blocked by 50 μM PPARγ agonist rosiglitazone.	(Jahoor et al., 2008)
	PPARβ/δ	200-300 μM OC12 acts as an agonist of transcriptional activity	
Human bronchial epithelial cells (BEAS-2B)	PPARγ	1nM of OC12 can interfere with the binding of 100 nM rosiglitazone, suggesting that OC12 has a strong binding affinity to the ligand binding domain of PPARγ	(Cooley et al., 2010)
Macrophage cells (RAW264.7) and a macrophage-like monocytic cell line (THP-1).	PPARγ	50 μM OC12 was sufficient to significantly reduced the mRNA and protein expression of PPARγ and PON-2 in THP-1 and RAW264.7 cells	(Bedi et al., 2016)
BEAS-2B	PPARγ	100 μM OC12 reduced PPARγ expression and lowered the expression of junctional proteins, eliminating barrier function in BEAS-2B cells. PPARγ agonist, Pioglitazone (PIO) (30 μM), reduced the antagonistic effects of OC12	(Bedi et al., 2017)

The results from Bedi et al. (2016) should not be considered to definitively determine that just PPARγ is involved in the interaction with OC12. This is because the 'PPARγ antagonist' that was used (GW9662) is in fact shown to also be an antagonist of PPARβ/δ and PPARα, although it is however a more potent antagonist of PPARγ than of PPARβ/δ and PPARα (Leesnitzer et al., 2002).

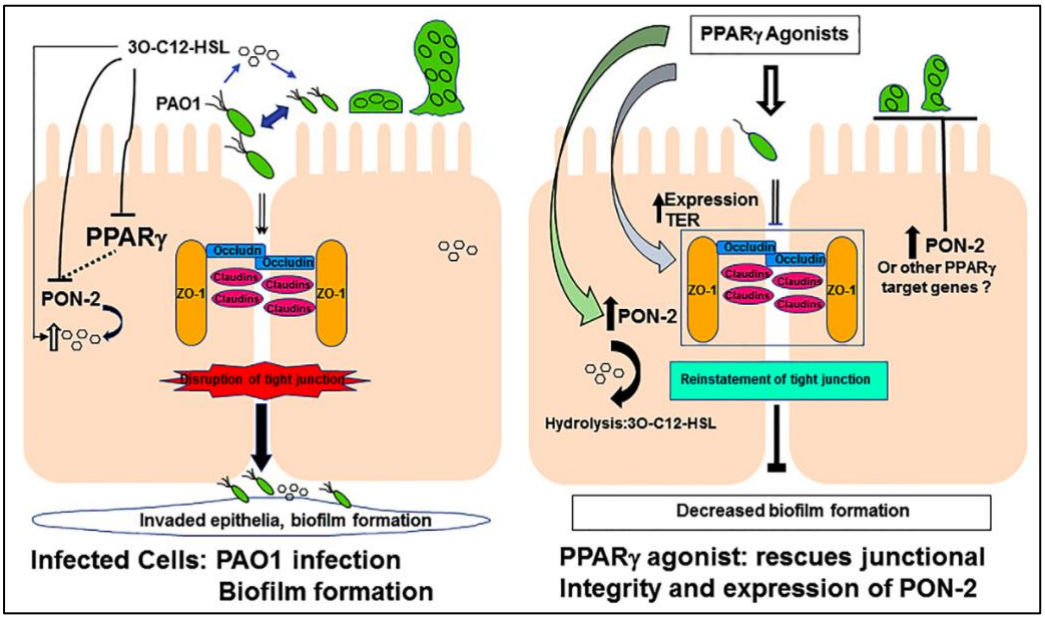

Figure 2.9. Schematic of PPARγ-mediated attenuated biofilm formation by *Pseudomonas aeruginosa* on epithelial cells. Upon infection of epithelial cells with *P. aeruginosa* (PAO1) and OC12, PPARγ, PON-2 and tight junction protein (ZO-1, claudin-4, and occluding) levels are reduced. All these events promote the permeation of bacterial colonies which form biofilms. Upon addition of PPARγ ligands, PPARγ receptors are activated, leading to increased expression of PON-2 and tight junction proteins; enhancing barrier function, hydrolysis of OC12 and weakening the potential for biofilm formation. Taken from Bedi et al. (2017).

2.5.1.3 Possibility of PPARs being receptor in amoeba

To date, PPARs have not been identified in amoebae or protists as a whole. However, peroxisomes are believed to be present in most, if not all eukaryotic cells and are used for processing lipids (Ludewig-Klingner et al., 2018). Recently, peroxisomes have been shown to be present in some amoeba (Jansen et al., 2021). Al-Hammadi (2020) found that blocking of PPARα reduced the negative effect of the long-chained lipid Cannabidiol (CBD) in the amoeba *Vermamoeba vermiformis*, and proposed that a non-genomic action of a PPAR-like molecule was in place. This involves PPAR binding to other proteins, meaning that recombination with RXR is not involved (Unsworth et al., 2018). This suggested that, despite the lack of RXR homologues in amoebae, PPARs might still be able to respond to long chain lipids. However, this might be a specifies-specific response, as blocking all PPAR-like receptors (with GW9662) did not alleviate the negative effect of CBD in *A. castellanii*, *Flamella arnhemensis*, *Hartmannella cantabrigiensis*, *Naegleria gruberi* and *Vahlkampfia avara.*

Al-Hammadi (2020) also examined the role of a GPCR in the interaction with CBD, specifically, blocking the serotonin 5-HT1A receptor (with [S]-WAY 100135 dihydrochloride)

alleviated the negative effect of CBD in *N. gruberi*. But once again, this was found to be species-specific and blocking this receptor had no alleviation effect on *A. castellanii*, *F. arnhemensis*, *H. cantabrigiensis*, *V. vermiformis* and *V. avara*. Considering that amoebae are known to possess many GPCRs (Baig, 2016; Senoo et al., 2016) together with evidence that some can bind long chain HSLs (Jaggupilli et al., 2018), they warrant further investigation.

2.5.2 G-Protein Coupled Receptors

2.5.2.1. Structure and function

G-protein coupled Receptors (GPCRs) are the largest family of membrane proteins and they are responsible for perception of molecules such as hormones (some of which are long chain lipids) and neurotransmitters, as well as having a role in light, smell and taste perception (Rosenbaum et al., 2009). More widely, GPCRs are responsible for multiple cellular process such as creating signal cascades which cause increases in intracellular Ca^{2+}, allowing actin cytoskeleton rearrangement (Dushek et al., 2008; Rosenbaum et al., 2009; York-Andersen et al., 2020). This is an important step in engulfing prey in phagocytes (Levin et al., 2016). Despite being involved in phagocytosis (Pan et al., 2016), GPCRs are not considered to be 'phagocytotic receptors' but instead are receptors that help to prime the cell for phagocytosis and modulate the cellular response to a phagocytotic particle (Freeman and Grinstein, 2014).

The general structure of GPCRs comprises of 7 hydrophobic transmembrane (TM) spanning alpha helices, separated by alternating intracellular and extracellular loop regions, with an extracellular Amino terminus (N- Terminus) and intracellular Carboxyl terminus (C-terminus) (Kaczor et al., 2014) (**Figure 2.10**). They are descendants of prokaryotic bacteriorhodopsins (DiBartolo and Booth, 2012; Evtikhov et al., 2017). GPCRs are separated into seven families based on their sequence and structural similarity; rhodopsin receptors (family A), secretin receptors (family B), glutamate receptors (family C), fungus pheromone receptors (family D), cAMP receptors (family E), frizzled/smoothened receptors (family F) and family O which is comprised of those GPCRs that do not fit into the other 6 categories (de Oliveira et al., 2019).

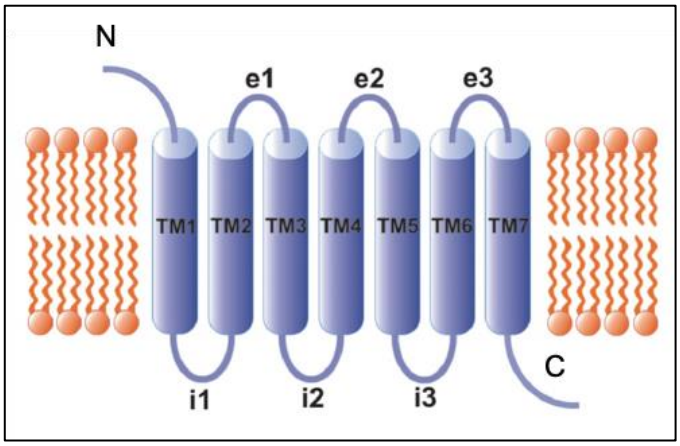

Figure 2.10. General topology of G-protein coupled receptors. Embedded in a lipid-bilayer are seven transmembrane helices (TM1-TM7), connected with 3 extracellular (e1-e3) and 3 intracellular (i1-i3) loops. Taken from Kaczor et al. (2014) and adapted to include annotation of the extracellular N- terminus (N) and the intracellular C-terminus (C).

GPCRs are responsible for the activation of intracellular heterotrimeric G proteins, which act as key downstream signalling molecules (Duc et al., 2015). G proteins are heterotrimeric as they have three subunits known as α, β, and γ. The α subunit is a GTP-binding domain with GTPase activity, referred to as Gα (de Oliveira et al., 2019). In their inactive state, GDP is bound to the Gα subunit. The Gα has different subtypes, including G_s, G_i (including G_t and G_o), G_q and $G_{12/13}$ (de Oliveira et al., 2019). The β, and γ, subunits form a complex together called the Gβγ dimer, regardless of the Gα subtype (de Oliveira et al., 2019).

There is variability in the GPCR structure, with the most variable structures being the N-terminus, the intracellular loop spanning TM5 and TM6 (i3 in **Figure 2.10**), and the C-terminus (Kobilka, 2007). G proteins interact with the C-terminus, whilst also interacting with specific residues that TM5 and TM6 possess. Therefore, the variability of the i3 loop – found between TM5 and TM6 – and the C-terminus allow for different G-protein subtypes to interact with the GPCR (Hollmann et al., 2005).

The binding of a ligand to a GPCR causes a conformational change which allows Gα subunits to exchange GDP for GTP, making the G protein active. This exchange allows for the separation of the Gα subunit and the Gβγ dimer (de Oliveira et al., 2019). These subunits are then both active and can go off to stimulate their respective downstream signalling factors and alter the production of second messengers (Tanase et al., 2012). For every GPCR that is activated, multiple G proteins can be activated which helps to amplify the signal from the very

beginning and allow further amplification in the signal transduction pathway (Tanase et al., 2012).

2.5.2.2 Evidence for interaction with HSLs

The interaction of GPCRs with HSLs has been seen by multiple studies (**Table 2.3**), and has been shown in both plant and animal cells, highlighting how widely they occur but also highlighting that they are a potential receptor for HSL perception in all eukaryotic cells.

A widely reported example is that of multiple bitter taste receptors interacting with OC12 (Ahmad and Dalziel, 2020). Bitter taste receptors were originally thought to be their own family of GPCRs, but more recent evidence suggests they are family A (rhodopsin-like) receptors (Di Pizio et al., 2016). The first reported example of an interaction of OC12 with bitter taste receptors was seen with receptor T2R38 in neutrophils (Maurer et al., 2015). T2R38 is found on the cell membrane and intracellularly, meaning that there are two possible mechanisms of OC12-T2R38 binding; OC12 diffusion through the cell membrane and/or binding to the receptor on the membrane (Maurer et al., 2015). Further investigation found that other taste receptors could also interact with other HSLs. Receptors T2R4 and T2R20 could both be activated by C8 and OC12, whilst receptor T2R14 was activated by C4, C8 and OC12 (Jaggupilli et al., 2018).

GPCRs in plants (mainly *Arabidopsis* spp.) have also been shown to interact with HSLs. Interaction of a GPCR (GCR1) with OC6 and OC8 resulted in the activation of Gα (GPA1) (Liu et al., 2012). This promoted Ca^{2+} influx into the cytosol, triggering activation of calmodulin and the transcriptional factor AtMYB44 to induce expression of HSL-regulated genes, such as cytokinin- and auxin-related genes (Zhao et al., 2016; Shrestha and Schikora, 2020). Jin et al. (2012) suggested that two *Arabidopsis* GPCR candidates (Cand2 and Cand7) are involved in HSL-mediated promotion of root elongation, as the *Cand2* and *Cand7* knock-out mutants “abolished the promotional effects” of OC6 or OC8 which suggested that binding with Cand2 and Cand7 is crucial for HSL-mediated root elongation.

Table 2.3 GPCRs involved in the perception of different length HSLs.

HSLs	Cell type	GPCR	Effect(s)	Reference
OC6 and OC8	*Arabidopsis*	Cand2 + Cand7	1 μM OC6 and 10 μM OC8 promoted Cand2 and Cand7 gene expression and cause root elongation.	(Jin et al., 2012)
		GCR1 (GPA1)	1 μM OC6 and 10 μM OC8 resulted in increase of relative root elongation, due to activation of GPA1 via GCR1 interaction; *gcr1-1* and *gpa1*mutants had no promotional effects when treated with HSLs. OC6 and OC8 both increased *GCR1* and *GPA1* gene expression in wildtype plants	(Liu et al., 2012)
OC12	Human cancer cell line; Caco-2	Protease activated receptor (PAR) 1 and 2	200 μM OC12 induced protease-activated receptor (PAR)-dependent signalling leading to disassembly of tight junctions	(Eum et al., 2014)
	Human neutrophils and cell line HL-60	T2R38	50-100 μM OC12 bound to T2R38 and acted as an agonist and resulted in the up-regulation of CD11b cell surface expression and enhanced phagocytosis.	(Maurer et al., 2015)
	Myeloid cells (U937)	T2R38	100 μM OC12 bound to T2R38 which co-localised with IQGAP1 when activated	(Gaida et al., 2016)
C8 and OC12	Human embryonic kidney (HEK293T) cell line	T2R4 and T2R20	T2R4 and T2R20 both had an increased calcium mobilisation when treated with C8 (50 and 200 μM, respectively) and OC12 (100 and 200 μM, respectively).	(Jaggupilli et al., 2018)
C4, C8 and OC12	HEK293T	T2R14	Increased calcium mobilisation by C4, C8 and OC12 (50 μM)	(Jaggupilli et al., 2018)

2.5.2.3 Possibility of GPCR and HSL binding in amoebae.

GPCRs are widespread among eukaryotic cells and have been shown to be present in amoebae. *D. discoideum,* although not a 'true' amoeba, has been shown to have at least 55 different GPCRs (Senoo et al., 2016) with some being used for prey detection and chemotaxis. For example, folic acid receptor 1 (fAR1) detects folic acid secreted by bacteria (Pan et al., 2016; Senoo et al., 2016). Heterotrimeric G proteins (and their activation by GPCRs) have been shown to be important in aggregation, cell differentiation and phagocytosis in *D. discoideum* (Gotthardt et al., 2006). GPCRs have also been shown in 'true' amoebae. Both *A. castellanii* and *Naegleria fowleri* have been shown to have structural homologs to human M_1 type muscarinic cholinergic receptors, believed to be bound to G_q subtypes, (Haga, 2013). The GPCR homolog, NF0059410, in *N. fowleri* is a G_q α subtype that is believed to be involved in neurochemotaxis, as the downstream signalling from this receptor promotes actin assembly (Baig, 2016). A G_q α subtype in *A. castellanii* is believed to be involved in proliferation, as the blocking of this receptor prevented cell propagation (Baig and Ahmad, 2017; Baig et al., 2018). Therefore, it is possible that GPCRs in amoebae might be able to detect HSLs and one way to study this is with the use of GPCR antagonists.

2.5.3 Receptor antagonists

Commercial antagonists or 'blockers' are widely used in research to deduce the function of a receptor of interest. For example, there are 'general' blockers which deduce the response of a family of receptors by blocking all receptors within that family, and there are also specific blockers which target certain receptors within the family. Gallein is a 'general' antagonist for all GPCRs as it inhibits the βγ complex, common to all (Lehmann et al., 2008), whereas PTX and Melittin are antagonists to certain G protein subtypes. PTX prevents G_i proteins from interacting with their GPCRs (including G_o and G_t receptors, but not G_z) (Mangmool and Kurose, 2011; de Oliveira et al., 2019), whereas melittin inhibits G_s protein activity (Fukushima et al., 1998). Similarly, with PPARs, there is a general antagonist (GW9662, Leesnitzer et al. [2002]), as well as more potent antagonists for the different PPAR subtypes; α (GW6471, Abu Aboud et al. [2013]), β/δ (GSK3787, Palkar et al. [2010]) and γ (T0070907, Lee et al. [2002a]).

2.6 Research questions and aims

The overall aim of this research was to determine how sensitive different amoebae are to HSLs and attempt to elucidate the eukaryotic receptor for HSL binding.

The specific objectives were to:

1) Evaluate the susceptibility of numerous amoeba species to the HSLs C4, C6, C8, C10, and C12.
2) With those that were susceptible, to:
    a. Evaluate their sensitivity to C12 variants, i.e. C12 vs HC12 vs OC12.
    b. Determine the Minimum Inhibitory Concentration (MIC), Inhibitory Concentration at 50% (IC50) and the Lethal Dose (LD) of the HSLs.
    c. To evaluate whether PPARs or GPCRs might be the receptor within amoebae, for HSLs.
    d. Assess the physiological effect of HSLs on amoeba cells.

3. Materials and Methodology

3.1 Organisms and Maintenance

3.1.1 *Escherichia coli*

Escherichia coli strain DH5α (obtained from Dr Karen Tait, Plymouth Marine Laboratory) was maintained as streak plates on Diagnostic Sensitivity agar (DST) with Chloramphenicol (30 µg/mL) (see **Appendix I**) and incubated at 30 °C for three days. Suspensions were prepared by pouring 5 mL of sterile water onto a streak plate and dislodging cells into suspension with a sterile spreader. Bacterial suspensions were made fresh on the day of an experiment.

The *E. coli* DH5α strain used is a transformed strain which includes a silenced *aiiA* plasmid carrying chloramphenicol resistance genes, and it is a HSL insensitive strain, therefore will not be effected by the HSLs examined in this study.

3.1.2 Amoebae

Amoebae (**Table 3.1**) were sub-cultured seven days prior to an experiment. A streak of *E. coli* DH5α was placed down the centre of a Non-nutrient agar (NNA) plate (see **Appendix I**), and a cube of agar from a previous amoebae culture, containing trophozoites, was placed at the top of the streak, amoeba side down, and incubated at room temperature for 7 days.

Amoebic suspensions were prepared by aseptically removing the bacterial strip and the agar block from the NNA plates. Then, 8 mL of amoeba saline (AS, see **Appendix I**) was aseptically poured onto the plates. The amoeba cells were dislodged with a sterile spreader and then aseptically poured into a tissue culture flask. The amoebae suspensions were prepared on the day of an experiment and stored at room temperature (*ca*. 23 ^{o}C) on a rotary shaker, to prevent cell settlement and cyst formation.

Table 3.1. Amoebae strains and their source. American Type Culture Collection (ATCC), Culture Collection of Algae and Protozoa (CCAP).

Amoeba Species	Source Code
Acanthamoeba castellanii	CCAP 1501/1A
Acanthamoeba polyphaga	CCAP 1501/18
Cochliopodium minus	CCAP 1537/1A
Echinamoeba silvestris	CCAP 1519/1
Flamella arnhemensis	CCAP 1525/2
Hartmannella cantabrigiensis	CCAP 1534/8
Hartmannella cantabrigiensis	CCAP 1534/11
Naegleria gruberi NEG-M	ATCC 30224
Phalansterium filosum	CCAP 1576/1
Rosculus hawesi	CCAP 1571/4
Saccamoeba limax	CCAP 1572/3
Tetramitus aberdonicus	CCAP 1588/4
Vahlkampfia avara	CCAP 1588/1A
Vannella placida	CCAP 1565/2
Vermamoeba vermiformis	CCAP 1534/7A
Vermamoeba vermiformis	CCAP 1534/14
Vexillifera bacillipedes	CCAP 1590/1

3.2 Experimental Compounds

3.2.1 Acyl Homoserine Lactones (HSLs)

Stock solutions (10 mM) of seven HSLs (SIGMA) (**Table 3.2**) were prepared in Dimethyl sulfoxide (DMSO) (SIGMA), separated into 100 µL aliquots and stored at -20 °C.

Table 3.2. Full name and code for each acylated homoserine lactone (HSL).

HSL full name	HSL code
N-Butyryl-DL-homoserine Lactone	C4
N-Hexanoyl-DL-homoserine Lactone	C6
N-Octanoyl-DL-homoserine Lactone	C8
N-Decanoyl-DL-homoserine Lactone	C10
N-Dodecanoyl-DL-homoserine Lactone	C12
N-(3-Hydroxydodecanoyl)-DL-homoserine Lactone	HC12
N-(3-oxo-dodecanoyl)-L-homoserine Lactone	OC12

3.2.2 Antagonists

Stock solutions of nine antagonists (TOCRIS) were prepared in either Ethanol, DMSO or Distilled water, at their respective stock concentrations and stored at -20 °C (4 °C for Pertussis Toxin), see **Table 3.3**.

Table 3.3. The antagonists, their targets, stock and working concentrations and storage information.

Antagonist (code)	Target	Concentration		Solvent	Exposure time	Storage
		Stock	Working			
GW9662 (GW)	General PPAR antagonist	10 mM	10 μM	Ethanol	30 min	-20 °C
Capsazepine (Cap)	General Vanilloid receptor antagonist	10 mM	10 μM	Ethanol	30 min	-20 °C
Gallein (Gal)	All GPCRs; a βγ complex inhibitor	10 mM	10 μM	DMSO	30 min	-20 °C
Haloperidol hydrochloride (Halo)	Dopamine & Serotonin receptors	10 mM	10 μM	Ethanol	30 min	-20 °C
Pertussis Toxin (PTX)	$G_{i/o}$ and G_t GPCR inhibitor	100 μg/mL	100 ng/mL	Distilled water	5 hr	4 °C
Melittin (Mel)	G_s GPCR inhibitor	0.35 mM	0.2 μM to 1 μM	Distilled water	30 min	-20 °C
SCH 23390 hydrochloride (SCH)	Selective Dopamine D1 inhibitor	10 mM	10 μM	Ethanol	30 min	-20 °C
EMD 281014 hydrochloride (EMD)	Selective Serotonin 5-HT2A inhibitor	10 mM	10 μM	Ethanol	30 min	-20 °C
ZM241385 (ZM)	Selective Adenosine A2 antagonist	10 mM	10 μM	DMSO	30 min	-20 °C

3.3 Cell counts

3.3.1 Bacterial Counts

Ten-fold dilutions of the bacterial suspension were made, down to 10^{-3}, using sterile water. Two drops of 4′,6-diamidino-2-phenylindole (DAPI) (SIGMA) were added to the 10^{-3} dilution and left to stain for 30 minutes. Sterile water (*ca*. 5 mL) and 200 µL of the 10^{-3} dilution were filtered through a 0.2 µm pore filter (Millipore), via suction, to ensure the filter had an equal distribution of bacterial cells on its surface. Using an epi-fluorescent microscope (x 1600 magnification), the bacterial cells on the filter were counted in randomly selected whipple grids, under UV light, until at least 400 cells had been counted. **Equation 1** was used to determine the bacterial cells/mL in the undiluted suspension.

Equation 1. Determination of bacterial cells per mL of the undiluted suspension.

$$\left(\frac{number\ of\ bacterial\ cells\ counted}{number\ of\ whipple\ grids\ counted}\right) \times\ 23068\ \times\ 10^3\ \times\ 5 = cells/mL$$

3.3.2 Amoebic Suspension Counts

Four haemocytometer counts were performed on each amoeba cell suspension, using a light microscope (x40 magnification). The average number of amoeba cells in the four haemocytometer grids (36 squares counted in total) was multiplied by 1 x 10^4 to determine amoebae cells/mL, shown in **Equation 2**.

Equation 2. Determination of amoeba cells per mL of suspension.

$$(total\ number\ of\ amoebae \div 36) \times\ (1\ \times 10^4) = cells/mL$$

3.3.3 Amoebic Counts on Experimental Plates

All experimental plates (**see 3.4**) had a piece of acetate, showing 5 counting grids, adhered to the base of the Petri dish. Amoeba cells were counted in each of the 5 counting grids using a light microscope (x40 magnification). These counts were first converted to natural log (Ln) amoeba cells/grid and then percentage population growth in the presence of Tests were compared to the Control, unless stated otherwise.

3.4 General experimental set up

All experiments were conducted in triplicate, unless stated otherwise. Non-Nutrient Agarose (NNAg) plates (see **Appendix I**) were poured on a spirit-levelled surface to ensure an even distribution of amoeba and bacterial cells post-inoculation. Agarose was used instead of agar, to ensure the plates were carbon free which prevented *E. coli* growth. These plates shall henceforth be known as "experimental plates".

E. coli and amoebic suspensions were prepared (**3.1.1 and 3.1.2**) and counted (**3.3.1 and 3.3.2**). The optimised starting concentration of cells on the surface of a NNAg experimental plate (90 cm diameter) was 5 x 10^6 *E. coli*/cm^2 and 15 amoeba cells/cm^2. Experimental plates were therefore inoculated with a 1 mL suspension containing 3.18 x 10^8 *E. coli* cells and 954 amoeba cells, with the volume being made up to 1 mL with AS (with/without HSL). On a spirit-levelled surface, in a Class 2 cabinet, the 1 mL mixture was poured onto an experimental plate and rotated to ensure the whole plate was covered with the suspension. When dry, the plates were incubated at 16 °C.

The Control experimental plates were counted on day 2 of incubation, and then every day until 3 cellular divisions had been reached (a minimum of 120 cells per grid on average). Only then were counts conducted on the remaining experimental plates (**3.3.3**). All amoeba counts were converted to Ln amoeba/grid and then an average percentage population density was calculated for each treatment, compared to the Control and presented as percentage population growth compared to Control (± SEM), unless otherwise stated.

3.5 HSL sensitivity screening

All 17 amoeba strains (**Table 3.1**) were grown on *E. coli* in the absence (Control 1) and presence of 200 µM HSLs (C4, C6, C8, C10 and C12) and 20 µL of DMSO (Control 2), following the method in **3.4**. The plates were then incubated and counts, in accordance with **3.3.3**, were conducted on all experimental plates, once 3 cellular divisions occurred in Control 1. Cell counts/grid were converted to Ln amoeba cells/grid and then percentage growth compared to Control (± SEM). The DMSO Control (Control 2) was used in this stage of screening to check that DMSO (the 'vehicle') (at 20 µL/mL) did not have a negative effect on amoebic population growth.

3.6 DMSO Controls

DMSO is the solvent in which HSLs were prepared (the 'vehicle'). HSL-sensitive amoeba strains were tested against various volumes of DMSO, from 0 to 40 µL (which would be present in HSL solutions up to 400 µM), following **3.4**. Amoeba cell counts were conducted on all experimental plates after at least 3 cellular divisions had occurred on the Control plates, in accordance with **3.3.3**. The cell counts were converted to Ln amoeba cells/grid and then the percentage population growth compared to Control (± SEM).

3.7 C12-HSL variants sensitivity screening

Amoeba strains which had been shown to be sensitive to C12, were also tested against the C12 variants HC12 and OC12. In accordance with **3.4**, amoebae were grown in the absence (Control) and presence of C12, HC12 and OC12 at 300 µM to identify any differences in the growth of the amoeba population in the presence of the variants. Amoeba cell counts were conducted on all experimental plates (**see 3.3.3**) once 3 cellular divisions had occurred on Control plates. The cell counts were converted to Ln amoeba cells/grid and then to percentage population growth compared to Control (± SEM).

3.8 HSL Dose Response experiments

Sensitive amoebae were tested in the absence (Control) and presence of various concentrations of C12 (0 to 600 µM) following the method in **3.4**. Amoeba cell counts were conducted on all experimental plates (**see 3.3.3**), after 3 cellular divisions had been reached on Control plates. The cell counts were converted to Ln amoeba cells/grid and then percentage population growth compared to Control (± SEM). This was plotted against LOG10 HSL concentration in a QtiPlot to determine the Inhibitory Concentration at 50% (IC50). The Minimum Inhibitory Concentration (MIC) and Lethal Dose (LD) values were estimated by regression analysis of the linear decline in percentage growth with increasing HSL concentration.

3.8.1 Growth experiment

One sensitive amoeba strain (*Vermamoeba vermiformis* CCAP1534/14) was subjected to daily counts within one of the dose response experiments (**3.8**) to determine the effect that HSLs had on the growth of the amoeba population over time; specifically looking at the lag phase and doubling times. Amoeba cell counts were conducted on all experimental plates in accordance with **3.3.3** including day 0 (when all plates had fully dried). All experimental plates were then

counted every 24 h for 9 days. The amoeba cells/grid from all experimental plates, at all time points, were first converted to amoeba cells/cm^2 (average number of cells/grid divided by 1.44) and then Ln amoeba cells/cm^2. The Ln amoeba cells/cm^2 was then plotted against time (d), and the lag phase, specific growth rate and doubling times were calculated using linear regression of the exponential phase. The gradient of this line provided the specific growth rate value (/d) and then the doubling time was calculated with **Equation 3**. The lag phase was estimated as the time taken (days) between inoculation (day 0) and the start of exponential growth.

Equation 3. Determination of amoeba doubling time.

$$\frac{LN(2)}{Specific\ Growth\ Rate} = Doubling\ time$$

3.9 Receptor blocking

Antagonists that were used, and their targets, are listed in **Table 3.3**. The flow chart which determined the order of blocker experiments is in **Appendix I, Table A.**

Amoebic cell suspensions (**3.1.2**) were split into 'blocked' and 'unblocked' cells. Receptor blockers (at the appropriate working concentrations) were added to 'blocked' amoebic suspensions for the required exposure time (**Table 3.3**), whist on the rotary shaker. Experiments were then conducted with both 'blocked and 'unblocked' amoebae, in accordance with **3.4**, in the absence (unblocked and blocked Control) and presence of 300 μM C12. Amoeba cell counts were conducted on all experimental plates after 3 cellular divisions had been reached on the Unblocked Control plates (**see 3.3.3**). Amoeba cell counts were then converted to Ln amoeba cells/grid and then to percentage population growth compared to Control (± SEM).

3.9.1 Melittin toxicity screening

Melittin has been shown to be toxic to different cells at various concentrations. The toxicity to amoebae was unknown. Therefore, dose response experiments (**3.8**) with the antagonist Melittin were conducted to determine potential toxicity of Melittin on amoeba. Amoeba were grown in the absence (Control) and after 30-minute exposure to Melittin (0.2 to 1 μM). Amoeba cell counts were conducted on all experimental plates once 120 amoeba cells were present on average per grid (3 cellular divisions) for the Control (**see 3.3.3**). Amoeba cell counts were then

converted to Ln amoeba cells/grid and then to percentage population growth compared to Control (± SEM).

3.10 Statistical analyses

Each treatment was compared using a One-way ANOVA, followed by post-hoc Tukey test using confidence limits of 95% ($P \leq 0.05$) and 99% ($P \leq 0.01$). https://astatsa.com/OneWay_Anova_with_TukeyHSD/.

4. Results

4.1 HSL sensitivity screening

Each of the 15 amoeba species (17 strains) was subjected to HSLs (C4-C12) at 200 µM (**see 3.5**) but only 4 species (5 strains) were sensitive and showed a reduction in population growth compared the Control (*Echinamoeba silvestris*, *Flamella arnhemensis*, *Naegleria gruberi* and both strains of *Vermamoeba vermiformis*). All were sensitive to C12 while *E. silvestris* and *V. vermiformis* (CCAP1534/14) were additionally sensitive to C6 and C10, respectively (**Table 4.1**). The two strains of *V. vermiformis*, CCAP 1534/7A and CCAP 1534/14, will henceforth be referred to as *V. vermiformis* (7A) and *V. vermiformis* (14), respectively.

4.2 DMSO controls

Since HSLs were dissolved in DMSO (the 'vehicle'), the sensitivity of *N. gruberi*, *V. vermiformis* (7A), *V. vermiformis* (14) and *F. arnhemensis* was tested against DMSO only, at volumes (10-40 µL) which were used to provide HSL concentrations at 100-400 µM (**see 3.6**). Results are presented in **Figure 4.1** and **Appendix II** (**Figures A-C**). DMSO did not significantly affect amoebic population growth, so the vehicle was considered inert and any effect of the addition of an HSL (in DMSO) to the amoeba culture was considered to be solely due to the HSL.

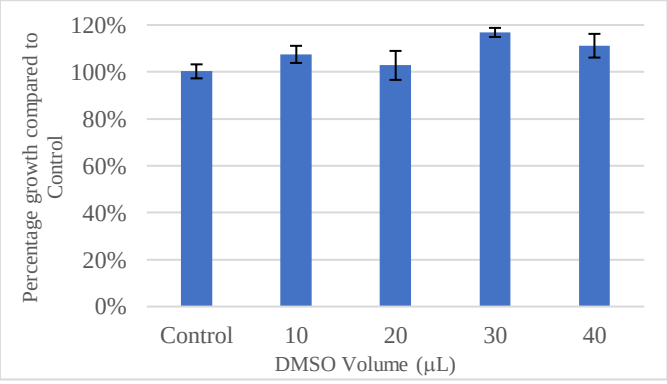

Figure 4.1 Percentage population growth of *Naegleria gruberi* in the presence of different DMSO volumes. Dose response experiments were carried out in which *N. gruberi* cells (15 amoeba/cm^2) were fed with *Escherichia coli* (5 x 10^6 cells/cm^2) in the absence (Control) and presence of DMSO (10-40 µL). Amoeba cell counts were conducted after 3 population divisions and the percentage population growth (compared to Control) was calculated. Data are presented as Average ± SEM, n=15. Statistical analysis by One-way ANOVA, P = 0.0544.

Table 4.1. Percentage population growth of amoebae, compared to the Control, in the presence of HSLs C4-C12. Data were statistically analysed using One-way ANOVAs (P<0.05 in 6 cases) and post-hoc tukey HSD tests (significant treatments in bold). n=10, except *Tetramitus aberdonicus* (n=5). *No significant treatment despite ANOVA P<0.05.

Amoeba species	**Strain source code**	**Control**	**C4**	**C6**	**C8**	**C10**	**C12**	**ANOVA P**
Acanthamoeba castellanii	CCAP1501/1A	100±2%	92±5%	99±1%	95±4%	99±2%	97±3%	0.4542
Acanthamoeba polyphaga	CCAP1501/18	100±3%	94±4%	92±4%	87±5%	91±4%	92±5%	0.3839
Cochliopodium minus	CCAP1537/1A	100±2%	99±2%	101±2%	98±2%	92±2%	92±3%	0.0132*
Echinamoeba silvestris	CCAP1519/1	100±1%	88±4%	**70±6%**	86±3%	78±4%	**38±11%**	$2.24x10^{-7}$
Flamella arnhemensis	CCAP1525/2	100±6%	89±16%	79±14%	89±13%	88±11%	**42±13%**	0.0313
Hartmannella cantabrigiensis	CCAP1534/8	100±2%	97±3%	100±1%	99±3%	101±2%	96±2%	0.4825
Hartmannella cantabrigiensis	CCAP1534/11	100±2%	95±2%	93±4%	95±3%	97±3%	96±3%	0.5555
Naegleria gruberi NEG-M	ATCC30224	100±4%	94±7%	92±5%	74±14%	72±11%	**57±11%**	0.0178
Phalansterium filosum	CCAP1576/1	100±13%	103±7%	112±6%	116±5%	109±7%	98±10%	0.6197
Rosculus hawesi	CCAP1571/4	100±3%	104±4%	98±3%	100±4%	102±3%	101±4%	0.8903
Saccamoeba limax	CCAP1572/3	100±3%	98±4%	97±3%	97±6%	87±7%	91±4%	0.4034
Tetramitus aberdonicus	CCAP1588/4	100±6%	94±3%	82±3%	89±6%	90±3%	84±3%	0.6611
Vahlkampfia avara	CCAP1588/1A	100±3%	99±4%	100±4%	103±2%	102±2%	107±2%	0.4867
Vannella placida	CCAP1565/2	100±2%	100±3%	97±2%	102±2%	94±2%	97±2%	0.386
Vermamoeba vermiformis	CCAP1534/7A	100±2%	98±3%	102±2%	96±3%	96±3%	**76±2%**	$4.68x10^{-7}$
Vermamoeba vermiformis	CCAP1534/14	100±2%	103±2%	91±1%	90±2%	**74±6%**	**72±4%**	$6.6x10^{-10}$
Vexillifera bacillipedes	CCAP1590/1	100±2%	97±2%	87±10%	101±1%	102±2%	102±2%	0.3912

4.3 C12 variant sensitivity

Three amoebae strains (*N. gruberi, V. vermiformis* [7A] and *V. vermiformis* [14]) were tested in the presence of 300 μM of C12, HC12 and OC12 (**see 3.7**).

4.3.1 *Naegleria gruberi*

Figure 4.2 shows that OC12 reduced the percentage growth of *N. gruberi* to 75% compared to the Control but this was not significantly different to Control (P=0.1469). C12 significantly reduced the percentage growth to 20% compared to the Control (P=0.001) while HC12 significantly reduced it to 59% (P=0.005). These reductions were themselves significantly different (C12 vs HC12, P=0.0058).

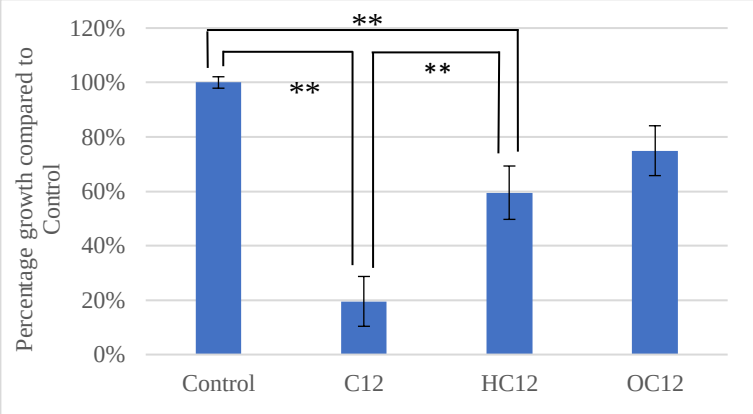

Figure 4.2 The effects of C12 variants on *Naegleria gruberi* population growth. *N. gruberi* cells (15 amoeba/cm^2) were fed with *Escherichia coli* (5 x 10^6 cells/cm^2) in the absence (Control) and presence of 300 μM C12, HC12 and OC12. Amoeba cell counts were conducted after 3 population divisions and the percentage population growth (compared to Control) was calculated. Data are presented as Average ± SEM, n=15. Statistical analyses using a post hoc tukey HSD test revealed significant results, ** = Significant difference (P<0.01).

4.3.2 *Vermamoeba vermiformis* (7A)

Figure 4.3 shows that OC12 reduced the percentage growth of *V. vermiformis* (7A) to only 97% compared to the Control which was not significant (P=0.8999). C12 significantly reduced the percentage growth to 70% compared to the Control (P=0.001) while HC12 significantly reduced it to 80% (P=0.005). These reductions were themselves not significantly different (P=0.1446).

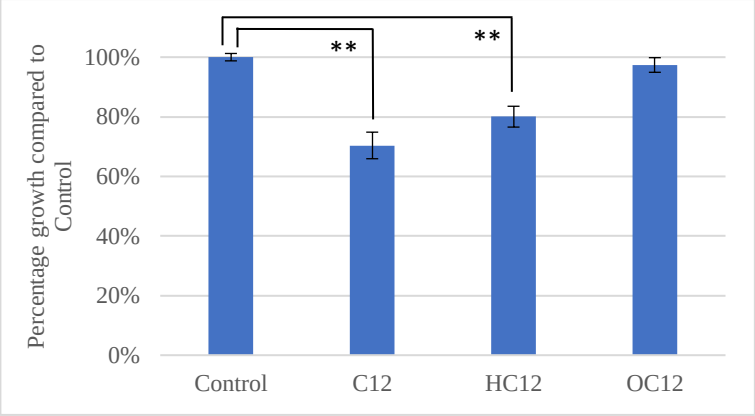

Figure 4.3 The effects of C12 variants on *Vermamoeba vermiformis* (7A) population growth. *V. vermiformis* (7A) cells (15 amoeba/cm^2) were fed with *Escherichia coli* (5 x 10^6 cells/cm^2) in the absence (Control) and presence of 300 µM C12, HC12 and OC12. Amoeba cell counts were conducted after 3 population divisions and the percentage population growth (compared to Control) was calculated. Data are presented as Average ± SEM, n=15. Statistical analyses using a post hoc tukey HSD test revealed significant results, ** = Significantly different to Control (P<0.01).

4.3.3 *Vermamoeba vermiformis* (14)

Figure 4.4 shows that *V. vermiformis* (14) was sensitive to all three variants, showing significant reductions in population growth compared to the Control, with C12 being 68% (P= 0.001), HC12 being to 70% (P=0.001) and OC12 being 77% that of the Control (P=0.001). These reductions were not themselves significantly different to each other (C12 vs HC12, P=0.8999, C12 vs OC12 P=0.1427, HC12 vs OC12 P=0.4163).

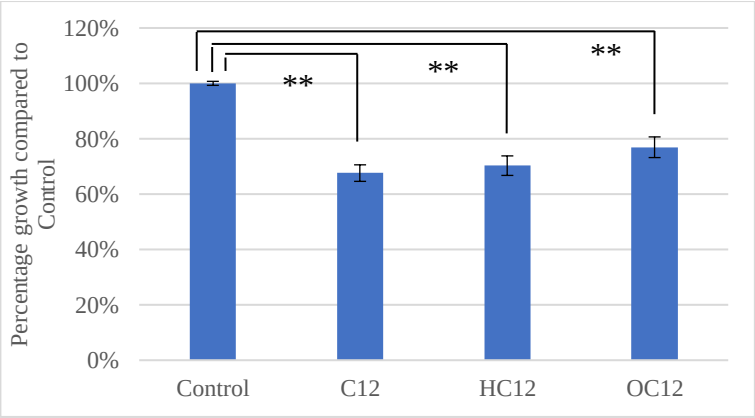

Figure 4.4 The effects of C12 variants on *Vermamoeba vermiformis* (14) population growth. *V. vermiformis* (14) cells (15 amoeba/cm^2) were fed with *Escherichia coli* (5 x 10^6 cells/cm^2) in the absence (Control) and presence of 300 µM C12, HC12 and OC12. Amoeba cell counts were conducted after 3 population divisions and the percentage population growth (compared to Control) was calculated. Data are presented as Average ± SEM n=15. Statistical analyses using a post hoc tukey HSD test revealed significant results, ** = Significantly different to Control (P<0.01).

Data therefore suggest that only *V. vermiformis* (14) was sensitive to OC12. All three strains were sensitive to C12 and HC12 either equally (the two *V. vermiformis* strains) or more so with C12 (*N. gruberi*). Further experiments focused solely on the effects of C12, as all 3 strains had the largest decrease in % population growth in the presence of this HSL.

4.4 Dose response experiments with C12

Dose response experiments (**see 3.8**) were carried out with C12 on *N. gruberi*, *V. vermiformis* (7A), *V. vermiformis* (14) and *F. arnhemensis* to determine the IC50, MIC and LD values.

4.4.1. *Naegleria gruberi*

Figure 4.5.A shows the Qti plot of percentage growth (compared to Control) against various concentrations of C12 (20 to 600 μM). *N. gruberi* exhibited a typical dose response, whereby population growth decreased as the C12 concentration (μM) increased. The IC50 was calculated as 132 ± 1.06 μM. The IC50 curve does not indicate the MIC and LD, these can be estimated from regression analysis of the linear decline in percentage population growth (**Figure 4.5.B**). A fitted line estimated the MIC as being 51 μM and the LD as 357μM.

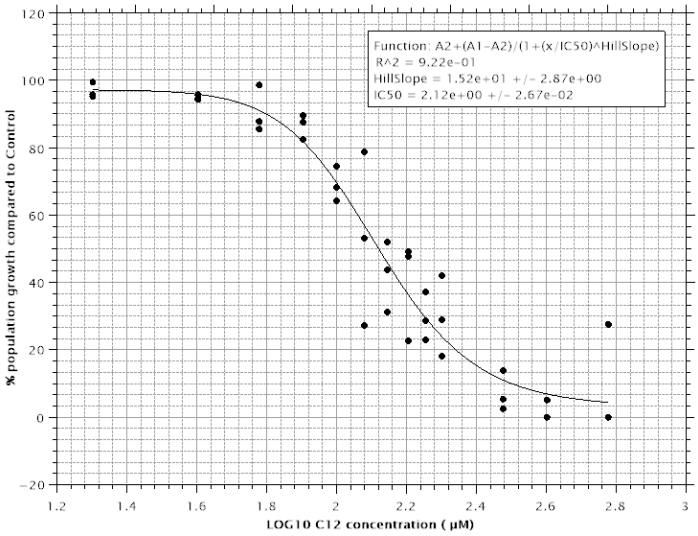

Figure 4.5.A. Qti plot of *Naegleria gruberi* C12 dose response data, showing the percentage population growth compared to Control, against LOG10 C12 concentration (μM). Dose response experiments were carried out in which *N. gruberi* cells (15 amoeba/cm^2) were fed with *Escherichia coli* (5 x 10^6 cells/cm^2) in the absence (Control) and presence of C12 (20-600 μM). Amoeba cell counts were conducted after 3 population divisions and the percentage population growth (compared to Control) was calculated.

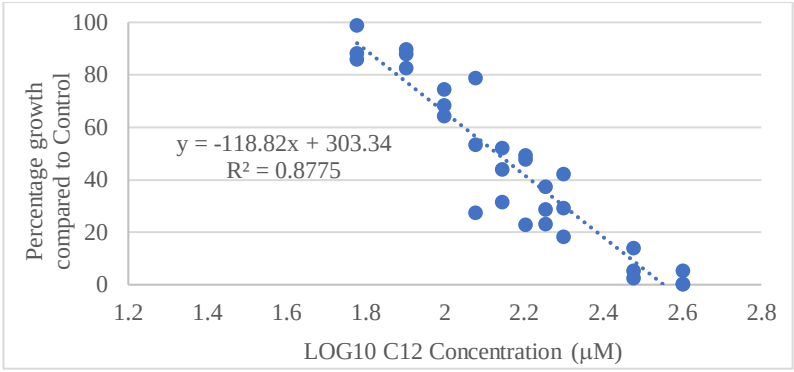

Figure 4.5.B. Linear regression analysis of dose response data for *Naegleria gruberi* with percentage population growth (compared to the Control), against LOG10 C12 concentration (µM). Dose response experiments were carried out in which *N. gruberi* cells (15 amoeba/cm^2) were fed with *Escherichia coli* (5 x 10^6 cells/cm^2) in the absence (Control) and presence of C12 (20-600 µM). Amoeba cell counts were conducted after 3 population divisions and the percentage population growth (compared to Control) was calculated.

4.4.2 *Vermamoeba vermiformis* (7A)

Figure 4.6.A shows the Qti plot of percentage growth (compared to Control) against various concentrations of C12 (20 to 300 µM). *V. vermiformis* (7A) exhibited a typical dose response, whereby *V. vermiformis* (7A) population growth decreased as the C12 concentration (µM) increased. Unfortunately, data using concentrations above 300 could not be attained due to time restrictions. Even so, the IC50 was calculated as 200 ± 1.36 µM and using regression analysis (**Figure 4.6.B**) the MIC and LD were estimated as being 69 µM and 541 µM, respectively.

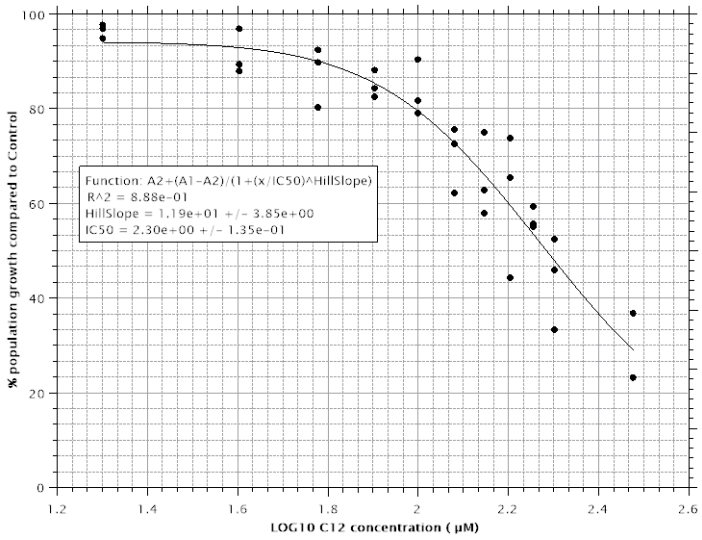

Figure 4.6.A. Qti plot of *V. vermiformis* (7A) C12 dose response data, showing the percentage population growth compared to Control, against LOG10 C12 concentration (µM). Dose response experiments were carried out in which *V. vermiformis* (7A) cells (15 amoeba/cm^2) were fed with *Escherichia coli* (5 x 10^6 cells/cm^2) in the absence (Control) and presence of C12 (20-300 µM). Amoeba cell counts were conducted after 3 population divisions and the percentage population growth (compared to Control) was calculated.

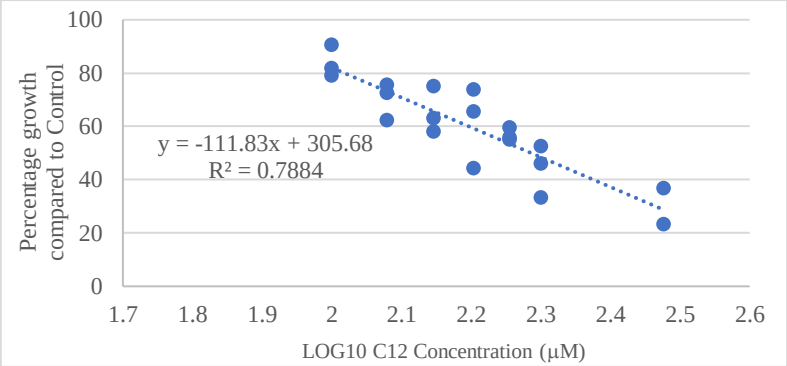

Figure 4.6.B Linear regression analysis of dose response data for *Vermamoeba vermiformis* (7A) with percentage population growth (compared to the Control) against LOG10 C12 concentration (µM). Dose response experiments were carried out in which *V. vermiformis* (7A) cells (15 amoeba/cm^2) were fed with *Escherichia coli* (5 x 10^6 cells/cm^2) in the absence (Control) and presence of C12 (20-300 µM). Amoeba cell counts were conducted after 3 population divisions and the percentage population growth (compared to Control) was calculated.

4.4.3 *Vermamoeba vermiformis* (14)

Due to time constraints, only one *V. vermiformis* (14) dose response experiment was conducted, which could not be fitted with a Qti Plot (**Figure 4.7)**. Data suggest that the effect of C12 on *V. vermiformis* (14) acts in a dose-dependent manner. The data provide estimations only for the MIC and the IC50 as being lower than 100 µM, and an estimation of the LD being between 300 µM and 400 µM.

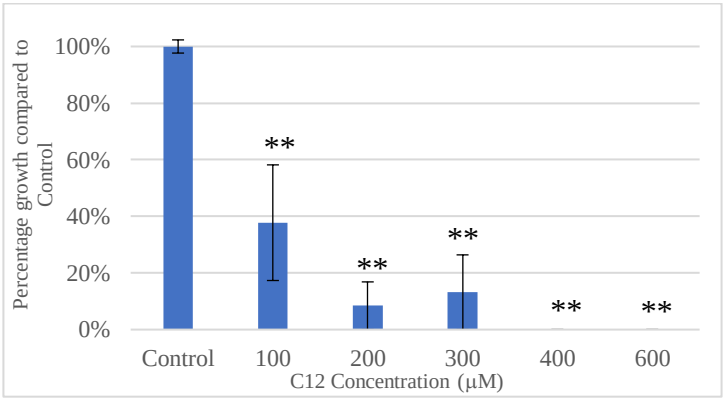

Figure 4.7. Dose response analysis from one experiment of the effects of ranging C12 concentrations from 0 µM to 600 µM on *Vermamoeba vermiformis* (14). A dose response experiment was carried out in which *V. vermiformis* (14) cells (15 amoeba/cm^2) were fed with *Escherichia coli* (5 x 10^6 cells/cm^2) in the absence (Control) and presence of C12 (100-600 µM). Amoeba cell counts were conducted after 3 population divisions and the percentage population growth (compared to Control) was calculated. Data are presented as Average ± SEM, n=5. Statistical analyses using a post hoc tukey HSD test revealed significant results, ** = Significantly different to Control (P<0.01).

4.4.4 *Flamella arnhemensis*

Data present in **Figure 4.8** suggest that the effect of C12 on *F. arnhemensis* acts in a dose-dependent manner. The data provide estimations only for the MIC and IC50 as being lower than 100 μM and the LD as higher than 400 μM, respectively. Time constraints prevented further C12 concentrations from being conducted.

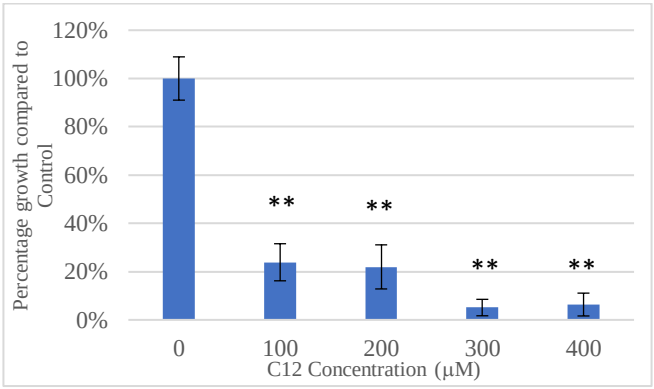

Figure 4.8. Percentage population growth of *Flamella arnhemensis* in the presence of ranging C12 concentrations. Dose response experiments were carried out in which *F. arnhemensis* (15 amoeba/cm^2) was fed with *Escherichia coli* (5 x 10^6 cells/cm^2) in the absence (Control) and presence of C12 (100-400 μM). Amoeba cell counts were conducted after 3 population divisions and the percentage population growth (compared to Control) was calculated. Data are presented as Average ± SEM, n=15. Statistical analyses using a post hoc tukey HSD test revealed significant results, ** = Significantly different to Control (P<0.01).

4.4.5 Summary of dose-response experiments

All amoeba strains tested, shown in **Table 4.2,** had an (estimated or determined) MIC value lower than 100 μM, and all LD values (estimated or determined) were higher than 300 μM.

Table 4.2. The MIC, IC50 and LD values (μM) of C12 with *N. gruberi, V. vermiformis* (7A), *V. vermiformis* (14) and *F. arnhemensis*. *N. gruberi* and *V. vermiformis* (7A) values were determined by Qti Plot and linear regression analysis. *V. vermiformis* (14) and *F. arnhemensis* values were estimated based on percentage population growth (compared to Control) and post hoc tukey HSD test significance.

Strain	MIC (μM)	IC50 (μM)	LD (μM)
N. gruberi	51	132	357
V. vermiformis (7A)	69	200	541
V. vermiformis (14)	<100	<100	300-400
F. arnhemensis	<100	<100	>400

V. vermiformis (14) appears to have a level of sensitivity similar to that of *N. gruberi* rather than *V. vermiformis* (7A) as their MIC and LD values are closer (**Table 4.2**). Similarly, *F. arnhemensis* has MIC and IC50 estimates similar to *N. gruberi*, compared to those of *V. vermiformis* (7A), however the LD estimate of more than 400 µM suggests that this parameter is closer to *V. vermiformis* (7A). However, the values for *V. vermiformis* (14) and *F. arnhemensis* are only estimates and further experimentation, with a wider range of C12 concentrations and subsequent analysis with Qti Plot and linear regression, is required to calculate the true values.

4.5 Effect of C12 on population growth

4.5.1 Population growth analysis

Daily counts during the *V. vermiformis* (14) dose response experiment allowed a preliminary evaluation of <u>when</u> C12 caused an effect, which then resulted in the observed reduction in population density (see **3.8.1**). **Figure 4.9** shows that there was an instantaneous (and significant) loss of cells at day 0 (by 20 minutes after drying) at the higher concentrations of 200, 300 and 400 µM.

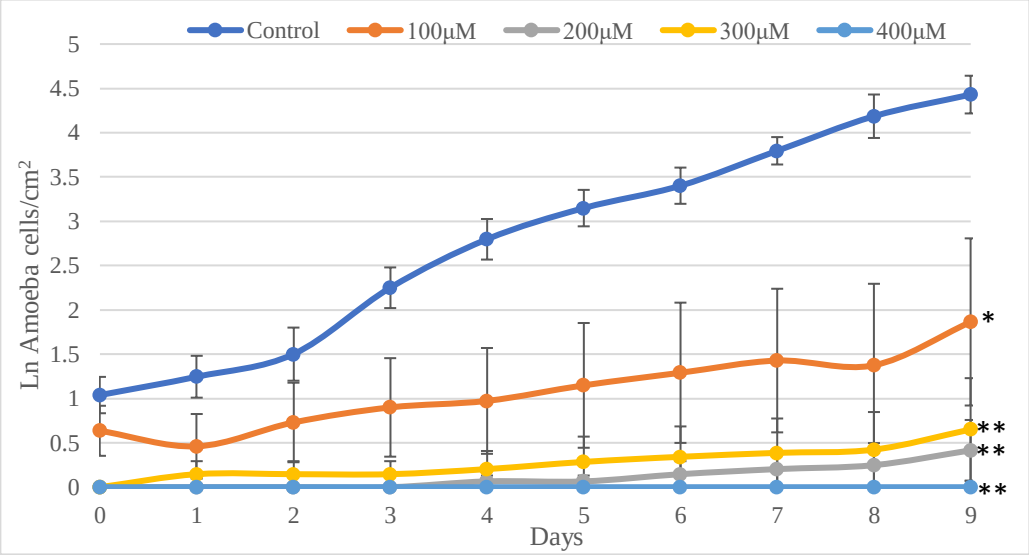

Figure 4.9. Comparison of the natural log of *Vermamoeba vermiformis* (14) against time (days), in the presence of C12 at 0, 100, 200, 300 and 400 µM. A dose response experiment was carried out in which *V. vermiformis* (14) cells (15 amoeba/cm^2) were fed with *Escherichia coli* (5 x 10^6 cells/cm^2) in the absence (Control) and presence of C12 (100-400 µM). Amoeba cells were counted daily for 9 days and the Ln amoeba cells/cm^2 was calculated. Data are presented as Average ± SEM, n=5. Significant results compared to Control (determined by post hoc tukey HSD test) at day 9 are shown. * = Significantly different to Control (P<0.05), ** = Significantly different to Control (P<0.01).

With 200 and 300 μM, the population started to increase after 3 days, suggesting the amoeba was below the detection limit of 1 cell/grid at day 0, rather than C12 being lethal to the whole population (which was observed at 400 μM). Although there was some instantaneous reduction in cell concentration with 100 μM C12, this was not significant, but the population did appear to have a 2-day lag period before positive growth of the population was observed (**Figure 4.9**). Population growth appeared slower, compared to the Control, in the presence of 100 μM C12 and this treatment was significantly different to the Control on day 3 ($P=0.019$); whereas other treatments were significantly different to the Control from day 0 ($P<0.01$ in all 3 treatments). For P values comparing all treatments to the Control, at all time points, **see Table B** (**Appendix II**).

4.5.2 Comparing growth rate as doubling time and lag phase

Data from **Figure 4.9** were used to estimate amoebic doubling times and lag phases in the presence of C12 (0-300 μM) (see **3.8.1**). **Figure 4.10** shows that the Control had a lag phase of ~1 day and a doubling time of ~2 days. With 100 μM, the lag phase and doubling times increased to ~2 days and ~5 days, respectively. At 200 and 300 μM, the lag phase and doubling time increased again to ~3 days and ~10 days, respectively.

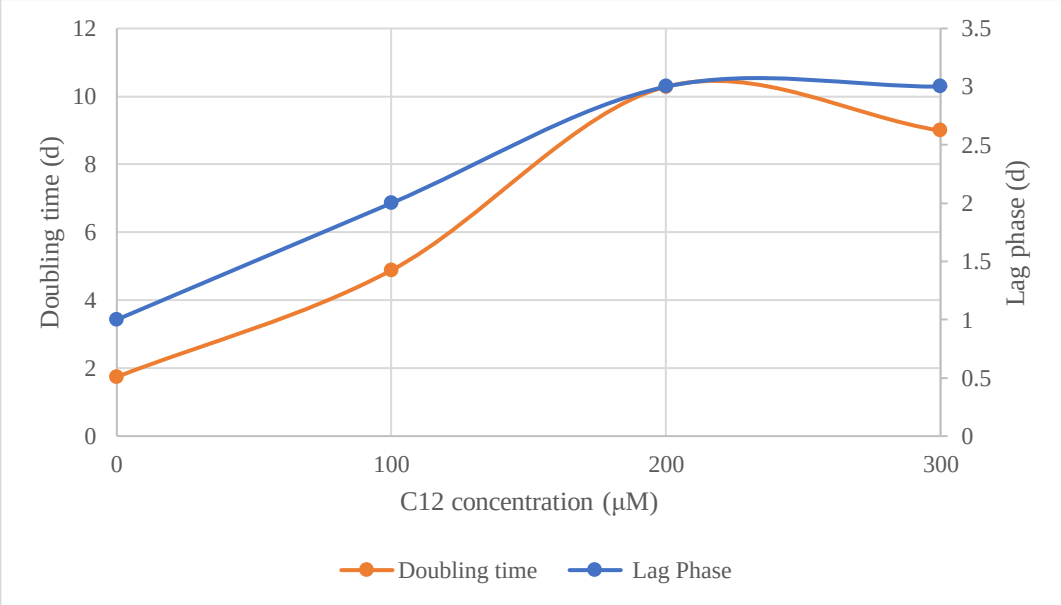

Figure 4.10 Relationship between C12 concentration and (i) lag phase (days) and (ii) the doubling time (days) of *V. vermiformis* (14). A dose response experiment was carried out in which *V. vermiformis* (14) cells (15 amoeba/cm^2) were fed with *Escherichia coli* (5 x 10^6 cells/cm^2) in the absence (Control) and presence of C12 (100-400 μM). Amoeba cell counts were conducted after 3 population divisions and Ln amoeba cells/cm^2 was calculated. The doubling time and the Lag phase were then calculated.

These preliminary data suggest that C12 initially causes dose-dependent growth arrest (lag phase) followed by a reduced growth rate (giving rise to longer doubling times than seen with the Control).

4.6 Receptor blocking

N. gruberi and *V. vermiformis* (7A) were subjected to receptor blocking experiments, see **3.9**.

4.6.1 PPAR, TRPV1 and Adenosine A2 receptor blocking

The blocking of PPARs, TRPV1 and Adenosine (A2) receptors was conducted on *N. gruberi* using GW9662 (GW), Capsazepine (Cap) and ZM241385 (ZM), respectively (**Figure 4.11**). Only PPARs and TRPV1 were blocked in *V. vermiformis* (7A) due to time constraints (**Figure 4.12**).

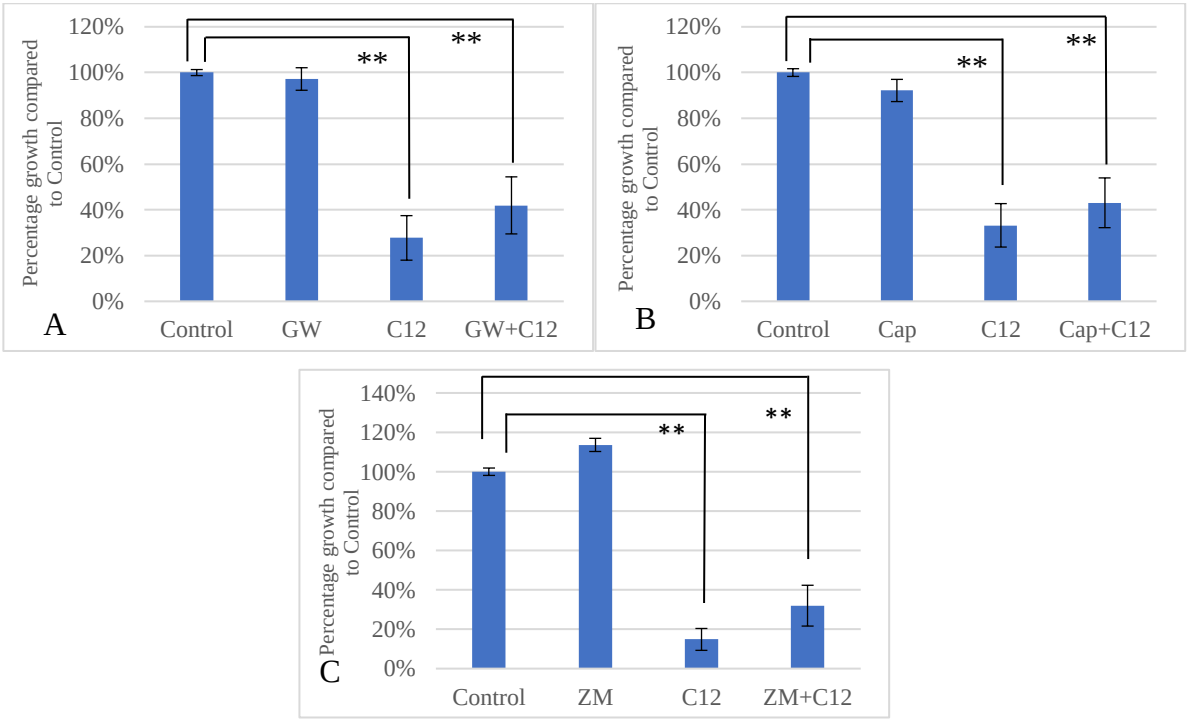

Figure 4.11. The effects of 10 µM of GW9662 (A), 10 µM of Capsazepine (B) and 10 µM of ZM241385 (C) on the percentage population growth (compared to Control) of *Naegleria gruberi* in the presence and absence of 300 µM of C12. GW9662 (GW), Capsazepine (Cap) and ZM241385 (ZM) were allowed to block *N. gruberi* cells for 30 minutes after which 'blocked' and 'unblocked' *N. gruberi* cells (15 amoeba/cm^2) were fed with *Escherichia coli* (5 x 10^6 cells/cm^2) in the absence (Control) and presence of C12 at 300 µM. Amoeba cell counts were conducted after 3 population divisions and the percentage population growth (compared to Control) was calculated. Data are presented as Average ± SEM, n=15. Statistical analyses using a post hoc tukey HSD test revealed significant results, ** = Significantly different to Control (P<0.01).

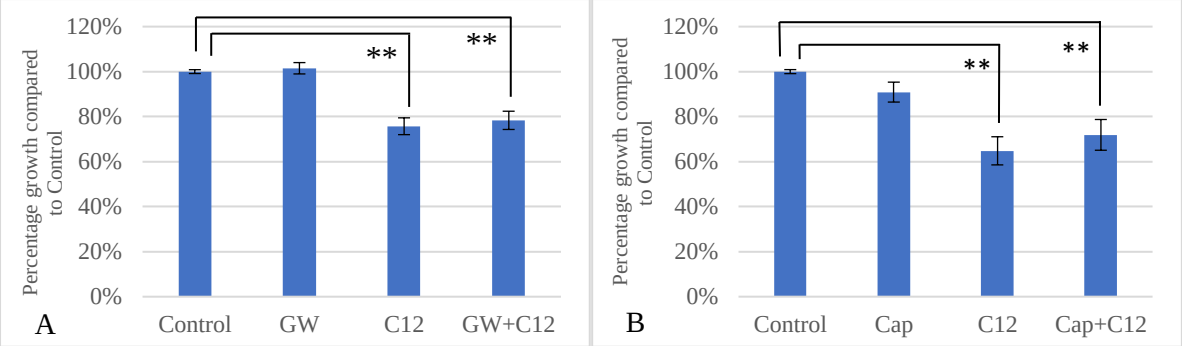

Figure 4.12. The effect of 10 µM of GW9662 (A) and 10 µM of Capsazepine (B) on the percentage population growth of *Vermamoeba vermiformis* (7A) in the presence and absence of 300 µM of C12. GW9662 (GW) and Capsazepine (Cap) were allowed to block *V. vermiformis* (7A) cells for 30 minutes after which 'blocked' and 'unblocked' *V. vermiformis* (7A) cells (15 amoeba/cm^2) were fed with *Escherichia coli* (5 x 10^6 cells/cm^2) in the absence (Control) and presence of C12 at 300 µM. Amoeba cell counts were conducted after 3 population divisions and the percentage population growth (compared to Control) was calculated. Data are presented as Average ± SEM, n=15. Statistical analyses using a post hoc tukey HSD test revealed significant results, ** = Significantly different to Control, ($P<0.01$).

Figures 4.11 and 4.12 show that GW and Cap did not alleviate the negative effect of C12 in either *N. gruberi* (42% and 43% growth, respectively) or *V. vermiformis* (7A) (78% and 72% growth respectively), suggesting that PPARs and TRPV1 are not involved in the interaction with C12 in either amoeba strain. ZM did not alleviate the negative effect of C12 on *N. gruberi* (32% growth) (**Figure 4.11**), suggesting that A2 is not involved in *N. gruberi*-C12 interaction.

4.6.2 Dopamine and Serotonin Blocking

Haloperidol hydrochloride (Halo) blocks both serotonin and dopamine receptors. Pertussis Toxin (PTX) blocks receptors Dopamine D2, Serotonin 5-HT1A and other $G_{i/o}$ and G_t-GPCRs. SCH23390 hydrochloride (SCH) blocks Dopamine D1 receptors and EMD281014 hydrochloride (EMD) blocks Serotonin 5-HT2A receptors. All 4 blockers were tested against *N. gruberi* (**Figure 4.13**) while only Halo and PTX were tested against *V. vermiformis* (7A) due to time constraints (**Figure 4.14**).

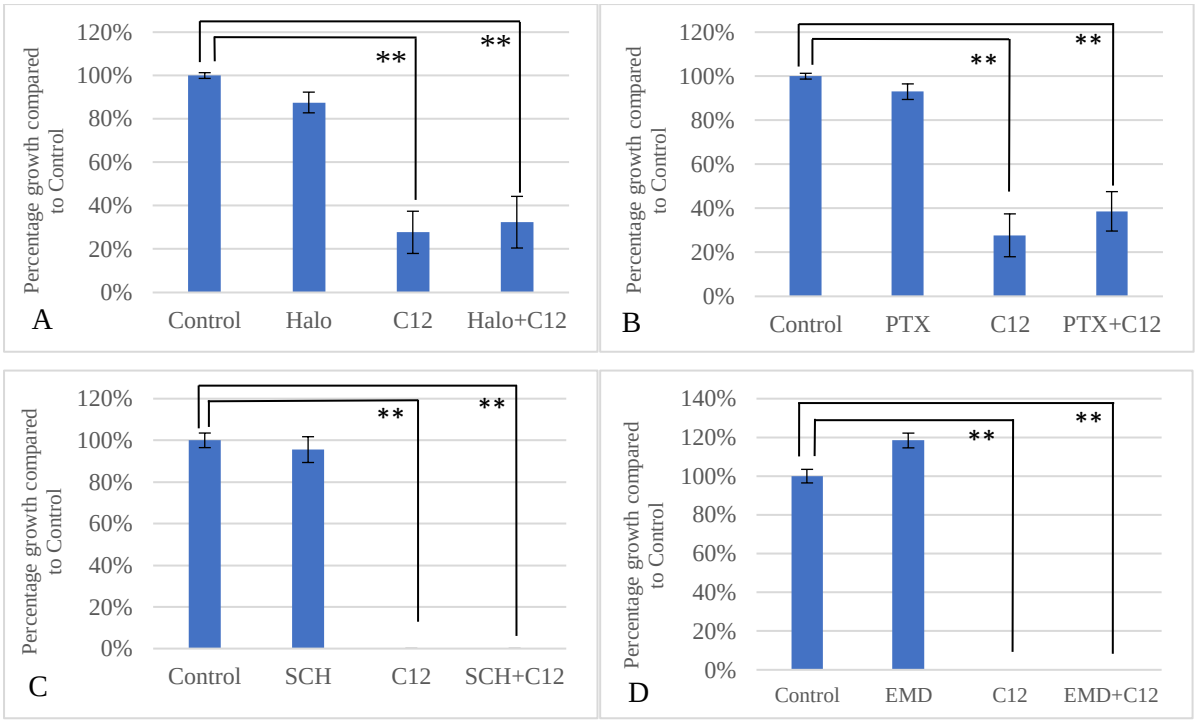

Figure 4.13 The effect of 10 µM of Haloperidol hydrochloride (A), 100 ng/mL of Pertussis Toxin (B), 10 µM of SCH23390 (C) and 10 µM of EMD281014 (D) on the percentage population growth of *Naegleria gruberi* in the presence and absence of 300 µM of C12. Haloperidol Hydrochloride (Halo), Pertussis Toxin (PTX), SCH23390 (SCH) and EMD281014 (EMD) were allowed to block *N. gruberi* cells for 30 minutes (5 h for PTX) after which 'blocked' and 'unblocked' *N. gruberi* cells (15 amoeba/cm^2) were fed with *Escherichia coli* (5 x 10^6 cells/cm^2) in the absence (Control) and presence of C12 at 300 µM. Amoeba cell counts were conducted after 3 population divisions and percentage population growth (compared to Control) was calculated. Data are presented as Average ± SEM, n=15; Halo and PTX, n=5; SCH and EMD. Statistical analyses using a post hoc tukey HSD test revealed significant results, ** = Significantly different to Control (P<0.01).

Figures 4.13 and 4.14 both show that blockers Halo and PTX could not alleviate the negative effect of C12 in neither *N. gruberi* (32% and 39% growth, respectively) nor *V. vermiformis* (7A) (76% and 75% growth, respectively). This suggests that Serotonin & Dopamine receptors, and other $G_{i/o}$ and G_t-GPCRs, are not involved in the C12 interaction with either amoeba strain. **Figure 4.13** shows that SCH and EMD did not alleviate the negative effect of C12 on *N. gruberi* (0% growth, compared to Control), suggesting that dopamine receptor D1 and serotonin receptor 5-HT2A are not involved in the *N. gruberi*-C12 interaction.

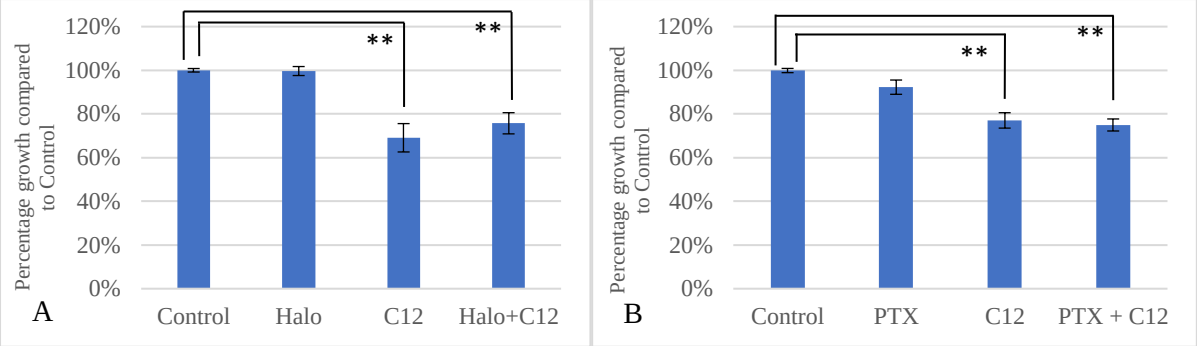

Figure 4.14 The effect of 10 µM of Haloperidol hydrochloride (A) and 100 ng/mL of Pertussis toxin (B) on the percentage population growth of *Vermamoeba vermiformis* (7A) in the presence and absence of 300 µM of C12. Haloperidol Hydrochloride (Halo) and Pertussis Toxin (PTX) were allowed to block *V. vermiformis* (7A) cells for 30 minutes and 5h, respectively after which 'blocked' and 'unblocked' *V. vermiformis* (7A) cells (15 amoeba/cm^2) were fed with *Escherichia coli* (5 x 10^6 cells/cm^2) in the absence (Control) and presence of C12 at 300 µM. Amoeba cell counts were conducted after 3 population divisions and the percentage population growth (compared to Control) was calculated. Data are presented as Average ± SEM, n=15. Statistical analyses using a post hoc tukey HSD test revealed significant results, ** = Significantly different to Control, ($P<0.01$).

4.6.3 GPCR Blocking

4.6.3.1. Blocking of all GPCRs with Gallein

Gallein (Gal) inhibits the βγ complex in GPCRs and is therefore considered to block all GPCRs. Gal blocking was performed on *N. gruberi* and *V. vermiformis* (7A) and was found (like all the other blockers) not to be toxic to *N. gruberi* (**Figure 4.15**) and *V. vermiformis* (7A) **(Figure 4.16**) (P=0.8999, compared to Control with both amoebae strains).

Figure 4.15 shows there was a significant reduction in percentage population growth of *N. gruberi* and *V. vermiformis* (7A) in the C12 treatment and although Gal alleviated some of this effect, it was not at 100% effective, since significant differences still remained between % growth with C12+Gal and the Control and Gal alone. This suggests that at 10 µM Gal partially blocks the amoeba-C12 interaction and that some form of GPCR may be involved in the interaction.

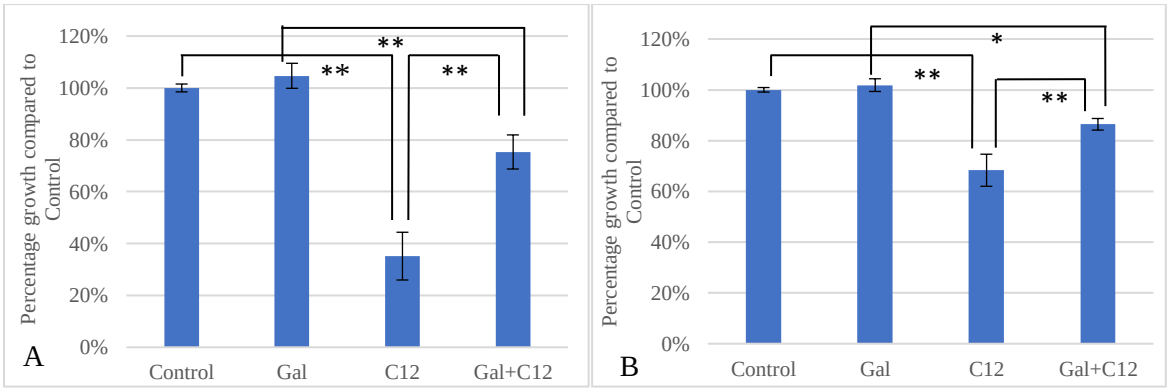

Figure 4.15 The effect of 10 µM of Gallein (Gal) on the percentage population growth of (A) *Naegleria gruberi* and (B) *V. vermiformis* (7A) in the presence and absence of 300 µM of C12. Gal was left to block amoeba cells for 30 minutes after which 'blocked' and 'unblocked' amoeba (15 amoeba/cm^2) were fed with *Escherichia coli* (5 x 10^6 cells/cm^2) in the absence (Control) and presence of C12 at 300 µM. Amoeba cell counts were conducted after 3 population divisions and the percentage population growth (compared to Control) was calculated. Data are presented as Average ± SEM, n=15. Statistical analyses using a post hoc tukey HSD test revealed significant results, * = Significant Difference (P<0.05), ** = Significant Difference (P<0.01).

4.6.3.2. Blocking of specific GPCR subtypes

Since treatment with Gal (**4.6.3.1**) indicated that GPCRs were involved in the interaction between C12 and both *N. gruberi* and *V. vermiformis* (7A), different subtypes of GPCRs were inspected for their contribution to this.

4.6.3.2.1. Blocking of $G_{i/o}$ and G_t-GPCRs

Pertussis Toxin (PTX) is not only an antagonist of the Dopamine D2 receptor and the Serotonin 5-HT1A receptor (see **4.6.2**) but is considered an antagonist of all $G_{i/o}$ and G_t-GPCRs. Results from PTX blocking experiments with *N. gruberi* (**Figure 4.13.B**) and *V. vermiformis* (**Figure 4.14.B**), whereby PTX did not block the effect of C12, suggest that $G_{i/o}$ and G_t-GPCRs are not involved in the amoeba-C12 interaction.

4.6.3.2.2. Blocking of G_s-GPCRs

Melittin (Mel) inhibits G_s-GPCRs and the normal working concentration is less than 1 µM (Sommer et al., 2012; Jamasbi et al., 2014; Kreinest et al., 2020). However, this antagonist has proven to be toxic to multiple cell types and model membranes at high concentrations (Jamasbi et al., 2014; Feng et al., 2020), including to the ciliate *Tetrahymena pyriformis* by a fellow researcher at Lancaster and so, Tims (2021) had used a working concentration of 0.3 µM instead. Toxicity tests were therefore performed on both *N. gruberi* and *V. vermiformis* (7A).

Figure 4.16 indicates no significant negative effect of melittin on the percentage population growths of *N. gruberi* and *V. vermiformis* (7A).

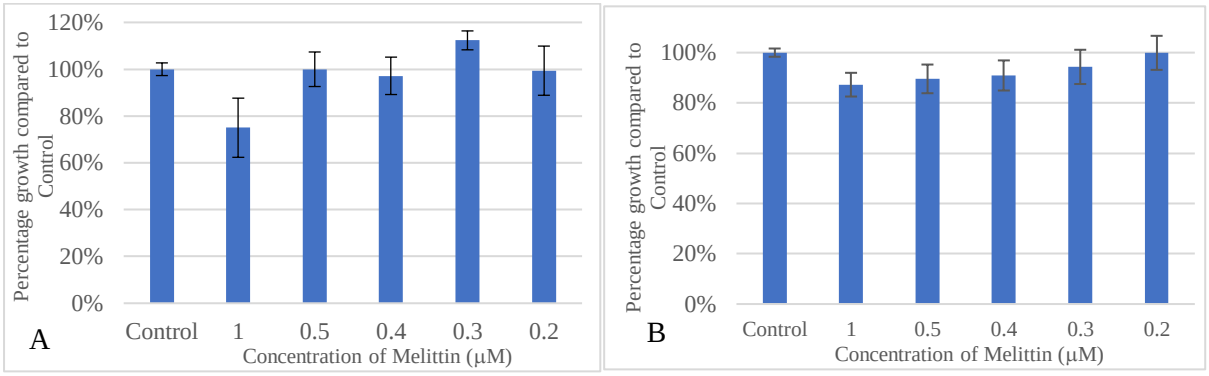

Figure 4.16. Melittin dose response with *Naegleria gruberi* (A) and *Vermamoeba vermiformis* (7A) (B) to assess potential toxicity. Dose response experiments were carried out in which amoeba cells (15 amoeba/cm^2) were fed with *Escherichia coli* (5 x 10^6 cells/cm^2) in the absence of melittin (Control) and after 30-minute exposure to melittin (0.2 to 1 μM). Amoeba cell counts were conducted after 3 population divisions and percentage population growth (compared to Control) was calculated. Data are presented as Average ± SEM, n=15 (A), n=20 (B). Statistical analysis by One-way ANOVA, P = 0.0662 (A) and P = 0.4584 (B).

The next stage of the research was to test whether Melittin could block the negative effect of C12 action against both amoebae, but time constraints prevented this from being carried out.

5. Discussion

5.1 Summary of major findings

The aim of this project was to evaluate the susceptibility of various amoebae to the HSLs C4, C6, C8, C10, and C12. Then with those that were susceptible to: (i) Evaluate their sensitivity to C12 variants (C12, HC12, OC12), (ii) determine the Minimum Inhibitory Concentration (MIC), Inhibitory Concentration at 50% (IC50) and the Lethal Dose (LD) of the HSLs, (iii) evaluate what the eukaryotic HSL receptor might be and, (iv) assess how the HSL might be affecting amoebic physiology/behaviour.

Seventeen amoeba strains (15 species) were tested against HSLs C4-C12 to determine their sensitivity. Five of those amoebae, *Naegleria gruberi, Vermamoeba vermiformis* (7A), *Vermamoeba vermiformis* (14), *Echinamoeba silvestris* and *Flamella arnhemensis*, exhibited a significant degree of sensitivity (i.e. a reduced population growth) to one HSL in particular, C12. Two amoebae exhibited dual HSL sensitivity with *E. silvestris* also sensitive to C6 and *V. vermiformis* (14) also sensitive to C10.

Further work with *N. gruberi, V. vermiformis* (7A) and *V. vermiformis* (14) showed that all three were sensitive to C12 and HC12 with *V. vermiformis* (7A) and (14) being equally sensitive to C12 and HC12, whereas *N. gruberi* was more sensitive to C12. Only *V. vermiformis* (14) was sensitive to OC12. Their MICs with C12 were all <100 μM, while their IC50s were 132, 200 and <100 μM for *N. gruberi*, *V. vermiformis* (7A) and *V. vermiformis* (14), respectively. The LD was >300 μM in all cases.

N. gruberi and *V. vermiformis* (7A) were both tested against a range of receptor antagonists in the presence/absence of C12. Both strains showed that the blocking of PPARs, TRPV1 and the Serotonin, Dopamine and Adenosine receptors, did not alleviate the negative effect of C12 However, the blocking of all GPCRs (using Gallein) did block the C12 action in both amoebae. Further work aimed to characterise which type of GPCR might be responsible. Blocking with PTX showed no alleviation of the C12 effect, therefore suggesting that $G_{i/o}$ and G_t GPCRs were not involved. Time constrains prevented the testing of further GPCR sub-types (*but later work has shown that the likely candidate(s) are members of the G_s GPCR group*).

With regards to the physiological effects of C12 on amoebae, a preliminary experiment with *V. vermiformis* (14) suggested that C12 acted in two ways and caused instantaneous cell death at high concentration and population growth inhibition at lower concentrations.

5.2. Sensitive amoeba species

Representative amoebae from across the phylogenetic tree (**Figure 5.1**) were tested against HSLs. These included members of the two sub-phyla of Amoebozoa (**Figure 5.1a**) and those naked amoebae that reside within the sub-phylum Percolozoa (**Figure 5.1.b**). The latter is part of the Excavata which is a sub-group of unicellular organisms that are within the domain Eukaryota (Simpson, 2003). The amoebae placed in this sub-group have a flagellate stage as part of their lifecycle, usually with 2 or 4 flagella (Simpson, 2003). Of the 4 genera tested within this sub-phylum, only *Naegleria* showed sensitivity to C12 (**Figure 5.1.b**).

Within the phylum Amoebozoa, two genera from the sub-phylum Conosa were tested. *Flamella* was sensitive to C12 whereas *Phalasterium* was not sensitive to any HSL (**Figure 5.1.a**). Four genera from the sub-phylum Lobosa, class Discosea (*Vannella, Vexillifera, Acanthamoeba* and *Cochliopodium*) also showed no sensitivity to HSLs (**Figure 5.1.a**). Within the class Tubulinea, both genera belonging to the order Echinamoebida exhibited sensitivity to at least one of the HSLs (*Echinamoeba* and *Vermamoeba*) while 3 strains of *Hartmannella/ Saccamoeba* did not (**Figure 5.1.a**). The latter result is interesting because, pre-2011, *V. vermiformis* had been classified as *Hartmannella vermiformis.* The obvious difference in HSL susceptibility between the two genera, together with *V. vermiformis* HSL susceptibility being similar to that of *Echinamoeba,* now lends further weight to the reclassification performed by Smirnov et al. (2011).

This author could only find one publication which suggests amoebae respond to HSLs. Cosson et al. (2002) found that the population growth of the slime mould *Dictyostelium discoideum* (which has an amoeba stage in its life cycle, **Figure 5.2a**) was reduced in the presence of wild-type *Pseudomonas aeruginosa* (OC12 and C4 positive) but increased in the presence of a *las* mutant (OC12 negative) and more so with the *rhl* mutant (C4 negative). Although not a 'true' amoeba (because it does not produce cysts upon starvation [**Figure 5.2b**], but instead, produces a migrating slug [**Figure 5.2a**] [Bozzaro, 2013]), it is a member of the Conosa, class Mycetozoa (**Figure 5.1a**). However, this 'amoeba' appears to respond negatively to the short-chained C4, whereas all 17 amoeba strains tested in the current student did not (**Table 4.1**). Considering that *D. discoideum* is considered to be the 'model' amoeba, and is intensively studied, it does not appear to correctly represent the 'true' amoebae with regards to HSL susceptibility.

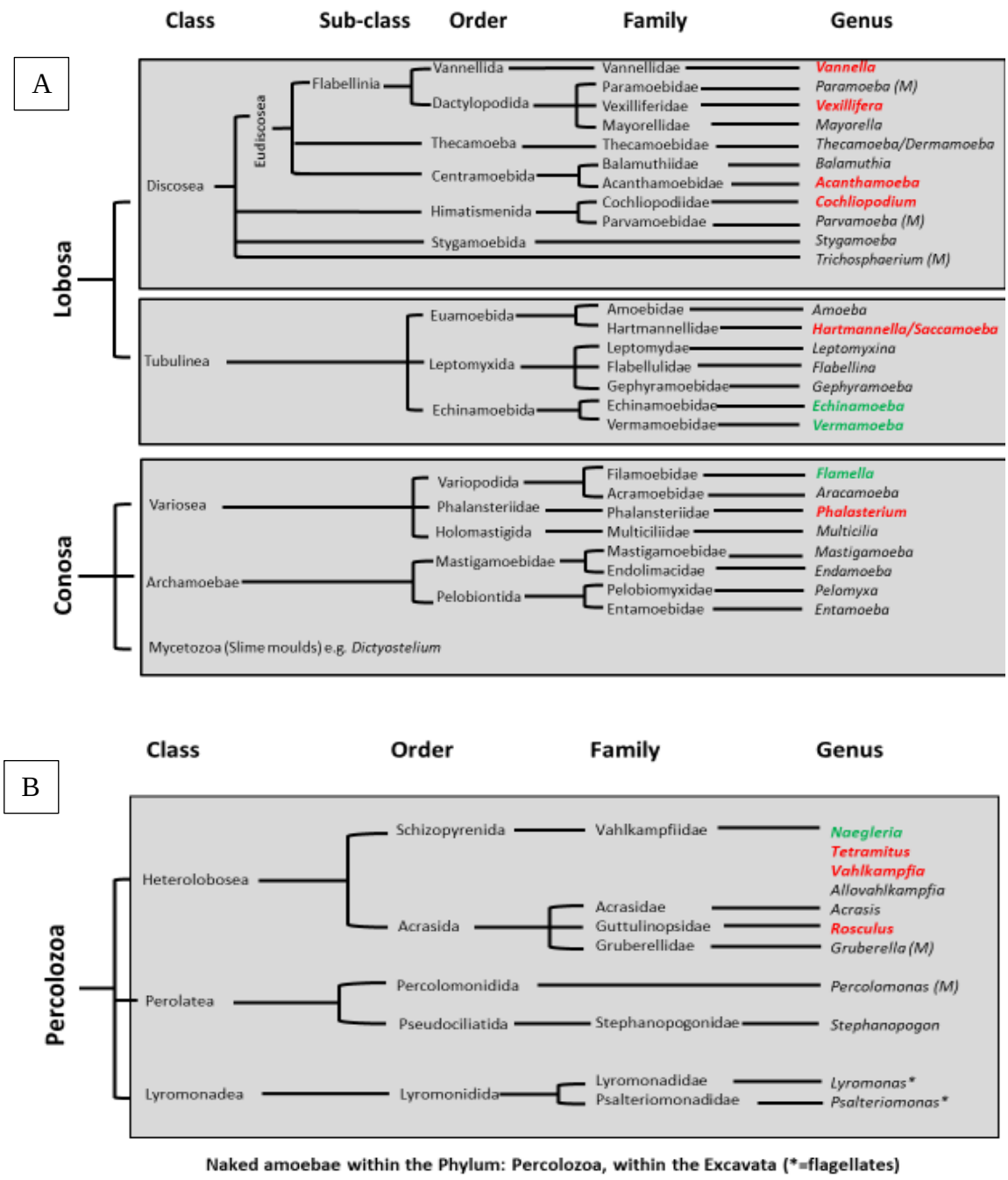

Figure 5.1. Phylogenetic trees of the phylum Amoebozoa; sub-phyla Conosa and Lobosa **(A),** and the naked amoebae that reside within the phylum of Percolozoa, within the Excavata **(B)**. Excavata is a sub-group within the Eukaryota domain. Species within the Excavata are classified based on flagellate structure. Amoebae within this grouping have both amoeboid and flagellate stages to their lifecycles. Amoebae genera that were tested in this study are shown by green and red font colours. Green indicates the HSL sensitive genera (to at least 1 HSL), red indicates those genera that were not HSL sensitive. *(M)*= marine species only. *= obligate flagellates.

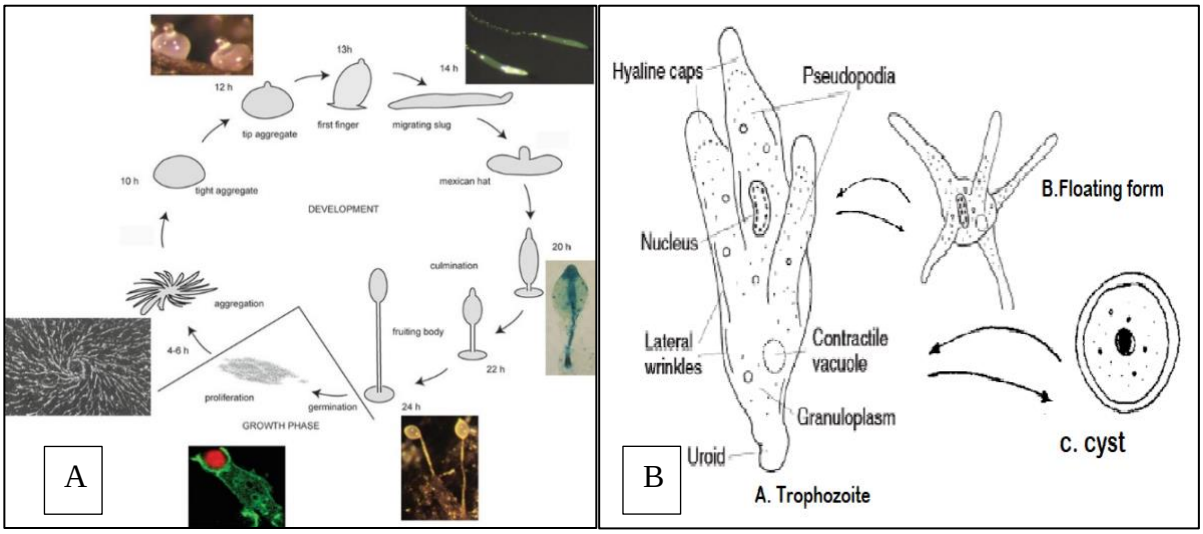

Figure 5.2. (A) Life cycle of *Dictyostelium discoideum*. The life cycle of *D. discoideum* consists of two phases, growth phase and development. Unicellular amoebae cells feed on bacteria and proliferate by binary fission. Starvation triggers development, leading to aggregation, and transformation into migrating slugs, and a fruiting body. Figure taken from Bozzaro (2013). **(B)** *Amoeba proteus* life cycle stages, taken from Al-Hammadi (2020).

In the current study, the four sensitive genera resided within three sub-phyla which suggests that phylogenetic relatedness plays no role in their HSL sensitivity. This is similar to the conclusion made by Al-Hammadi (2020) when examining amoeba sensitivity to another long chain lipid, Cannabidiol (CBD). In her study, more amoebae were sensitive to CBD (than they were to HSLs here), i.e., *Acanthamoeba castellanii*, *Hartmannella cantabrigiensis*, *Vahlkampfia avara*, *N. gruberi*, *F. arnhemensis* and *V. vermiformis*. Interestingly, *E. silvestris* was not sensitive to CBD but was sensitive to HSLs (**Figure 5.1a**). Even so, in her study all CBD-sensitive strains spanned four sub-phyla and no link to phylogenetic relatedness could be found and there was also no obvious link with the location (and date) from where the amoebae were isolated (Al-Hammadi, 2020).

It is therefore currently unclear as to why certain amoebae are sensitive to HSLs while some are not. This is addressed further in 5.4 after a comparison of how amoebic sensitivity to C12 (and its variants) compares with the sensitivity demonstrated by other eukaryotic cell types.

5.3. Amoebic C12-sensitivity

All five sensitive amoebae responded negatively to C12. The MIC, IC50 and LD values were determined for two strains (*N. gruberi* and *V. vermiformis* [7A]) and estimated for another two (*V. vermiformis* [14] and *F. arnhemensis*) (**Table 4.2**). Data revealed inter-strain differences with regards to IC50 values, however two features were common to all four strains, i.e., their

MIC values were <100 μM and their LD values were >300 μM. Comparison of these data with those of other eukaryotic cells with C12 is difficult, as most studies have used OC12 as the sole HSL in experiments (see below). This author could find only one publication (Chhabra et al., 2003) which stated that C12 reduced murine (BALB/c) splenocyte proliferation with an IC50 value of 52 μM. Although lower than the calculated IC50s for *N. gruberi* and *V. vermiformis* (7A) (132 and 200 μM, respectively), further work on *V. vermiformis* (14) and *F. arnhemensis* might show more similarity with this published IC50 value as both have estimated IC50 values <100 μM.

As previously stated, most published work has concentrated on OC12, possibly because OC12 is produced by *P. aeruginosa* which is an opportunistic pathogen of particular research interest (de Bentzmann and Plésiat, 2011; Turkina and Vikström, 2019). In the current study, three strains were tested against the three C12 variants (C12, OC12 and HC12). *N. gruberi*, *V. vermiformis* (7A) and *V. vermiformis* (14) were all sensitive to HC12 in addition to C12 with both *V. vermiformis* strains being equally sensitive to C12 and HC12, while *N. gruberi* was more sensitive to C12. Surprisingly, only *V. vermiformis* (14) was sensitive to OC12. This difference between *V. vermiformis* strains was unexpected particularly because these amoebae are the most closely related strains out of all the HSL-sensitive amoebae tested. However, *V. vermiformis* (14) was also sensitive to C10 while *V. vermiformis* (7A) was not (**Table 4.1**). This result further substantiates that phylogenetic relatedness is not closely linked with the presence of, and/or, degree of HSL sensitivity in amoebae.

Unfortunately, the MIC, IC50 and LD values for OC12 with *V. vermiformis* (14) were not determined in the current study. However, its response to OC12 (at 300 μM) was not significantly different to its response to C12 (**Figure 4.4**) which infers that their parameter values might also be equivalent, i.e., MIC <100 μM, IC50 <100 and LD >300<400 μM (as determined with C12, **Figure 4.7**). Comparison of these estimated values with those for OC12 in the literature was more fruitful, although most papers do not state MIC, IC50 or LD values and have not been included below.

A number of studies have tested OC12 on the inhibition of human peripheral blood mononuclear cells (PBMCs) proliferation and recorded IC50 values ranging from 10 to 60 μM (Chhabra et al., 2003; Hooi et al., 2004; Huynh, 2008). OC12 also inhibited the release of IL-1 and IL-2 in PBMCs, with IC50 values of 18 and 4 μM respectively (Hooi et al., 2004; Huynh,

2008). Inhibition of IL-2 release has also been recorded in anti-CD3/anti-CD28 antibody activated T cells at an IC50 value of 49 μM (Hooi et al., 2004). Data on OC12 MIC values are rarer, but some are available for macrophages and mast cells. Both Tateda et al. (2003) and Zhang et al. (2014) recorded a MIC of >6<12 μM with bone derived and blood-derived macrophages, respectively (IC50s were 25 and >12<25 μM, respectively). Li et al. (2009) recorded a MIC of 25-50 μM with mast cells (IC50 50-100 μM), whilst Taguchi et al. (2014) suggested a MIC of 10 μM on cell viability and apoptosis of Caco-2 cells (IC50 ≥100 μM). Most recently, OC12 was found to reduce the viability of mice epithelial cells (CT-26) with a suggested MIC of 200 μM (Tao et al., 2021).

All published OC12 MIC values therefore lie between 6 and 50 μM, with the exception of Tao et al. (2021), whilst IC50 values lie between 10 and 100 μM which correlates with the response of *V. vermiformis* (14) to OC12 (both parameter values at <100 μM). Although difficult to extrapolate to the amoebic response to C12, values recorded in the current study are in the same ballpark as published values, which suggests that the response of amoebae to HSLs might be similar in nature to that of other eukaryotic cells. However, the lack of studies on HSLs other than OC12 on other cell types does hinder the comparison somewhat.

This author found only one publication (Chhabra et al., 2003) which directly compared the effect of C12, OC12 and HC12 (on murine splenocyte proliferation) and found that IC50 values did differ (52, 4 and 12.5 μM, respectively) suggesting that OC12 is far more potent than HC12, which itself is more potent than C12. Another publication (Khambati et al., 2017) found that OC12 (at 10 μM) inhibited mast cell degranulation and the release of Tumour Necrosis Factor (TNF) and Cysteinyl Leukotrienes (CysLT), but that 100 μM of C12 was required to induce the same response. In addition, Song et al. (2019) found that OC12 induced greater apoptosis in CD4+ T cells than C12. These few studies contradict the findings of the current study whereby C12 was either equally or more effective than HC12, and two out of three strains did not respond to OC12 at all. So, what else is known about the difference between these three C12 variants?

C12 is the most stable variant in alkaline environments (Tait and Havenhand, 2013) where the high pH leads to both pH-mediated lactonolysis and the "Claisen-like" rearrangement. For example, seawater has an alkaline pH which can result in hydrolysis of the homoserine lactone ring. This process is known as base-catalysed lactonolysis and causes an open ring structure,

which turns HSLs into homoserines (HS) that cannot function as biologically active molecules (Joint et al., 2002; Yates et al., 2002; Kaufmann et al., 2005; Williams, 2007). This has been shown to be a particularly problematic with oxo- and hydroxy- variants due to their electronegative substitutions at C3 (Yates et al., 2002). Donation of ions to the carbonyl group makes the lactone ring more resistant to hydroxide ions in alkali environments but having an oxo or hydroxy substitution at C3 decreases the electron-donating-potential and leads to reduced stability of the lactone ring in alkali environments (Yates et al., 2002). Others have also considered that oxo-variants are subjected to an additional degradation method; the so called "Claisen-like" re-arrangement (Kaufmann et al., 2005; Williams, 2007). This process acts via intramolecular alkylation of the β-ketoamide moiety to form tetramic acids (Kaufmann et al., 2005) (**Figure 5.3**). The β-ketoamide moiety is only present on oxo- substitutes as it includes the ketone group at the C3 position (Hodgkinson et al., 2011).

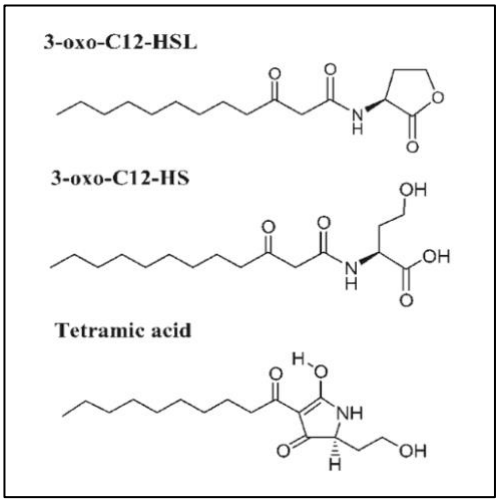

Figure 5.3. OC12 and its base-catalysed hydrolysis products. 3-oxo-C12-HS produced by base-catalysed lactonolysis, and tetramic acid produced by "Claisen-like" rearrangement. Taken from Williams (2007).

In addition, Hmelo and Van Mooy (2009) found that all HSLs tested had a higher degradation rate in natural seawater than artificial, with oxo-HSLs still having a higher degradation rate than unsubstituted. The authors suggested that this might be due to enzymatic hydrolysis, in addition to pH-mediated lactonolysis and the "Claisen-like" rearrangement.

Enzymatic hydrolysis of the lactone ring of HSLs can occur via lactonase enzymes, which is a pH-independent process. A lactonase (AidP) produced by *Planococcus versutus* showed a higher level of activity towards oxo-variants than unsubstituted HSLs (See-Too et al., 2018). However, Wong et al. (2013) showed that oxo-variants were degraded at a slower rate than

unsubstituted HSLs by an unnamed lactonase produced by *Trichosporon loubieri*. Chan et al. (2011) also found that the lactonase activity of *Acinetobacter* degraded OC12 to a lesser extent than HC12 and C12. This suggests that microbially-produced lactonases act on HSLs differently.

Oxo- substituted HSLs are additionally susceptible to modification of activity by oxidoreductases. These cause a reduction from oxo to hydroxy at the C3 position, ultimately altering HSL activity but not degrading them (Uroz et al., 2005; Chan et al., 2011). This suggests there may be more ways of affecting the activity and degradation of oxo-substituted than un-substituted HSLs.

Finally, C12 is more hydrophobic than its variants, as determined by the, (i) critical concentration required to form spherical micelles or aggregates in solution (the CMC value) and, (ii) predicted octanol/water partition coefficient (the Log P value). The CMC value is lower for C12 (4 μM) compared to OC12 (247 μM) (Davis et al., 2011; Gahan et al., 2020) and HC12 is not able to form micelles (Davis et al., 2011), suggesting that C12 is more hydrophobic than OC12 and both are more hydrophobic than HC12. Predicted Log P values confirm this trend, with the value for C12 (3.38) being higher that of OC12 (2.23) which is itself higher than HC12 (1.96). In addition, Log P values for the open ring structure of OC12 (OC12-HS) (1.89) and C12 tetramic acid (3.83) suggest that OC12-HS is the least hydrophobic of the C12 variants (and equivalent to HC12) whilst C12 tetramic acid is more hydrophobic than C12 (Davis et al., 2011). There is therefore clear evidence that hydrophobicity changes with C12 structural variation and this could impact on the extent to which they interact with biological membranes (Davis et al., 2010), as this is an important prerequisite to interacting with their cellular target (whether it be an internal target or one which that is membrane-bound.)

5.4. HSL interactions with the plasma membrane

5.4.1. HSL movement across the plasma membrane without receptor involvement

It is thought that HSLs are able to cross the cell membrane of eukaryotic cells without the aid of membrane receptors and then bind to intracellular receptors (Kaplan and Greenberg, 1985; Shiner et al., 2005). This is considered to be feasible due to HSLs being amphiphilic and structurally similar to the lipids that make up the cell membrane (hydrophilic head [lactone ring] and a hydrophobic tail [carbon chain]) (Coquant et al., 2020). All eukaryotic cell membranes essentially comprise the same components, i.e., lipid-bilayers with proteins,

carbohydrates (in the form of glycoproteins and glycolipids) and cholesterols (Alberts et al., 2002). However, the plasma membrane composition can vary between cell types and organisms (Guidotti, 1972; Quinn et al., 1980; Casares et al., 2019), Data on the composition of the plasma membranes of amoebae are rare (**Table 5.1**).

Table 5.1. Plasma membrane compositions of different cell types across different organisms. nr= not reported.

Cell type	Phospholipid %	Protein %	Carbohydrate %	Reference
Amoeba proteus	36	49	15	Topf and Stockem, 1996
Acanthamoeba castellanii	27	37	37 (Phosphoglycan)	Korn and Wright, 1973
Human Red blood cell	35.1	39.5	5.8	de Oliveira and Saldanha, 2010
Rat liver cells Mouse Liver cells HeLa cells	42 54 40	58 46 60	5-10 2-4 2.4	Guidotti, 1972
Ulva lactuca	20.3	nr	nr	Kostetsky et al., 2018

Potential differences in amoebic membrane lipid content might account for the difference in their susceptibility to HSL. The lipid composition of *Amoeba proteus* (unknown HSL sensitivity) and *A. castellanii* (HSL-insensitive) plasma membranes did differ (36 and 27%, respectively) (**Table 5.1**). Unfortunately, published data could not be obtained for the membrane compositions of the other amoebae tested in the current study, to evaluate whether there might be a link between plasma membrane lipid content and HSL sensitivity.

In addition to lipid content *per se*, the types of lipid, such as cholesterol and phosphatidylcholine (PC), can also change between cell type. Once again, data for amoebae are rare and incomplete (**Table 5.2**). However, what the data do highlight is that different species of the same genus, *Entamoeba histolyitca* and *E. invadens*, can have differences in lipid compositions, particularly PC (with their Cholesterol:phospholipid ratio [C:P] being equivalent). Data for *V. vermiformis* strains 7A and 14 could not be located, to see if their PC/cholesterol content differed (as did their susceptibilities to OC12 and C10). *D. discoideum* is suggested to be HSL-sensitive (Cosson et al., 2002) and was found to have a higher PC and PI content than *A. castellanii* (determine as HSL-insensitive in the current study) but no data

could be found on cholesterol for either species (**Table 5.2**). The lack of information on cholesterol content is particularly unfortunate as Davis et al. (2010) found that OC12 interacted with artificial cell membranes in areas of higher cholesterol concentration, indicating that these areas might be important for the HSL interaction, and strain differences in cholesterol composition might be related to HSL-sensitivity.

Table 5.2 Lipid composition differences in the plasma membrane of protists and *Ulva.* Phosphatidylcholine (PC), Phosphatidylinositol (PI), Phosphatidylethanolamine (PE) Sphingomyelin (SM), Cholesterol:phospholipid ratio (C:P). nr = not reported, np= not present.

Cell	PC	PI	PE	Cholesterol	SM	C:P	Reference
Amoeba proteus	nr	nr	nr	32%	nr	nr	Topf and Stockem, 1996
Acanthamoeba castellanii	19%	nr	47%	nr	nr	nr	Korn and Wright, 1973
	18.6%	0.2%	47.2%	nr	nr	nr	Ulsamer et al., 1971
Entamoeba histolytica	13%	1-10%	34%	nr	nr	0.87	Aley et al., 1980; Castellanos-Castro et al., 2020
Entamoeba invadens	38.3%	3.7%	30.1%	nr	9.3%	0.93	van Vliet et al., 1976; Das et al., 2002
Discoideum discoideum	28.8%	7.8%	27.8%	nr	nr	nr	Weeks and Herring, 1980
Tritrichomonas foetus	nr	nr	nr	20-30%	nr	nr	Rosa et al., 2014
Ulva fenestrata	np	0.9-1.7%	1.9-2.8%	nr	nr	nr	Kostetsky et al., 2004

HSLs have been found to insert into the lipid bilayer of both T-lymphocyte membranes and artificial membranes (Davis et al., 2010). Hydrophobicity should influence how HSLs insert into the membrane, i.e., HSLs with a higher hydrophobicity should insert easier. Considering C12 was shown to be more hydrophobic than OC12 which was itself more hydrophobic than HC12 (Davis et al., 2011; Gahan et al., 2020), it would be expected that C12 would cross the membranes easier than OC12, and both C12 and OC12 would cross easier than HC12 but this was not the case in the current study. Instead, all three amoeba strains were most sensitive to the HSLs at both ends of the hydrophobicity spectrum (C12 and HC12) and only one strain was sensitive to the intermediate, OC12. In addition, if crossing the plasma membrane was solely down to the hydrophobicity, one would also expect amoebae to only be susceptible to

the more hydrophobic longer-chain HSLs. But, *E. silvestris* was sensitive to the shorter chain C6, indicating that this sensitivity may not be governed solely by the hydrophobicity of the HSL.

It therefore appears unlikely that HSLs influence amoebae by solely crossing the amoeba plasma membrane 'unaided' and suggests that a membrane-bound receptor is involved.

5.4.2. HSL movement across the plasma membrane with receptor involvement

Davis et al. (2010) found that the insertion of OC12 into the plasma membrane of T lymphocytes (**5.4.1**), indicated a "cooperative binding pattern". The authors suggested that this strongly implied the presence of an unidentified OC12 receptor at the cell surface. Indeed, Shiner et al. (2006) had previously reported that OC12 influenced calcium signalling in host cells and suggested that OC12 interacted with an unknown membrane-bound receptor in order to do this. Subsequent work by others has identified multiple cell-specific transmembrane receptors that have been shown to interact with OC12, OC8 and even OC6. These receptors include Taste receptors such as T2R38 (Tizzano et al., 2010; Gaida et al., 2016; Jaggupilli et al., 2018), Toll-like receptor 2/4 (Lu et al., 2012), Cand2 and Cand7 (Jin et al., 2012) and GCR1 (Liu et al., 2012).

Because a receptor mediated HSL-eukaryote interaction allows for the uptake of OC6 (Jin et al., 2012), it might explain why *E. silvestris* was susceptible to C6 in the current study. Considering a receptor might be involved in the action of HSLs against amoebae, a series of membrane-bound, and one internal receptor (as a Control), were evaluated for their ability to block the negative action of C12 if they themselves were blocked with specific antagonists.

5.5 HSL-Receptor interaction

5.5.1 Proposed internal eukaryotic HSL receptors - PPARs

Peroxisome proliferator-activated receptors (PPARs) have been proposed as the receptors for OC12, where it acts as an antagonist to PPARγ and an agonist to PPARβ/δ (Cooley et al., 2008; Jahoor et al., 2008). No interaction of HSLs with PPARα have been reported to date. However, PPARs are not believed to be the receptor responsible in all mammalian cell types. Khambati et al. (2017) found that the effects of OC12 on bone marrow derived murine mast cells could not be blocked by the specific PPARγ antagonist, T0070907.

To date, PPARs have not been identified in amoebae, or protists as a whole. However, peroxisomes are believed to be present in most, if not all, eukaryotic cells (including amoebae) (Jansen et al., 2021), where they are used for processing lipids (Ludewig-Klingner et al., 2018). Al-Hammadi (2020) found that pre-blocking *V. vermiformis* (14) with GW6471 (antagonist of PPARα), prior to CBD treatment, reduced the negative effect of this long-chained lipid which suggested that the amoeba possessed a PPAR-like molecule. She proposed that this PPAR-like molecule was inducing a non-genomic response (due to the instantaneous effect of CBD), whereby it was binding to proteins outside the nucleus, such as Syk, LAT and PKC. However, this was found to be genus-specific as pre-blocking with even the general PPAR blocker (GW9662) did not alleviate the negative effect of CBD on *A. castellanii, F. arnhemensis, H. cantabrigiensis, N. gruberi* and *Vahlkampfia avara*.

In the current study, pre-blocking *V. vermiformis* (7A) and *N. gruberi* with GW9662 (a general PPAR blocker) did not alleviate the negative effects of C12, suggesting these internal receptors play no role in the interaction between these amoebae and HSLs and lends weight to the possibility of their being a plasma membrane-bound receptor which interacts with C12. Amoebae are known to possess many trans-membrane GPCRs (Baig, 2016; Senoo et al., 2016) and considering that long-chain HSLs can interact with GPCRs, albeit in other cell types (Jaggupilli et al., 2018), they do warrant further investigation.

5.5.2 Proposed membrane-bound eukaryotic HSL receptors - GPCRs

GPCRs are 7-trans-membrane (TM) receptors which bind to intracellular heterotrimeric G proteins. They comprise 3 subunits, α, β, and γ. The β and γ subunits form a complex called the Gβγ dimer (de Oliveira et al., 2019) which can be blocked with the antagonist Gallein. Ligand binding to the GPCR causes a conformational change which reduces the affinity of GDP to bind to the Gα subunit. There then follows a sequential dissociation of the GDP-Gα complex from the GPCR, an interaction of GTP with Gα, and dissociation of heterotrimeric complex Gα–βγ into the Gα subunit and βγ dimer (Pierce et al., 2002).

The α subunit has multiple subtypes, namely G_s, G_i (including G_t and G_o), G_q and $G_{12/13}$ (de Oliveira et al., 2019); each with their own specific blocker. G_s enhances adenylyl cyclase activity (Tilley, 2011) while G_i reduces it (Sunahara and Taussig, 2002). G_q activates phospholipase Cb while $G_{12/13}$ stimulates the guanine nucleotide exchange factor of small GTPases of the Rho family (Wang et al., 2021). The extent to which different Gα subtypes are present in eukaryotes varies, with humans having 16 Gα subtypes (Milligan and Kostenis,

2006; Jelinek et al., 2021) and the plant *Arabidopsis thaliana* only having four; one typical (GPA1) and 3 atypical, known as extra-large G protein alpha (Liu et al., 2021).

With regards to amoebae, *D. discoideum*, *Naegleria fowleri* and *E. histolytica* possess 14, 13 and 2 Gα subtypes, respectively (Eichinger et al., 2005; Bosch and Siderovski, 2013; Bosch et al., 2022). However, it has proven difficult to classify amoeba and other protist G proteins into the classical mammalian subtypes of G_s, G_i, G_q and $G_{12/13}$ (Kostiou et al., 2016).
When *N. gruberi* and *V. vermiformis* (7A) were pre-blocked with Gallein (to block the Gβγ dimer common to all GPCRs), the negative action of C12 was alleviated and therefore suggested that the HSL was interacting with a GPCR. The study then aimed to identify the nature of the alpha subunit of this GPCR.

5.5.2.1 $G_{i/o}$ and G_t GPCRs

Pertussis toxin (PTX) is an inhibitor of G_i GPCRs, including G_o and G_t GPCRs (TOCRIS, 2021). It catalyses the ADP-ribosylation of these $G\alpha_i$ subunits, uncoupling them from their cognate membrane-bound receptor and thus preventing their activation (Watts and Neve, 2005). When tested on *N. gruberi* and *V. vermiformis* (7A), no blocking of C12 activity was observed, indicating that $G_{i/o}$ and G_t GPCRs were not involved in the amoeba-C12 interaction. Within this α subtype are Opioid receptors (Holzer, 2009), Adenosine A1 (Chen et al., 2014), Dopamine D2 (Gonzalez-Iglesias et al., 2008) and Serotonin 5-HT1A and 1B (Gadgaard and Jensen, 2020); all of which have been implicated as possible receptors for CBD (Bih et al., 2015; Silvestro et al., 2020). The latter three receptors were further investigated here, with *N. gruberi* only, and Adenosine A2 (antagonist ZM241385), Dopamine D1 (antagonist SCH 23390 hydrochloride) and 5-HT2A (antagonist EMD281014) were all shown not to alleviate the negative effect of C12. Since there are multiple forms of Dopamine and Serotonin receptors, both *N. gruberi* and *V. vermiformis* (7A) were also tested with Haloperidol hydrochloride which blocks Serotonin 5-HT1A, 2A and 2C and Dopamine D1-5 (Li et al., 2016). Once again, no alleviation of the C12 effect was recorded. Thus, it appears unlikely that C12 interacts with Opioid, Adenosine, Dopamine and Serotonin receptors (or any other $G_{i/o}$ and G_t receptor) in these amoebae.

The author had expected to record an interaction between C12 and Serotonin receptors, only because Al-Hammadi (2020) found that blocking the serotonin 5-HT1A receptor alleviated the negative effect of CBD in *N. gruberi*. But once again, it appears that the interaction between amoebae and CBD differs to that of C12, even though they are both long-chained lipids.

5.5.2.2 G_s GPCRs

Melittin is a G_s GPCR antagonist that inhibits GDP release, rendering the G_s α subunit inactive (Fukushima et al., 1998; TOCRIS, 2019). However, it has been shown to be toxic to different cell types (Sommer et al., 2012; Jamasbi et al., 2014; Kreinest et al., 2020), particularly at concentrations >0.5 μM (Kreinest et al., 2020). The ciliate *Tetrahymena pyriformis* has been found to be particularly sensitive to concentrations >0.3 μM (Tims, 2021). Toxicity tests with both *N. gruberi* and *V. vermiformis* (7A) showed a negative reaction to Melittin at 1 μM but this was not significant. Even so, the working concentration decided upon was a cautious 0.5 μM. The next stage would have been to test each amoeba with Melittin but time constraints prevented this.

However, work at Lancaster University during 2021/22 did test Melittin against *N. gruberi* and found that it alleviated the negative effects of C12 in a dose-dependent matter, with Melittin having an MIC of >0.01<0.1μM for 100% blocking of this interaction (Raistrick, 2022). Raistrick (2022) also tested *N. gruberi* with YM254890 which blocks all G_q GPCRs (e.g. 5-HT2A and 2C [Cussac et al., 2002; Cussac et al., 2008]) and found that it did not alleviate the C12 effects. Thus, the G_s GPCRs seem to be a strong candidate for the C12 receptor in this amoeba.

There are many types of G_s GPCRs in animal cells but they all function via adenylyl cyclase activation (Godinho et al., 2015). Data on plant cell G protein activation of adenylyl cyclase is rare. However, Lomovatskaya et al. (2011) found that suramin, which uncouples G proteins from their receptors, inhibited membrane bound adenylyl cyclase by 93-95% in potato plants, suggesting the presence of G_s activity. Reports on the involvement of G_s GPCRs with HSLs are also very rare (**Table 2.3**). In the human cancer cell line Caco-2, 200 μM of OC12 induced protease-activated receptor (PAR)-dependent signalling leading to disassembly of tight junctions (Eum et al., 2014). PAR2 (GPR11), not PAR1, was found to interact with G_s α subunits (and those of $G_{q/11}$ and $G_{12/13}$) (Zhao et al., 2015a; Kennedy et al., 2020). In *Arabidopsis thaliana* the presence of 1 μM OC6 and 10 μM OC8 resulted in an increase of relative root elongation due to interaction with the GPCR (GCR1) and the G protein GPA1 (Liu et al., 2012); which is also susceptible to G_s agonists, such as cholera toxin (Ma et al., 1990). Evidence could not be found for PAR2 existing in amoebae or other protists, however, GPA1 was found to be present (see 5.6.1.1).

5.6 The G_s GPCRs

5.6.1 Presence and role of G_s GPCRs in amoebae

There are many receptors that have been identified as G_s bound GPCRs (Godinho et al., 2015) but their interaction with HSLs, and whether they exist in amoebae, is largely unknown. However, the current study discounted the presence/C12-interaction of some G_s GPCRs (5.5.2.1). These included Adenosine A2 and Dopamine D1 and D5, all of which are G_s GPCRs (Plouffe and Tiberi, 2013; Carpenter et al., 2016; Li et al., 2016; Gao et al., 2018).

5.6.1.1 GPA1 and its GPCRs

GPA1 is the Gα subunit that interacts with the HSL-interactive GPCR (GCR1) in *A. thaliana* (Liu et al., 2012*)*. It is also a Gα subunit that acts as a negative regulator of the pheromone response pathway in the yeast *Saccharomyces cerevisiae*, and G_{olf} is suggested to act in the same manner (Crowe et al., 2000). The GPA1 in the fungus *Cryptococcus neoformans* regulates adenylyl cyclase, leading to an increase in cAMP (Alspaugh et al., 2002) and thus shows that the classical G_s protein mechanism is conserved between mammalian cells and fungi. Furthermore, one of the two Gα proteins in *E. histolytica* (EhGα1) has similarity to the GPA1 of *A. thaliana* and *S. cerevisiae* (Bosch et al., 2012), suggesting EhGα1 may function as a $G_{s/olf}$ subunit in this amoeba, but to date, the GPCR it interacts with has not been identified.

GPA1 is also present in the widely studied *D. discoideum* (i.e., Gα1) (Dictybase, 2019). Whilst its similarity to the GPA1 of *E. histolytica* and *A. thaliana* is still to be determined, it has been shown that Gα1 (and Gα2) are 35% structurally identical to yeast (unspecified) GPA1, and to mammalian G_s (Pupillo et al., 1989). However, despite this structural similarity, Gα1 does not affect adenylyl cyclase (so not a G_s) and instead, Gα2 activates adenylyl cyclase in a G_s-like manner with the suggested GPCR being cAR1 (Pupillo et al., 1989; Pupillo et al., 1992; Dharmawardhane et al., 1994). Thus, despite both Gα subtypes being identical in structural similarity to human G_s proteins, they act via separate mechanisms.

Gα2 is now one of the most studied *D. discoideum* Gα subtypes and is widely reported to play a role in cAMP chemotaxis and the aggregation of cells into a migrating slug during starvation (**Figure 5.2**) (Tariqul Islam et al., 2018), in a typical G_s GPCR fashion. Other GPCRs (and Gα subtypes) have been found in *D. discoideum* but have different physiological effects.

5.6.1.2 Gα4 and its GPCRs

The Gα4 subunit of *D. discoideum* is not as well studied as Gα2, but Gα4 has been shown to have a 41% identity to Gα2 (Hadwiger et al., 1991); no reference to homology to human G_s proteins could be found. Gα4 is reported to play a role in the chemotaxis of cells to folic acid (Hadwiger et al., 1994) which is used to detect bacterial prey (Pan et al., 1972; Pan et al., 2016). Folic acid detection by GPCRs (folate receptors fAR1 and 2), on the amoeba membrane results in a signal cascade allowing the cells to move towards, and engulf, prey. The detection of folic acid by amoeboid cells causes activation of adenylyl cyclase, which is impaired in cells lacking Gα4 (Hadwiger et al., 1994), suggesting that Gα4 acts in a 'typical' mammalian G_s protein fashion.

Gα4 is also suggested to be involved in phagocytotic uptake, as it is present at the early stages of phagocytosis (Gotthardt et al., 2006). Gα4 null cells were found to have an uptake rate of fluorescent beads that was 50% lower than that of wildtype cells (Gotthardt et al., 2006). Pan et al. (2016) also found that Gα4 null mutants had a significantly lower rate of engulfment and ingestion (Pan et al., 2016). Because of this role in phagocytotic uptake, Gα4 is suggested to bring about actin polymerisation for engulfment and ingestion (Pan et al., 2016).

5.6.1.3. Beta adrenergic receptors

To date, no adrenergic receptor homologs have been found in amoebae, however their presence/activity has been alluded to via receptor blocking experiments.

The presence of G_s GPCRs in *E. invadens* has been noted by Coppi et al. (2002). They showed that epinephrine induced encystment, with the authors suggesting the involvement of a beta-1-adrenergic receptor, a G_s GPCR, at the cell surface. This was further supported by the fact that blocking of Beta-2-adrenergic receptors (via ICI-118,551, 500 μM) did not alleviate encystment in the presence of epinephrine but, blocking of Beta-1-adrenergic receptors (via Metaprolol and Timolol, 500 μM) did. In addition, Frederick and Eichinger (2004) demonstrated that epinephrine led to an increase in adenylyl cyclase activity and that cAMP increased during early encystment.

In a review by Krishna et al. (1984) the first report of beta-adrenergic receptors in *Acanthamoeba* was discussed. Epinephrine was found to induced adenylyl cyclase in *Acanthamoeba culbertsoni* and that the binding of epinephrine to the amoeba membranes was inhibited by the general Beta-adrenergic antagonist, propranolol. They, together with Aqeel et

al. (2015), also stated that propranolol inhibited epinephrine-induced encystment and Aqeel et al. (2015) further showed that propranolol (250 and 500 μM) reduced amoeba concentration compared to control and "adversely affected *A. castellanii* viability". These studies suggest that beta-adrenergic receptors (G_s GPCR) might be present in *Acanthamoeba* and are important in encystment, growth and proliferation.

5.6.2 G_s GPCR signalling pathways

The presence of G_s GPCRs in amoebae has been linked to physiological responses such as encystment, chemotaxis, phagocytosis, population growth and viability (5.6.1) but the mechanisms involved still require elucidation. Cell growth is tightly regulated by a variety of signal transduction pathways, and very few have been described for amoebae.

The stimulatory G protein family (G_s), which also includes G_{olf} proteins (Jones and Reed, 1989), have the ability to bind to and activate the $G_{s/olf}$ subtype of GPCRs. After G_s protein activation and dissociation of the active GTP-G_s α subunit, the G_s subunit is able to activate any form of available membrane-bound adenylyl cyclase (AC; AC1–AC9) (Sadana and Dessauer, 2009). These then catalyse the conversion of adenosine triphosphate (ATP) to 3',5'-cyclic AMP (cAMP), an important secondary messenger, and pyrophosphate.

As demonstrated in 5.6.1, all the G_s GPCRs known/inferred to exist in amoeba activate membrane-bound ACs and, interestingly, enhanced interactions of G_s and ACs have been associated with the ease in which G_s can be extracted from membranes with Triton X-100 (TX100) (Toki et al., 1999). TX100 is one of the most widely used non-ionic surfactants for lysing cells to extract membrane proteins, with the polar head group of TX100 molecules disrupting the hydrogen bonding present within the cell's lipid bilayer (Koley and Bard, 2010). However, the presence of cholesterol makes membranes more resistant to TX100 penetration, irrespective of the host phospholipid type (Nyholm and Slotte, 2001). This might suggest that detectable interactions of G_s and AC occur only in membranes with a lower cholesterol content, which links to a potential theory that variations in plasma membrane lipid composition is involved in determining the sensitivity of different amoebae to HSLs (see 5.4.1). However, Davis et al. (2010) actually found that OC12 interacts with areas of high cholesterol concentration (rafts) in artificial cell membranes, so the potential link between plasma membrane cholesterol levels and HSLs is currently unclear.

cAMP can directly regulate various biological processes or behaviours of cells, including cell metabolism, gene expression, cell growth, differentiation and apoptosis (Chin et al., 2002). However, one of the hallmarks of cAMP is its ability to inhibit proliferation in some cell types, but stimulate proliferation in others (Dumaz and Marais, 2005). This outcome on cell proliferation is primarily accredited to crosstalk from cAMP to one of four mitogen-activated protein kinase (MAPK) cascades (that comprise RAS/RAF/MEK/ERK), by either activating protein kinase A (PKA) (Tilley, 2011), ion channels (Bradley et al., 2005) or cAMP-activated exchange proteins (Epac) (Gloerich and Bos, 2010). Of the three, PKA is the most well-known cAMP effector.

Activated PKA phosphorylates Raf but instead of phosphorylating 4 sites (which activates Raf) it only phosphorylates two sites, thus rendering Raf inactive (Dumaz and Marais, 2005). As a consequence, the downstream MEK/ERK pathway is not activated and normal cellular proliferation and survival is lost (Dhanasekaran et al., 1998; Roberts and Der, 2007). When activated, ERK phosphorylates many substrates and in so doing, regulates numerous cellular functions such as gene expression, metabolism, morphology and proliferation. However, when MEK/ERK is not activated, proliferation does not occur and cell cycle progression is reported to be halted at G1 (Sebolt-Leopold et al., 1999; Pearson et al., 2001). The MEK/ERK pathway therefore plays an important role in determining cell responses such as proliferation, differentiation, senescence and survival (Sebolt-Leopold and Herrera, 2004).

Knowledge as to whether HSLs interfere with the G_s GPCR only or one or more components of its downstream pathway(s) is very limited and contradictory. To date, GPA1 is the only G_s GPCR which both interacts with a HSL and for which a homologue exists in amoebae (Pupillo et al., 1989, 1992; Dharmawardhane et al., 1994; Bosch et al., 2012). If C12 did stimulate a G_s GPCR in amoebae, it would be expected that the membrane-associated ACs would be activated and cellular cAMP would increase. However, there is a report which suggests that C12, but not C10, inhibits AC in the yeast *Candida albicans* (Hogan et al. 2004); a cell whereby the predominant GPCR type is G_s and where cell differentiation (from a virulent yeast to a virulent fungal form) is known to involve the cAMP-dependent-PKA pathway (Gao et al., 2018). There is also one report on OC12 being able to activate ERK, which led to a decrease in cell viability in Caco-2 cells (Shimizu et al., 2015).

The results of this study and work by Raistrick (2022) clearly suggest that G_s GPCRs are in some way involved in the interaction between C12 and amoebae as their blocking, with Melittin, significantly reduced the negative effect of this HSL on the population growth of *N. gruberi* at least (Raistrick, 2022). Further experiments are required to confirm whether a similar response occurs in *V. vermiformis*, and indeed the other HSL-sensitive amoebae.

5.7 Response of amoeba cells to HSLs

Whatever the mechanism by which C12 (and in some cases C6 and C10) interacts with its target(s) in amoebae, a measurable physiological response to C12 was recorded with all sensitive strains, i.e., reduced population growth at 3/4 days. This parameter is the culmination of a series of stages which includes amoebic feeding, assimilation of nutrients, cell growth and cell division. Because these stages were not examined in isolation here, it is unknown which stage or stages are specifically affected by C12. However, some clues can be gathered from the preliminary experiment with *V. vermiformis* (14) whereby population growth was monitored daily for 9 days in the presence of 4 concentrations of C12 (100–400 μM). This experiment suggested that C12 acted in two ways on the amoeba cells; instantaneous cell death (at high concentration) and population growth reduction (at lower concentrations).

5.7.1. Instantaneous cell death

C12 was found to be instantaneously lethal to *V. vermiformis* (14) at concentrations ≥200 μM. Amoeba cell concentration reduced to below the counting threshold (1 cell/grid) at 200 and 300 μM after which, some recovery of the population was evident. However, at 400 μM there was no amoebic recovery and 100% of the population was destroyed.

Cell death is normally programmed (apoptosis) or un-planned (necrosis). Apoptosis is characterized by cell shrinkage, membrane blebbing, nuclear fragmentation, chromatin condensation, and chromosomal DNA fragmentation (He et al., 2009). While necrosis is characterized by cell swelling and rupture of the cytoplasmic membrane, which results in the release of the cellular content (Proskuryakov et al., 2003). The latter is an uncontrolled and passive process that usually affects many cells whereas apoptosis is controlled, energy-dependent and affects individual cells or clusters (Elmore, 2007). The two processes can occur independently, sequentially, as well as simultaneously because they are considered to share the same biochemical network; the “apoptosis-necrosis continuum” (Zeiss, 2003). The type, degree and duration of stimuli can determine the path a cell takes within this continuum and a

variety of stimuli such as heat, radiation, hypoxia and cytotoxic drugs have been shown to induce apoptosis at low concentration but necrosis at higher concentration (Elmore, 2007).

OC12 has long been known to induce apoptosis in a variety of cell types (Tateda et al., 2003; Li et al., 2004; Shiner et al., 2006; Taguchi et al., 2014; Zhang et al., 2014; Kumar et al., 2018) (see 5.7.2.1) but its induction of necrosis in such cells is poorly studied. However, a study by Balhouse et al. (2017) did find that OC12 could induce necrosis in malignant human breast adenocarcinoma cells (MDA-MB-231). They treated the cells with various concentrations of OC12 and, after 48h, found that the cell concentration was significantly reduced in a dose dependent manner (MIC >50<100 μM); similar to the current study. Further experiments with 400 μM OC12 revealed that the cells (52% remaining, compared to the Control) showed a significant increase in necrosis level, but not in apoptosis level. In addition, less than 10% of these cells were entering the S-phase of the cell cycle so more than 90% were not proliferating (Balhouse et al., 2017) (see 5.7.2.2). Although no data were presented for the levels of proliferation, apoptosis and necrosis in cells treated with lower OC12 concentrations, the authors suggested that the observed reduction in cell number, at these lower concentrations, might be more due to a combination of apoptosis and a reduced number of cells entering the S-phase (reduced proliferation) rather than necrosis (Balhouse et al., 2017).

The current study did not assess whether those amoeba cells that remained after C12 treatment were apoptotic and/or necrotic, and what proportion were entering the S-phase of the cell cycle, however future work should address this, not only at 3/4 days but throughout the growth phase of the amoeba population. Even so, the current study showed that treatment of *V. vermiformis* (14) with 400 μM C12 resulted in 0% survival of cells, which strongly suggests that necrosis was the over-riding mechanism. Instantaneous cell death also occurred with 200 and 300 μM (also probably due to necrosis) however, the population then increased but with a lower growth rate compared to the Control. This might suggest a possible switch from necrosis being the dominant process to a combination of apoptosis and reduced proliferation, as suggested by Balhouse et al. (2017). And interestingly, increases in cAMP, which can be induced by G_s GPCRs (the putative HSL amoeba receptors, see 5.6), is considered to play a role in the cell cycle, proliferation and apoptotic processes of cells (Chin et al., 2002).

5.7.2. Population growth reduction

Population growth rate is the net result of the balance between cell birth (proliferation) and cell death and as such, a positive growth rate indicates that birth is greater than death. In the current study, C12 affected the population growth rate of *V. vermiformis* (14); reducing it at 100 µM (compared to the Control) and reducing it even further at 200 and 300 µM. Considering the dominant cell death mechanism might be apoptosis (after instantaneous necrosis had ended) evidence suggests that the observed reduction in population growth might be due to: (i) an increase in apoptosis with an unaffected proliferation rate, (ii) a reduced proliferation rate with an unaffected apoptosis rate or, (iii) a reduction in both proliferation and apoptosis rates.

5.7.2.1. Apoptosis

Apoptosis, or programmed cell death (PCD), is an essential mechanism for the development and homeostasis of multicellular organisms via the elimination of aged or abnormal cells through a sequence of programmed events that are regulated by environmental signals (Arends and Wyllie, 1991). Apoptosis typically initiates at a single discrete focus, or a small number of discrete foci, and then spreads rapidly throughout the cell at a consistent velocity, for example, at ~30 µM min^{-1} in *Xenopus laevis* egg extracts (Cheng and Ferrell, 2018).

PCD processes, although not their speed, have been identified in protists, including the amoebae *Dictyostelium* (Cornillon et al., 1994), *Acanthamoeba* (Feng et al., 2009), *Entamoeba* (Villalba et al., 2007), *Naegleria* (Zeouk et al., 2021), and the parasitic protozoans *Trypanosoma* (Nguewa et al., 2004), *Leishmania* (Lee et al., 2002b) and *Plasmodium* (Al-Olayan et al., 2002). However, as to why these protists might possess a mechanism to destroy themselves is currently unclear. It has been suggested that parasitic protozoa might use PCD within a host, to limit the parasite load which would allow enhanced reproduction and increase the spread of the parasite in the longer term (Al-Olayan et al., 2002; Nguewa et al., 2004). As for amoebae, Koutsogiannis et al. (2019) suggested it might be a mechanism to prevent the spread of 'endosymbiotic' pathogenic bacteria and viruses through local populations. Even so, the mechanism by which PCD occurs in protists does differ to that in mammalian cells, principally because protists lack caspases, a family of cysteine protease which are unequivocally important in mammalian apoptosis (Elmore, 2007). For example, caspases are known to be absent in *D. discoideum* (Olie et al., 1998), *A. castellanii* (Clarke et al., 2013) and *N. gruberi* (Fritz-Laylin et al., 2010).

Even though protists generally lack caspases, some possess caspase-like molecules (metacaspases and paracaspases). Metacaspases are present in parasitic protozoa such as *Plasmodium falciparum* (Meslin et al., 2007), *Trypanosoma brucei* (Szallies et al., 2002), *Leishmania major* (González et al., 2007) and *Leishmania donovani* (Lee et al., 2007). In these cells, metacaspases have been linked to growth reduction, respiratory dysfunction and cellular death. With regards to amoebae, *A. castellanii* possesses a metacaspase (Acmcp) (Trzyna et al., 2008) while *D. discoideum* possesses a paracaspase (Ddpcp) (Uren et al., 2000). However, it is considered unlikely that they are involved in PCD but rather, they play a role in the formation, regulation and/or function of the contractile vacuole (Saheb et al., 2014). The PCD mechanism in *Naegleria* has not yet been widely characterized (Zeouk et al., 2021) and no evidence for the presence of a metacaspase or paracaspase can be found by the author.

Although there are published reports of chemical stimuli inducing apoptosis in amoebae (Koutsogiannis et al., 2019) the author could find no reports of HSLs inducing apoptosis in these cells. Thus, whether C12 is inducing apoptosis in *V. vermiformis* (and the other sensitive amoebae) remains to be elucidated. This contrasts with more information being available on OC12 inducing apoptosis in a variety of other cell types (Tateda et al., 2003; Li et al., 2004; Shiner et al., 2006; Taguchi et al., 2014; Zhang et al., 2014; Kumar et al., 2018).

Apoptosis in other cell types can been shown to be mediated through the G_s GPCR beta-adrenergic receptors, via effects on cyclic AMP, in cardiomyocytes (Communal et al., 1999; Zaugg et al., 2000; Zhu et al., 2001), thymocytes (Gu et al., 2000), lymphoma cells (Yan et al., 2000) and mesangial cells (Mühl et al., 1996). In amoeba, such receptors have only been shown to be involved in encystation (see 5.6.1) and it is currently unknown if they are involved in apoptosis. Histamine receptor 2 is a G_s GPCR that has also been implicated in apoptosis in neutrophils (Hur et al., 2003). Treatment with histamine has been shown to increase phagocytosis in *A. proteus*, though no reference to a receptor was made (Csaba et al., 1984). There have been no reports of either of these receptors interacting with HSLs.

5.7.2.2. Proliferation

The cell cycle is an ordered sequence of cellular events that occur in preparation for cell division. It is a four-stage process in which the cell increases in size (G1-phase), copies its DNA (S-phase), prepares for cell division (G2-phase), and then divides by mitosis (M-phase) (Maton et al., 1997). In mammalian cells, the longest phase is G1 (Cooper, 2001) whereas in amoebae (and other protists) the longest phase is G2 (Anwar et al., 2020; de Carvalho Clímaco

et al., 2022). The G2 phase in amoebae is preceded by a short S-phase (Jantzen et al., 1990; Huber, 2014) and is followed by an even shorter M phase (Pérez-Posada et al., 2020).

The presence or absence of a G1-phase in amoebae has proved controversial (Zada-Hames and Ashworth, 1978; Stöhr et al., 1987; Jantzen et al., 1990; Byers et al., 1991; Dvorak et al., 1995; Lohia, 2003; Podlipaeva et al., 2013; Pérez-Posada et al., 2020) but it now appears to be strongly influenced by the methodology used. It has been found that a G1-phase is a characteristic of cells within a synchronized amoeba population whereas a G1 phase is largely un-detectable in an asynchronous population (de Carvalho Clímaco et al., 2022). However, one recent study (Bínová et al., 2021) detected a G1 phase in an asynchronous *A. castellanii* population and proposed that an undetectable G1 in other asynchronous cultures was due to the G1 phase being 'lost' via flow cytometric analysis of isolated nuclei (compared to whole cells); based on the nuclear fragility observed when testing several nuclear purification and fixation protocols on *D. discoideum* (Chen et al., 2004).

Control of the cell-cycle occurs via 'checkpoints' which are surveillance mechanisms that monitor the order, integrity, and fidelity of the major events of the cell cycle, and are predominantly at the G1/S transition, the intra-S (spindle) and the G2/M transition (Barnum and O'Connell, 2014). Checkpoints are regulated by Cyclin-dependent kinases (CDKs) whose actions are dependent on the binding of regulatory subunits known as cyclins (Pines, 1995), which are synthesized and destroyed at specific times during the cell cycle (Hershko, 1997).

Humans possess 20 CDKs and approximately 30 cyclin genes (Malumbres, 2011) while the amoeba *D. discoideum* possesses 7 CDKs and 9 cyclins (Cao et al., 2014). However, whilst this species is often used to represent amoebae in general, its life cycle differs from that of 'true' amoebae (**Figure 5.2**), so differences in the function of their CDK/cyclin system might be expected (Bínová et al., 2021). Indeed, a marked difference has been observed, with *A. castellanii* and *Capsaspora owczarzaki* both possessing only one CDK (CDK1-like and CDK1-3-like, respectively) (Mengue et al., 2016; Pérez-Posada et al., 2020) and 14 and 3 putative cyclin sequences, respectively (Pérez-Posada et al., 2020; Bínová et al., 2021). This suggests remarkable simplicity of the cell cycle regulatory machinery in these true amoebae. Even simpler is *E. histolytica* which possesses no checkpoints at all (Banerjee et al., 2002) and although potential cyclins and CDKs have been identified in its genome, the likely absence of other cell cycle proteins suggests a unique cell cycle regulation mechanism in this amoeba (Anamika et al., 2008).

5.7.2.3 HSLs and proliferation

The only study the author could find regarding the effect of a HSL on cell-cycle progression was for the malignant breast cancer cells studied by Balhouse et al. (2017) (see 5.7.1) whereby less than 10% of surviving cells were entering the S-phase. This suggested that OC12 arrested the cells in G1-phase, which has also been reported to occur in these cells upon treatment with algal phytochemicals (Murad et al., 2016). G1 cell-cycle arrest is possible in amoebae and has been demonstrated in *A. castellanii* cells after treatment with Nisin (de Carvalho Clímaco et al., 2022). However, as stated previously, amoebae cells spend most time in the G2-phase of the cell cycle (Huber, 2014; Anwar et al., 2020; de Carvalho Clímaco et al., 2022).

During the G2-phase, amoebae would be feeding on their prey, assimilating nutrients and increasing in size. The G2/M checkpoint would then prevent cells from entering the M-phase (mitosis) if the DNA was damaged and afford the cells the opportunity to repair the damaged DNA or, if the damage is irreparable, checkpoint signalling might activate pathways that lead to apoptosis (Wang et al., 2009). Although not a HSL, G2-phase arrest has been reported to be induced in the ciliate *Tetrahymena pyriformis* by another long-chain lipid, delta-9-tetrahydrocannabinol (THC). This compound caused a decrease in cellular growth and division which was temporary (McClean and Zimmerman, 1976). Further work showed that cells were briefly arrested in the G2 phase, which caused a delay in cell division and was accompanied by a reduction in cAMP levels (Zimmerman et al., 1981). THC has been found to reduce the population growth of *N. gruberi* (Pringle et al., 1979) and *D. discoideum* (Bram and Brachet, 1976) but the cell-cycle stages were not examined.

The isomer of THC, i.e., CBD can also reduce amoebic population growth (Pringle et al., 1979; Dey et al., 2010; Al-Hammadi, 2020) but once again these studies did not examine its effect on the cell-cycle phases. However, CBD does arrest feeding in amoebae (Al-Hammadi, 2020) and in *T. pyriformis* (Jaisswar, 2020; Tims, 2021) which would be occurring in the G2-phase. At high concentrations CBD can also induce instantaneous death in the *T. pyriformis* population (Wanlahbeh, 2020); as was recorded for amoebae with C12 in the current study. Future work could therefore determine whether C12 arrests phagocytosis in amoebae, as does CBD, to see if further similarities exist between the action of these long-chain lipids and whether G_s GPCRs are involved as they are known to be in *A. proteus* and *D. discoideum*, (Csaba et al., 1984; Gotthardt et al., 2006).

5.8. Future work and technical challenges

5.8.1. Future work

The main body of future work leading on from this study, and that of Raistrick (2022), would involve the examination of other HSL-sensitive amoebae strains in the presence of C12 and melittin. In addition, with HSL-sensitive amoebae, antagonistic blocking of C12 on effectors in the MEK/ERK pathway and G_s GPCRs shown to affect growth and feeding, such as fAR1/2 (antagonists unknown) and beta-adrenergic receptors (via propranolol and metaprolol) could provide crucial evidence as to the mechanism in which C12 reduces population growth in amoebae. Furthermore, assessment of C10 and C6 should also be tested on their respective sensitive amoebae strains to see if they interact in the same way (and with the same receptor type) as C12. This would provide confirmation of how HSLs of all lengths and hydrophobicities are able to interact with eukaryotic cells.

Morphological changes to amoeba cells were not examined in this study however could prove to be an interesting examination. This would identify if the cell structure changes as a result of the presence of C12 (and other HSLs). The work could include observations of changes in shape and/or size of the cell, i.e. if the cell rounds up to produce a pseudocyst, and to identify changes in vacuole number and/or volume. Single cell microscopy and light scattering techniques could prove very useful in assessing these morphological changes.

A study on the effect of C12 on the amoebic cell-cycle would also be essential, not only because there are currently no publications on this topic (along with the potential involvement of G_s GPCRs), but because anecdotal observations by the author strongly suggest that C12 influences cell-cycle progression. In particular, it was noticed in the current study that some experiments involving C12 ‘behaved’ and resulted in a significant reduction in amoebic population. However, some experiments did not ‘behave’ and in these, C12 had very little effect on the cells. Although all amoeba cultures were routinely grown for 7 days prior to an experiment, the cultures were not synchronous. So, the proportion of cells within each phase of the cell-cycle was unknown and could have varied at the start of each experiments (even if they do spend the majority of their time in G2-phase). If amoebae are more sensitive to C12 during a particular phase, then this variation might explain the disparity in C12 susceptibility between experiments. Ideally, synchronous cultures should be used.

5.8.2. Technical challenges

5.8.2.1. Obtaining synchronous cultures

Methods for obtaining synchronous cultures are broadly split into two categories, 'induction synchrony' and 'selection synchrony'. The former induces cells to divide synchronously by means of some form of exogenous treatment which can be chemical or physical, e.g., temperature and starvation (Lloyd et al., 1975; King and Hyams, 1982). Temperature shifts are commonplace in macrophage research and have also been used successfully with *D. discoideum* (Maeda, 1986). However, this cannot be performed with 'true' amoebae as they form cysts in unfavourable conditions (Smirnov and Brown, 2004; Smirnov, 2008). Serum starvation is commonly used to synchronise *E. histolytica* cells (Gangopadhyay et al., 1997) while starvation of prey for 3 days, followed by quail egg albumin for 1h and cell-washing, has been successful with *A. proteus* (Podlipaeva et al., 2013).

The use of cell cycle inhibitors has been shown to induce synchronicity in a range of cell types (Kung et al., 1990; Davis et al., 2001; Szczepański et al., 2019). Different inhibitors stop the cell cycle from progressing at different stages however, others, such as aphidicolin (APH) and hydroxyurea (HU) halt cells at the G1/S boundary (Bucknall et al., 1973; Yarbro, 1992). The latter has been successfully used to synchronise cells of *Capsaspora owczarzaki* (Pérez-Posada et al., 2020) and *E. histolytica* (Austin and Warren, 1983). However, neither of these agents induce synchronicity in *A. castellanii* (Bínová et al., 2021). Induced synchrony can however cause metabolic stress to the organism and at the extreme, those that arrest the M phase, such as microtubule disrupting agents, are rarely used as they are often too toxic (Davis et al., 2001).

Selection synchrony selects cells at a particular stage of a cycle, separates them from the rest of the culture and allows them to naturally go through their cycle (Lloyd et al., 1975). One method of selection synchrony with amoebae, and other protists and yeasts, was proposed by Lloyd et al. (1975) in which, cultures of exponentially growing *A. castellanii* cells were centrifuged at low speed. The effluent containing the smallest sized amoebae provided a culture which went on to exhibit synchronous cell division. As the amoebae cells used in selection synchrony cultures remain undamaged by toxic chemicals and physical conditions, the use of the selection synchrony method proposed by Lloyd et al. (1975), may be better suited to producing synchronous cultures of amoebae for cell cycle monitoring.

It is therefore clear that not all methods have been tested on all amoebae and that one method might be suitable for one genus/species but not another. However, in order to fully evaluate the effect of C12 on the whole cell-cycle, synchronous cultures will have to be used (so a G1-phase is included) and it should be the cells that are analysed, not isolated nuclei.

5.8.2.2. Cell cycle analysis

The effect of C12 on the different phases of the cell cycle could potentially be performed with the use of Fluorescent Ubiquitination-based Cell Cycle Indicator (Fucci) which analyses whole cells. The cell nuclei, when treated with Fucci (and Fucci 2), fluoresce different colours in G1, S, G2 and M phases (Sakaue-Sawano et al., 2008; Mort et al., 2014) (**Figure 5.3)**. Although originally developed for mammalian cells (hence the long G1 phase in Figure 5.3), it has been used in non-mammalian cell types, e.g., zebrafish (z-Fucci) and Drosophila (Fly-Fucci) (Zielke and Edgar, 2015).

Fucci uses fluorescent probes fused with licensing factor Cdt1 and its inhibitor Geminin. In the original Fucci system monomeric Kusabira Orange (mKO2) and monomeric Azami Green (mAG) are fused to Cdt1 and Geminin respectively (Sakaue-Sawano et al., 2008). mKO2-Cdt1 peaks in G1 before DNA replication, resulting in a red phase, and begins to decline after initiation of S phase, whilst mAG-Geminin begins to increase in S phase, creating an orange phase. By G2, mKO2-Cdt1 has been degraded and as such mAG-Geminin is predominant, resulting in a green phase. Geminin degradation is high during mitosis and G1, allowing G1 to remain dominated by mKO2-Cdt1 (Sakaue-Sawano et al., 2008; Zielke and Edgar, 2015). It is possible to measure how long each stage takes by using Fucci and Fluorescence-activated cell sorting (FACS) machine.

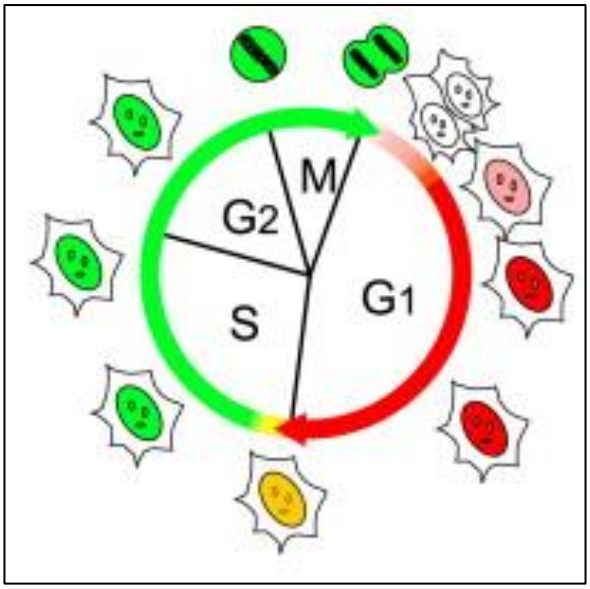

Figure 5.3. Fucci labels individual G1 phase nuclei in red and S phase nuclei in orange, with G2/M phase nuclei in green. Taken from Sakaue-Sawano et al., (2008).

Use of Fucci could be feasible with a synchronous amoeba cultures but as yet, there is no clear evidence that Cdt1 or Geminin homologues exist in amoebae (although the lack of homologues does not necessarily mean they are not present).

5.9 Conclusions and future impact

In conclusion, this work suggests amoebae HSL sensitivity is not correlated to phylogeny which begs the question, why are some amoebae are sensitive, and others are not?

One theory is that the plasma membrane composition is important for HSL interaction with crucial factors including hydrophobicity and the presence of appropriate membrane bound receptors. C12, HC12 and OC12 have different hydrophobicity values, and in contrast to previous work, this study suggests that hydrophobicity does not play a role in amoeba-HSL interaction. Instead suggesting the presence of a membrane bound receptor in this interaction, likely G_s GPCRs, with suggested G_s GPCRs in amoebae being beta-adrenergic receptors, amongst others. This study therefore supports the theory of membrane bound receptor HSL interaction.

C12 was found to cause instantaneous death at high concentrations, suggesting a necrosis pathway, but lower concentrations caused slow growth rates, suggesting an inhibition of cell proliferation pathway, most likely via cAMP mediated MEK/ERK. The ability of C12 to prevent the proliferation of certain amoebae by way of G_s GPCR activation, could allow C12

to be examined as an anti-cancer drug. OC12 has already been seen to inhibit the proliferation of breast cancer cell lines MCF-7, BR293 and MDA-MB-468 by way of STAT3 inhibition, as well as induce apoptosis in MCF-7 and MDA-MB-468 cells (Li et al., 2004).

Thus, the work performed in the current study and by others, suggest that long chain HSLs that have the ability to reduce cell proliferation and the possibility to induce cellular apoptosis, such as C12 and OC12, could be extremely useful interkingdom signalling molecules that could have implications for cancer treatments.

6. Acknowledgements

A massive thank you to Dr Jackie Parry for her continued support and help with this project, also a thank you to her husband, Mick, for building the level surface needed for the inoculation of each experiment, and a thank you to Janice Drinkall for her continued help with laboratory elements and help in maintenance of amoeba populations.

Also thank you to my family for their support through the struggles that I experienced over the course of this project. To my dad, for taking the time to help solve a structural engineering issue regarding the level surface and spirit leveller, the majority of the results of this project would not have been obtained without his help. To my Mum, for proof reading this thesis and helping me to explain topics more clearly, and to my brother, Andrew, who helped explain the chemical mechanisms of HSL degradation.

References

Abu Aboud, O., Wettersten, H. & Weiss, R. (2013) Inhibition of PPARα induces cell cycle arrest and apoptosis, and synergizes with glycolysis inhibition in kidney cancer cells. *PloS one,* 8(8)**,** e71115.

Ahmad, R. & Dalziel, J. (2020) G Protein-Coupled Receptors in Taste Physiology and Pharmacology. *Frontiers in pharmacology,* 11**,** 587664.

Al-Hammadi, I. (2020) *Actions of Cannabinoids on Amoebae.* PhD Lancaster University.

Al-Olayan, E., Williams, G. & Hurd, H. (2002) Apoptosis in the malaria protozoan, *Plasmodium berghei:* a possible mechanism for limiting intensity of infection in the mosquito. *International journal for parasitology,* 32(9)**,** 1133-1143.

Alberts, B., Johnson, A., Lewis, J., Raff, M., Roberts, K. & Walter, P. (2002) The Lipid Bilayer. *Molecular Biology of the Cell.* 4th ed. New York: Grand Science.

Aley, S., Scott, W. & Cohn, Z. (1980) Plasma membrane of *Entamoeba histolytica*. *The Journal of experimental medicine,* 152(2)**,** 391-404.

Alfiniyah, C., Bees, M. & Wood, A. *Quorum Machinery: Effect of the las System in rhl Regulation of P. aeruginosa*. AIP Conference Proceedings. 2019.

Allen, P. & Dawidowicz, E. (1990) Phagocytosis in *Acanthamoeba:* I. A mannose receptor is responsible for the binding and phagocytosis of yeast. *Journal of cellular physiology,* 145(3)**,** 508–513.

Alonso, S., Stange, M. & Beta, C. (2018) Modelling random crawling, membrane deformation and intracellular polarity of motile amoeboid cells. *PloS one,* 13(8)**,** e0201977.

Alsam, S., Sissons, J., Dudley, R. & Khan, N. (2005) Mechanisms associated with *Acanthamoeba castellanii* (T4) phagocytosis. *Parasitology research,* 96(6)**,** 402–409.

Alspaugh, J., Pukkila-Worley, R., Harashima, T., Cavallo, L., Funnell, D., Cox, G., Perfect, J., Kronstad, J. & Heitman, J. (2002) Adenylyl cyclase functions downstream of the Galpha protein Gpa1 and controls mating and pathogenicity of *Cryptococcus neoformans*. *Eukaryotic cell,* 1(1)**,** 75-84.

Anamika, K., Bhattacharya, A. & Srinivasan, N. (2008) Analysis of the protein kinome of *Entamoeba histolytica*. *Proteins,* 71(2)**,** 995-1006.

Anwar, A., Siddiqui, R. & Khan, N. (2020) Whole Organism Model to Study Molecular Mechanisms of Differentiation and Dedifferentiation. *Biology,* 9(4)**,** 79.

Aqeel, Y., Siddiqui, R., Manan, Z. & Khan, N. (2015) The role of G protein coupled receptor-mediated signaling in the biological properties of *Acanthamoeba castellanii o*f the T4 genotype. *Microbial pathogenesis,* 81**,** 22-27.

Arends, M. & Wyllie, A. (1991) Apoptosis: mechanisms and roles in pathology. *International review of experimental pathology,* 32**,** 223-254.

Austin, C. & Warren, L. (1983) Induced division synchrony in *Entamoeba histolytica.* Effects of hydroxyurea and serum deprivation. *The American journal of tropical medicine and hygiene,* 32(3)**,** 507-511.

Baig, A. (2016) Primary Amoebic Meningoencephalitis: Neurochemotaxis and Neurotropic Preferences of *Naegleria fowleri*. *ACS chemical neuroscience,* 7(8)**,** 1026–1029.

Baig, A. & Ahmad, H. (2017) Evidence of a M1-muscarinic GPCR homolog in unicellular eukaryotes: featuring *Acanthamoeba s*pp bioinformatics 3D-modelling and experimentations. *Journal of receptor and signal transduction research,* 37(3)**,** 267-275.

Baig, A., Rana, Z., Tariq, S., Lalani, S. & Ahmad, H. (2018) Traced on the Timeline: Discovery of Acetylcholine and the Components of the Human Cholinergic System in

a Primitive Unicellular Eukaryote *Acanthamoeba* spp. *ACS chemical neuroscience,* 9(3)**,** 494-504.
Balhouse, B., Patterson, L., Schmelz, E., Slade, D. & Verbridge, S. (2017) N-(3-oxododecanoyl)-L-homoserine lactone interactions in the breast tumor microenvironment: Implications for breast cancer viability and proliferation in vitro. *PloS one,* 12(7)**,** e0180372.
Bandara, H. M., Herpin, M. J., Kolacny, D., Harb, A., Romanovicz, D. & Smyth, H. D. (2016) Incorporation of Farnesol Significantly Increases the Efficacy of Liposomal Ciprofloxacin against *Pseudomonas aeruginosa* Biofilms in Vitro. *Molecular Pharmaceuticals,* 13(8)**,** 2760–2770.
Banerjee, S., Das, S. & Lohia, A. (2002) Eukaryotic checkpoints are absent in the cell division cycle of *Entamoeba histolytica*. *Journal of Biosciences* 27**,** 567-572.
Barnum, K. & O'connell, M. (2014) Cell cycle regulation by checkpoints. *Methods in molecular biology,* 1170**,** 29-40.
Bassler, B. L., Wright, M., Showalter, R. E. & Silverman, M. R. (1993) Intercellular signalling in *Vibrio harveyi:* sequence and function of genes regulating expression of luminescence. *Molecular Microbiology,* 9(4)**,** 773-786.
Basson, M. A. (2012) Signalling in cell differentiation and morphogenesis. *Cold Spring Harbour Perspectives in Biology,* 4(6)**,** a008151.
Bedi, B., Maurice, N. M., Ciavatta, V. T., Lynn, K. S., Yuan, Z., Molina, S. A., Joo, M., Tyor, W. R., Goldberg, J. B., Koval, M., Hart, C. M. & Sadikot, R. T. (2017) Peroxisome proliferator-activated receptor-γ agonists attenuate biofilm formation by *Pseudomonas aeruginosa*. *FASEB Journal,* 31(8)**,** 3608–3621.
Bedi, B., Yuan, Z., Joo, M., Zughaier, S. M., Goldberg, J. B., Arbiser, J. L., Hart, C. M. & Sadikot, R. T. (2016) Enhanced Clearance of *Pseudomonas aeruginosa* by Peroxisome Proliferator-Activated Receptor Gamma. *Infection and Immunity,* 84(7)**,** 1975-1985.
Bih, C., Chen, T., Nunn, A., Bazelot, M., Dallas, M. & Whalley, B. (2015) Molecular Targets of Cannabidiol in Neurological Disorders. *Neurotherapeutics,* 12(4)**,** 699-730.
Bosch, D., Jeck, W. & Siderovski, D. (2022) Self-activating G protein α subunits engage seven-transmembrane Regulator of G protein Signaling (RGS) proteins and a Rho guanine nucleotide exchange factor effector in the amoeba *Naegleria fowleri*. Journal of Biological Chemistry.
Bosch, D., Kimple, A., Muller, R., Giguère, P., Machius, M., Willard, F., Temple, B. & Siderovski, D. (2012) Heterotrimeric G-protein signaling is critical to pathogenic processes in *Entamoeba histolytica*. *PLoS pathogens,* 8(11)**,** e1003040.
Bosch, D. & Siderovski, D. (2013) G protein signaling in the parasite *Entamoeba histolytica*. *Experimental & molecular medicine,* 45(3)**,** e15.
Bozzaro, S. (2013) The Model Organism *Dictyostelium discoideum*. In: Eichinger, L. & Rivero, F. (eds.) *Dictyostelium discoideum Protocols, Methods in Molecular Biology.* Springer Science+Business Media.
Bradley, J., Reisert, J. & Frings, S. (2005) Regulation of cyclic nucleotide-gated channels. *Current opinion in neurobiology,* 15(3)**,** 343-349.
Bram, S. & Brachet, P. (1976) Inhibition of proliferation and differentiation of *Dictyostelium discoideum* by tetrahydrocannabinol and cannabinol. In: Nahas, G., Paton, W. & Idanpaan-Heikkila, J. (eds.) *Marihuana: chemistry, biochemistry and cellular effects.* New York: Springer-Verlag.
Bucknall, R., Moores, H., Simms, R. & Hesp, B. (1973) Antiviral effects of aphidicolin, a new antibiotic produced by *Cephalosporium aphidicola*. *Antimicrobial agents and chemotherapy,* 4(3)**,** 294-298.

Byers, T., Kim, B., King, L. & Hugo, E. (1991) Molecular aspects of the cell cycle and encystment of *Acanthamoeba*. *Reviews of infectious diseases,* 13**,** S373–S384.
Byers, T. J. (1986) Molecular Biology of DNA in *Acanthamoeba, Amoeba, Entamoeba,* and *Naegleria*. *International Review of Cytology,* 99**,** 311-341.
Bär, A., Phukan, N., Pinheiro, J. & Simoes-Barbosa, A. (2015) The Interplay of Host Microbiota and Parasitic Protozoans at Mucosal Interfaces: Implications for the Outcomes of Infections and Diseases. *PLoS neglected tropical diseases,* 9(12)**,** e0004176.
Bínová, E., Bína, D. & Nohýnková, E. (2021) DNA content in *Acanthamoeba* during two stress defense reactions: Encystation, pseudocyst formation and cell cycle. *European Journal of Protistology,* 77**,** 125745.
Cagnol, S. & Chambard, J. (2010) ERK and cell death: mechanisms of ERK-induced cell death--apoptosis, autophagy and senescence. *The FEBS journal,* 277(1)**,** 2-21.
Camilli, A. & Bassler, B. L. (2006) Bacterial small-molecule signaling pathways. *Science,* 311(5764)**,** 1113-1116.
Cao, L., Chen, F., Yang, X., Xu, W., Xie, J. & Yu, L. (2014) Phylogenetic analysis of CDK and cyclin proteins in premetazoan lineages. *BMC evolutionary biology,* 14**,** 10.
Cao, Z., Liao, Q., Su, M., Huang, K., Jin, J. & Cao, D. (2019) AKT and ERK dual inhibitors: The way forward? *Cancer letters,* 459**,** 30-40.
Carpenter, B., Nehmé, R., Warne, T., Leslie, A. & Tate, C. (2016) Structure of the adenosine A(2A) receptor bound to an engineered G protein. *Nature,* 536(7614)**,** 104-107.
Casares, D., Escribá, P. & Rosselló, C. (2019) Membrane Lipid Composition: Effect on Membrane and Organelle Structure, Function and Compartmentalization and Therapeutic Avenues. *International journal of molecular sciences,* 20(9)**,** 2167.
Castellanos-Castro, S., Bolaños, J. & Orozco, E. (2020) Lipids in *Entamoeba histolytica*: Host-Dependence and Virulence Factors. *Frontiers in cellular and infection microbiology,* 10**,** 75.
Castillo-Juárez, I., Maeda, T., Mandujano-Tinoco, E., Tomás, M., Pérez-Eretza, B., García-Contreras, S., Wood, T. & García-Contreras, R. (2015) Role of quorum sensing in bacterial infections. *World journal of clinical cases,* 3(7)**,** 575–598.
Chan, K., Atkinson, S., Mathee, K., Sam, C., Chhabra, S., Cámara, M., Koh, C. & Williams, P. (2011) Characterization of *N*-acylhomoserine lactone-degrading bacteria associated with the *Zingiber officinale* (ginger) rhizosphere: Co-existence of quorum quenching and quorum sensing in *Acinetobacter* and *Burkholderia*. *BMC Microbiology,* 11**,** 51.
Charlton, T. S., De Nys, R., Netting, A., Kumar, N., Hentzer, M., Givskov, M. & Kjelleberg, S. (2000) A novel and sensitive method for the quantification of *N*-3-oxo-acylhomoserine lactones using gas chromatography-mass spectrometry: application to a model bacterial biofilm. *Environmental Microbiology,* 2**,** 530 –541.
Chen, G., Shaulsky, G. & Kuspa, A. (2004) Tissue-specific G1-phase cell-cycle arrest prior to terminal differentiation in *Dictyostelium*. *Development,* 131(11)**,** 2619-2630.
Chen, J., Lee, C. & Chern, Y. (2014) Chapter One - Adenosine Receptor Neurobiology: Overview. *International Review of Neurobiology,* 119**,** 1-49.
Cheng, X. & Ferrell, J. (2018) Apoptosis propagates through the cytoplasm as trigger waves. *Science,* 361(6402)**,** 607–612.
Chhabra, S. R., Harty, C., Hooi, D. S., Daykin, M., Williams, P., Telford, G., Pritchard, D. I. & Bycroft, B. W. (2003) Synthetic analogues of the bacterial signal (quorum sensing) molecule N-(3-oxododecanoyl)-L-homoserine lactone as immune modulators. *Journal of Medicinal Chemistry,* 46(1)**,** 97-104.

Chin, K., Yang, W., Ravatn, R., Kita, T., Reitman, E., Vettori, D., Cvijic, M., Shin, M. & Iacono, L. (2002) Reinventing the wheel of cyclic AMP: novel mechanisms of cAMP signaling. *Annals of the New York Academy of Sciences,* 968**,** 49-64.

Chinetti, G., Fruchart, J. & Staels, B. (2000) Peroxisome proliferator-activated receptors (PPARs): nuclear receptors at the crossroads between lipid metabolism and inflammation. *Inflammation Research,* 49(10)**,** 497-505.

Churchill, M. & Chen, L. (2011) Structural basis of acyl-homoserine lactone-dependent signaling. *Chemical reviews,* 111(1)**,** 68-85.

Clarke, M., Lohan, A., Liu, B., Lagkouvardos, I., Roy, S., Zafar, N., Bertelli, C., Schilde, C., Kianianmomeni, A., Bürglin, T., Frech, C., Turcotte, B., Kopec, K., Synnott, J., Choo, C., Paponov, I., Finkler, A., Heng Tan, C., Hutchins, A., Weinmeier, T., Rattei, T., Chu, J., Gimenez, G., Irimia, M., Rigden, D., Fitzpatrick, D., Lorenzo-Morales, J., Bateman, A., Chiu, C., Tang, P., Hegemann, P., Fromm, H., Raoult, D., Greub, G., Miranda-Saavedra, D., Chen, N., Nash, P., Ginger, M., Horn, M., Schaap, P., Caler, L. & Loftus, B. (2013) Genome of *Acanthamoeba castellanii* highlights extensive lateral gene transfer and early evolution of tyrosine kinase signaling. *Genome biology,* 14(2)**,** R11.

Communal, C., Singh, K., Sawyer, D. & Colucci, W. (1999) Opposing effects of beta(1)- and beta(2)-adrenergic receptors on cardiac myocyte apoptosis : role of a pertussis toxin-sensitive G protein. *Circulation,* 100(22)**,** 2210-2212.

Cooley, M., Chhabra, S. R. & Williams, P. (2008) N-Acylhomoserine Lactone-Mediated Quorum Sensing: A Twist in the Tail and a Blow for Host Immunity. *Chemistry & Biology,* 15(11)**,** 1141-1147.

Cooley, M., Whittall, C. & Rolph, M. (2010) *Pseudomonas* signal molecule 3-oxo-C12-homoserine lactone interferes with binding of rosiglitazone to human PPARγ. *Microbes and infection,* 12(3)**,** 231-237.

Cooper, S. (2001) Revisiting the relationship of the mammalian G1 phase to cell differentiation. *Journal of theoretical biology,* 208(4)**,** 399-402.

Coppi, A., Merali, S. & Eichinger, D. (2002) The enteric parasite *Entamoeba* uses an autocrine catecholamine system during differentiation into the infectious cyst stage. *The Journal of biological chemistry,* 277(10)**,** 8083-8090.

Coquant, G., Grill, J. & Seksik, P. (2020) Impact of N -Acyl-Homoserine Lactones, Quorum Sensing Molecules, on Gut Immunity. *Frontiers in immunology,* 11**,** 1827.

Cornillon, S., Foa, C., Davoust, J., Buonavista, N., Gross, J. & Golstein, P. (1994) Programmed cell death in *Dictyostelium*. *Journal of cell science,* 107**,** 2691-2704.

Cosson, P., Zulianello, L., Join-Lambert, O., Faurisson, F., Gebbie, L., Benghezal, M., Van Delden, C., Curty, L. & Köhler, T. (2002) *Pseudomonas aeruginosa* virulence analyzed in a *Dictyostelium discoideum* host system. *Journal of bacteriology,* 184(11)**,** 3027-3033.

Csaba, G., Muzsnai, A., László, V. & Darvas, Z. (1984) A New Method for the Quantitative Determination of Phagocytosis in Amoeba Effect of histamine on the phagocytotic capacity of *Amoeba proteus*. *Cytologia,* 49(4)**,** 691-695.

Cugini, C., Calfee, M., Farrow, J., Morales, D., Pesci, E. & Hogan, D. (2007) Farnesol, a common sesquiterpene, inhibits PQS production in *Pseudomonas aeruginosa*. *Molecular microbiology,* 65(4)**,** 896–906.

Cussac, D., Boutet-Robinet, E., Ailhaud, M., Newman-Tancredi, A., Martel, J., Danty, N. & Rauly-Lestienne, I. (2008) Agonist-directed trafficking of signalling at serotonin 5-HT2A, 5-HT2B and 5-HT2C-VSV receptors mediated Gq/11 activation and calcium mobilisation in CHO cells. *European journal of pharmacology,* 594(1-3)**,** 32-38.

Cussac, D., Newman-Tancredi, A., Duqueyroix, D., Pasteau, V. & Millan, M. (2002) Differential activation of Gq/11 and Gi(3) proteins at 5-hydroxytryptamine(2C) receptors revealed by antibody capture assays: influence of receptor reserve and relationship to agonist-directed trafficking. *Molecular pharmacology,* 62(3)**,** 578-589.

Cutler, A. & Davies, K. (1998) Antigen Clearance. *In:* Delves, P. (ed.) *Encyclopaedia of Immunology* Second ed.: Elsevier Academic Press.

Danilov, V., Zavilgelsky, G., Zarubina, A. & Mazhul, M. (2008) The role of *luxCDE* genes in bioluminescence of bacteria. *Moscow University Biological Sciences Bulletin,* 63(2)**,** 57-61.

Das, S., Stevens, T., Castillo, C., Villasenõr, A., Arredondo, H. & Reddy, K. (2002) Lipid metabolism in mucous-dwelling amitochondriate protozoa. *International journal for parasitology,* 32(6)**,** 655-675.

Das, T., Sabir, S., Chen, R., Farrell, J., Kriel, F., Whiteley, G., Glasbey, T., Manos, J., Willcox, M. & Kumar, N. (2022) Halogenated Dihydropyrrol-2-One Molecules Inhibit Pyocyanin Biosynthesis by Blocking the *Pseudomonas* Quinolone Signalling System. *Molecules,* 27(4)**,** 1169.

Davis, B., Jensen, R., Williams, P. & O'shea, P. (2010) The interaction of *N*-acylhomoserine lactone quorum sensing signaling molecules with biological membranes: implications for inter-kingdom signaling. *PloS one,* 5(10)**,** e13522.

Davis, B., Richens, J. & O'shea, P. (2011) Label-free critical micelle concentration determination of bacterial quorum sensing molecules. *Biophysical journal,* 101(1)**,** 245-254.

Davis, P., Ho, A. & Dowdy, S. (2001) Biological methods for cell-cycle synchronization of mammalian cells. *BioTechniques,* 30(6)**,** 1322-1331.

Dayel, M., Holleran, E. & Mullins, R. (2001) Arp2/3 complex requires hydrolyzable ATP for nucleation of new actin filaments. *Proceedings of the National Academy of Sciences of the United States of America,* 98(26)**,** 14871–14876.

De Bentzmann, S. & Plésiat, P. (2011) The *Pseudomonas aeruginosa* opportunistic pathogen and human infections. *Environmental microbiology,* 13(7)**,** 1655–1665.

De Carvalho Clímaco, M., De Oliveira, Y., Ramos, A., Ramos-De-Souza, J., Silva, A., Jain, S., Rott, M., Scher, R., Correa, C., Barbosa, A. & Dolabella, S. (2022) Nisin Induces Cell-Cycle Arrest in Free-Living Amoebae *Acanthamoeba castellanii*. *Acta parasitologica,* 67(1)**,** 511-517.

De Oliveira, P., Ramos, M., Amaro, A., Dias, R. & Vieira, S. (2019) Gi/o-Protein Coupled Receptors in the Aging Brain. *Frontiers in aging neuroscience,* 11**,** 89.

De Oliveira, S. & Saldanha, C. (2010) An overview about erythrocyte membrane. *Clinical hemorheology and microcirculation,* 44(1)**,** 63-74.

Declerck, P., Behets, J., De Keersmaecker, B. & Ollevier, F. (2007) Receptor-mediated uptake of *Legionella pneumophila* by *Acanthamoeba castellanii* and *Naegleria lovaniensis*. *Journal of applied microbiology,* 103(6)**,** 2697–2703.

Defronzo, R., Ferrannini, E., Groop, L., Henry, R., Herman, W., Holst, J., Hu, F., Kahn, C., Raz, I., Shulman, G., Simonson, D., Testa, M. & Weiss, R. (2015) Type 2 diabetes mellitus. *Nature Reviews Disease Primers,* 1**,** 15019.

Dey, R., Pernin, P. & Bodennec, J. (2010) Endocannabinoids inhibit the growth of free-living amoebae. *Antimicrobial agents and chemotherapy,* 54(7)**,** 3065-3067.

Dhanasekaran, N., Tsim, S., Dermott, J. & Onesime, D. (1998) Regulation of cell proliferation by G proteins. *Oncogene,* 17(11)**,** 1383-1394.

Dharmawardhane, S., Cubitt, A., Clark, A. & Firtel, R. (1994) Regulatory role of the G alpha 1 subunit in controlling cellular morphogenesis in *Dictyostelium*. *Development,* 120(12)**,** 3549–3561.

Di Pizio, A., Levit, A., Slutzki, M., Behrens, M., Karaman, R. & Niv, M. (2016) Comparing Class A GPCRs to bitter taste receptors: Structural motifs, ligand interactions and agonist-to-antagonist ratios. *Methods in cell biology,* 132**,** 401–427.

Dibartolo, N. & Booth, P. (2012) The Membrane Factor: Biophysical Studies of Alpha Helical Transmembrane Protein Folding. In: Egelman, E. (ed.) *Comprehensive Biophysics.* Elsevier.

Dictybase (2019) *Gene Information for gpaA.* Available at: http://dictybase.org/gene/DDB_G0283349 [Accessed 24th June 2022].

Duc, N. M., Kim, H. R. & Chung, K. Y. (2015) Structural mechanism of G protein activation by G protein-coupled receptor. *European journal of pharmacology,* 763**,** 214–222.

Dumaz, N. & Marais, R. (2005) Integrating signals between cAMP and the RAS/RAF/MEK/ERK signalling pathways. *FEBS Journal,* 272**,** 3491-3504.

Dushek, O., Mueller, S., Soubies, S., Depoil, D., Caramalho, I., Coombs, D. & Valitutti, S. (2008) Effects of intracellular calcium and actin cytoskeleton on TCR mobility measured by fluorescence recovery. *PloS one,* 3(12)**,** e3913.

Dvorak, J., Kobayashi, S., Alling, D. & Hallahan, C. (1995) Elucidation of the DNA Synthetic Cycle of *Entamoeba* Spp. Using Flow Cytometry and Mathematical Modeling. *Eukaryotic Microbiology,* 42(5)**,** 610-616.

Eichinger, L., Pachebat, J., Glöckner, G., Rajandream, M., Sucgang, R., Berriman, M., Song, J., Olsen, R., Szafranski, K., Xu, Q., Tunggal, B., Kummerfeld, S., Madera, M., Konfortov, B., Rivero, F., Bankier, A., Lehmann, R., Hamlin, N., Davies, R., Gaudet, P., Fey, P., Pilcher, K., Chen, G., Saunders, D., Sodergren, E., Davis, P., Kerhornou, A., Nie, X., Hall, N., Anjard, C., Hemphill, L., Bason, N., Farbrother, P., Desany, B., Just, E., Morio, T., Rost, R., Churcher, C., Cooper, J., Haydock, S., Van Driessche, N., Cronin, A., Goodhead, I., Muzny, D., Mourier, T., Pain, A., Lu, M., Harper, D., Lindsay, R., Hauser, H., James, K., Quiles, M., Madan Babu, M., Saito, T., Buchrieser, C., Wardroper, A., Felder, M., Thangavelu, M., Johnson, D., Knights, A., Loulseged, H., Mungall, K., Oliver, K., Price, C., Quail, M., Urushihara, H., Hernandez, J., Rabbinowitsch, E., Steffen, D., Sanders, M., Ma, J., Kohara, Y., Sharp, S., Simmonds, M., Spiegler, S., Tivey, A., Sugano, S., White, B., Walker, D., Woodward, J., Winckler, T., Tanaka, Y., Shaulsky, G., Schleicher, M., Weinstock, G., Rosenthal, A., Cox, E., Chisholm, R., Gibbs, R., Loomis, W., Platzer, M., Kay, R., Williams, J., Dear, P., Noegel, A., Barrell, B. & Kuspa, A. (2005) The genome of the social amoeba *Dictyostelium discoideum*. *Nature,* 435(7038)**,** 43-57.

Eickhoff, M. & Bassler, B. (2018) SnapShot: Bacterial Quorum Sensing. *Cell,* 174(5)**,** 1328.

Elgaml, A., Higaki, K. & Miyoshi, S. (2014) Effects of temperature, growth phase and *luxO*-disruption on regulation systems of toxin production in *Vibrio vulnificus* strain L-180, a human clinical isolate. *World Journal of Microbiology & Biotechnology,* 30(2)**,** 681–691.

Elmore, S. (2007) Apoptosis: a review of programmed cell death. *Toxicologic pathology,* 35(4)**,** 495-516.

Eum, S., Jaraki, D., Bertrand, L., András, I. & Toborek, M. (2014) Disruption of epithelial barrier by quorum-sensing *N*-3-(oxododecanoyl)-homoserine lactone is mediated by matrix metalloproteinases. *The American Journal of Physiology-Gastrointestinal and Liver Physiology,* 306(11)**,** G992–G1001.

Evans, R. M., Barish, G. D. & Wang, Y.-X. (2004) PPARs and the complex journey to obesity. *Nature medicine,* 10(4)**,** 355–361.

Evtikhov, N., Pérez-Pérez, A., Jiménez-Cortegana, C., Carmona-Fernández, A., Vilariño-García, T. & Sánchez-Margalet, V. (2017) Pancreastatin Signaling. Mechanisms of Action. *Reference Module in Neuroscience and Biobehavioral Psychology.* Elsevier.

Federle, M. & Bassler, B. (2003) Interspecies communication in bacteria. *The Journal of clinical investigation,* 112(9)**,** 1291–1299.
Feng, J., Zhu, R., Jiang, F., Xie, J., Gao, C., Li, M., Jin, H. & Fu, D. (2020) Melittin-encapsulating peptide hydrogels for enhanced delivery of impermeable anticancer peptides. *Biomaterials science,* 8**,** 4559.
Feng, Y., Hsiao, Y., Chen, H., Chu, C., Tang, P. & Chiu, C. (2009) Apoptosis-like cell death induced by *Salmonella* in *Acanthamoeba rhysodes*. *Genomics,* 94(2)**,** 132-137.
Fouque, E., Trouilhé, M.-C., Thomas, V., Hartemann, P., Rodier, M.-H. & Héchard, Y. (2012) Cellular, biochemical, and molecular changes during encystment of free-living amoebae. *Eukaryotic cell,* 11(4)**,** 382-387.
Frans, I., Michiels, C. W., Bossier, P., Willems, K. A., Lievens, B. & Rediers, H. (2011) *Vibrio anguillarum* as a fish pathogen: virulence factors, diagnosis and prevention. *Journal of Fish Diseases,* 34**,** 643-661.
Frederick, J. & Eichinger, D. (2004) *Entamoeba invadens c*ontains the components of a classical adrenergic signaling system. *Molecular and biochemical parasitology,* 137(2)**,** 339-343.
Freeman, S. & Grinstein, S. (2014) Phagocytosis: receptors, signal integration, and the cytoskeleton. *Immunological reviews,* 262(1)**,** 193-215.
Fritz-Laylin, L., Prochnik, S., Ginger, M., Dacks, J., Carpenter, M., Field, M., Kuo, A., Paredez, A., Chapman, J., Pham, J., Shu, S., Neupane, R., Cipriano, M., Mancuso, J., Tu, H., Salamov, A., Lindquist, E., Shapiro, H., Lucas, S., Grigoriev, I., Zacheus Cande, W., Fulton, C., Rokhsar, D. & Dawson, S. (2010) The genome of *Naegleria gruberi i*lluminates early eukaryotic versatility. *Cell,* 140(5)**,** 631-642.
Fukushima, N., Kohno, M., Kato, T., Kawamoto, S., Okuda, K., Misu, Y. & Ueda, H. (1998) Melittin, a metabostatic peptide inhibiting Gs activity. *Peptides,* 19(5)**,** 811–819.
Gadgaard, C. & Jensen, A. (2020) Functional characterization of 5-HT1A and 5-HT1B serotonin receptor signaling through G-protein-activated inwardly rectifying K+ channels in a fluorescence-based membrane potential assay. *Biochemical pharmacology,* 175**,** 113870.
Gahan, C., Patel, S., Boursier, M., Nyffeler, K., Jennings, J., Abbott, N., Blackwell, H., Van Lehn, R. & Lynn, D. (2020) Bacterial Quorum Sensing Signals Self-Assemble in Aqueous Media to Form Micelles and Vesicles: An Integrated Experimental and Molecular Dynamics Study. *The journal of physical chemistry B,* 124(18)**,** 3616-3628.
Gaida, M., Dapunt, U. & Hänsch, G. (2016) Sensing developing biofilms: the bitter receptor T2R38 on myeloid cells. *Pathogens and disease,* 74(3)**,** ftw004.
Galicia-Garcia, U., Benito-Vicente, A., Jebari, S., Larrea-Sebal, A., Siddiqi, H., Uribe, K., Ostolaza, H. & Martín, C. (2020) Pathophysiology of Type 2 Diabetes Mellitus. *International journal of molecular sciences,* 21(17)**,** 6275.
Gangopadhyay, S., Ray, S., Kennady, K., Pande, G. & Lohia, A. (1997) Heterogeneity of DNA content and expression of cell cycle genes in axenically growing *Entamoeba histolytica* HM1:IMSS clone A. *Molecular and biochemical parasitology,* 90(1)**,** 9-20.
Gao, Z., Inoue, A. & Jacobson, K. (2018) On the G protein-coupling selectivity of the native A2B adenosine receptor. *Biochemical pharmacology,* 151**,** 201–213.
Gervois, P., Torra, I. P., Fruchart, J. C. & Staels, B. (2000) Regulation of lipid and lipoprotein metabolism by PPAR activators. *Clinical chemistry and laboratory medicine,* 38(1)**,** 3-11.
Gilbert, S. (2000) *Developmental Biology.* Sixth ed. Sunderland, Massachusetts: Sinauer Associates Inc.

Gloerich, M. & Bos, J. (2010) Epac: defining a new mechanism for cAMP action. *Annual review of pharmacology and toxicology,* 50**,** 355-375.
Godinho, R., Duarte, T. & Pacini, E. (2015) New perspectives in signaling mediated by receptors coupled to stimulatory G protein: the emerging significance of cAMP efflux and extracellular cAMP-adenosine pathway. *Frontiers in pharmacology,* 6**,** 58.
Gonzalez-Iglesias, A., Murano, T., Li, S., Tomić, M. & Stojilkovic, S. (2008) Dopamine inhibits basal prolactin release in pituitary lactotrophs through pertussis toxin-sensitive and -insensitive signaling pathways. *Endocrinology,* 149(4)**,** 1470-1479.
González, I., Desponds, C., Schaff, C., Mottram, J. & Fasel, N. (2007) Leishmania major metacaspase can replace yeast metacaspase in programmed cell death and has arginine-specific cysteine peptidase activity. *International journal for parasitology,* 37(2)**,** 161-172.
Gotthardt, D., Blancheteau, V., Bosserhoff, A., Ruppert, T., Delorenzi, M. & Soldati, T. (2006) Proteomics fingerprinting of phagosome maturation and evidence for the role of a G alpha during uptake. *Molecular & cellular proteomics,* 5(12)**,** 2228–2243.
Gotthardt, D., Warnatz, H. J., Henschel, O., Brückert, F., Schleicher, M. & Soldati, T. (2002) High-resolution dissection of phagosome maturation reveals distinct membrane trafficking phases. *Molecular biology of the cell,* 13(10)**,** 3508-3520.
Griffiths, A. J. (1969) Encystment in Amoebae. In: Rose, A. H. & Wilkinson, J. F. (eds.) *Advances in Microbial Physiology.* Academic Press.
Grygiel-Górniak, B. (2014) Peroxisome proliferator-activated receptors and their ligands: nutritional and clinical implications - a review. *Nutrition Journal,* 13**,** 17.
Gu, C., Ma, Y., Benjamin, J., Littman, D., Chao, M. & Huang, X. (2000) Apoptotic signaling through the beta -adrenergic receptor. A new Gs effector pathway. *The Journal of biological chemistry,* 275(27)**,** 20726–20733.
Guidotti, G. (1972) Membrane Proteins. *Annual Review of Biochemistry,* 41**,** 731-752.
Hadwiger, J., Lee, S. & Firtel, R. (1994) The G alpha subunit G alpha 4 couples to pterin receptors and identifies a signaling pathway that is essential for multicellular development in *Dictyostelium*. *Proceedings of the National Academy of Sciences of the United States of America,* 91(22)**,** 10566–10570.
Hadwiger, J., Wilkie, T., Strathmann, M. & Firtel, R. (1991) Identification of *Dictyostelium G* alpha genes expressed during multicellular development. *Proceedings of the National Academy of Sciences of the United States of America,* 88(18)**,** 8213-8217.
Haga, T. (2013) Molecular properties of muscarinic acetylcholine receptors. *Proceedings of the Japan Academy Series B, Physical and biological sciences,* 89(6)**,** 226-256.
Hancock, J. (2017) *Cell Signalling.* Fourth ed. Oxford: Oxford University Press.
Hawver, L., Jung, S. & Ng, W. (2016) Specificity and complexity in bacterial quorum-sensing systems. *FEMS microbiology reviews,* 40(5)**,** 738–752.
He, S., Wang, L., Miao, L., Wang, T., Du, F., Zhao, L. & Wang, X. (2009) Receptor interacting protein kinase-3 determines cellular necrotic response to TNF-alpha. *Cell,* 137(6)**,** 1100-1111.
Heming, M., Gran, S., Jauch, S. L., Fischer-Riepe, L., Russo, A., Klotz, L., Hermann, S., Schäfers, M., Roth, J. & Barczyk-Kahlert, K. (2018) Peroxisome Proliferator-Activated Receptor-γ Modulates the Response of Macrophages to Lipopolysaccharide and Glucocorticoids. *Frontiers in Immunology,* 9**,** 893.
Hentzer, M., Riedel, K., Rasmussen, T., Heydorn, A., Andersen, J., Parsek, M., Rice, S., Eberl, L., Molin, S., Høiby, N., Kjelleberg, S. & Givskov, M. (2002) Inhibition of quorum sensing in *Pseudomonas aeruginosa* biofilm bacteria by a halogenated furanone compound. *Microbiology,* 148(1)**,** 87–102.

Hershko, A. (1997) Roles of ubiquitin-mediated proteolysis in cell cycle control. *Current opinion in cell biology,* 9(6)**,** 788-799.
Hogan, D. A., Vik, A. & Kolter, R. (2004) A *Pseudomonas aeruginosa* quorum-sensing molecule influences *Candida albicans* morphology. *Molecular microbiology,* 54(5)**,** 1212–1223.
Hollmann, M., Strumper, D., Herroeder, S. & Durieux, M. (2005) Receptors, G proteins, and their interactions. *Anesthesiology,* 103(5)**,** 1066–1078.
Holzer, P. (2009) Opioid receptors in the gastrointestinal tract. *Regulatory peptides,* 155(1-3)**,** 11-17.
Hooi, D., Bycroft, B., Chhabra, S., Williams, P. & Pritchard, D. (2004) Differential immune modulatory activity of Pseudomonas aeruginosa quorum-sensing signal molecules. *Infection and immunity,* 72(11)**,** 6463-6470.
Huber, R. (2014) The cyclin-dependent kinase family in the social amoebozoan *Dictyostelium discoideum*. *Cellular and molecular life sciences,* 71(4)**,** 629-639.
Hughes, D. & Sperandio, V. (2008) Inter-kingdom signalling: communication between bacteria and their hosts. *Nature Reviews Microbiology,* 6**,** 111–120.
Hur, J., Kang, M., Park, J., Lee, S., Bae, Y., Lee, S., Park, Y. & Kwak, J. (2003) Pro-apoptotic effect of high concentrations of histamine on human neutrophils. *International immunopharmacology,* 3(10-11)**,** 1491-1502.
Huynh, T. (2008) *The Effects of Pseudomonas aeruginosa Quorum Sensing Signalling Molecules on Human T cell Function.* PhD University of Nottingham.
Jaggupilli, A., Singh, N., Cruz De Jesus, V., Duan, K. & Chelikani, P. (2018) Characterization of the Binding Sites for Bacterial Acyl Homoserine Lactones (AHLs) on Human Bitter Taste Receptors (T2Rs). *ACS Infectious Diseases,* 4(7)**,** 1146-1156.
Jahoor, A., Patel, R., Bryan, A., Do, C., Krier, J., Watters, C., Wahli, W., Li, G., Williams, S. C. & Rumbaugh, K. P. (2008) Peroxisome proliferator-activated receptors mediate host cell proinflammatory responses to *Pseudomonas aeruginosa* autoinducer. *Journal of Bacteriology,* 190(13)**,** 4408-4415.
Jaisswar, C. (2020) *Study of the effects of the Cannabinoids Anandamide and Cannabidiol on the feeding processes of Tetrahymena pyriformis.* MSc by Research Lancaster University.
Jamasbi, E., Batinovic, S., Sharples, R., Sani, M., Robins-Browne, R., Wade, J., Separovic, F. & Hossain, M. (2014) Melittin peptides exhibit different activity on different cells and model membranes. *Amino acids,* 46(12)**,** 2759–2766.
Janeway, C. A., Travers, P., Walport, M., & Shlomchik, M. (eds.) (2001). *Immunobiology: The Immune System in Health and Disease*. 5th ed. New York: Garland Science.
Jansen, R., Santana-Molina, C., Van Den Noort, M., Devos, D. & Van Der Klei, I. (2021) Comparative Genomics of Peroxisome Biogenesis Proteins: Making Sense of the PEX Proteins. *Frontiers in cell and developmental biology,* 9**,** 654163.
Jantzen, H., Schulze, I. & Stöhr, M. (1990) The importance of mitotic control for establishment of developmental competence in *Acanthamoeba castellanii*. *Journal of Cell Science,* 97**,** 715-724.
Jelinek, V., Mösslein, N. & Bünemann, M. (2021) Structures in G proteins important for subtype selective receptor binding and subsequent activation. *Communications biology,* 4(1)**,** 635.
Jin, G., Liu, F., Ma, H., Hao, S., Zhao, Q., Bian, Z., Jia, Z. & Song, S. (2012) Two G-protein-coupled-receptor candidates, Cand2 and Cand7, are involved in *Arabidopsis* root growth mediated by the bacterial quorum-sensing signals *N*-acyl-homoserine lactones. *Biochemical and biophysical research communications,* 417(3)**,** 991–995.

Joint , I., Tait , K., Callow , M., Callow , J., Milton , D., Williams , P. & Cámara, M. (2002) Cell-to-cell communication across the prokaryote-eukaryote boundary. *Science,* 298(5596)**,** 1207.

Joint, I., Tait, K. & Wheeler, G. (2007) Cross-kingdom signalling: exploitation of bacterial quorum sensing molecules by the green seaweed *Ulva*. *Philosophical transactions of the Royal Society of London. Series B, Biological sciences,* 362(1483)**,** 1223–1233.

Kaczor, A., Bartuzi, D. & Matosiuk, D. (2014) Modeling the Active Conformation of Human μ Opioid Receptor. *Letters in Drug Design & Discovery,* 11(9)**,** 1053-1061.

Kaneshiro, E. (1995) Amoeboid Movement, Cilia, and Flagella. In: Sperelakis, N. (ed.) *Cell Physiology Source Book.* Elsevier Academic Press.

Kaplan, H. B. & Greenberg, E. P. (1985) Diffusion of autoinducer is involved in regulation of the *Vibrio fischeri l*uminescence system. *Journal of Bacteriology,* 163(3)**,** 1210-1214.

Karlsson, T., Turkina, M., Yakymenko, O., Magnusson, K. & Vikström, E. (2012) The *Pseudomonas aeruginosa N*-acyl homoserine lactone quorum sensing molecules target IQGAP1 and modulate epithelial cell migration. *PLoS pathogens,* 8(10)**,** e1002953.

Kaufmann, G., Sartorio, R., Lee, S., Rogers, C., Meijler, M., Moss, J., Clapham, B., Brogan, A., Dickerson, T. & Janda, K. (2005) Revisiting quorum sensing: Discovery of additional chemical and biological functions for 3-oxo-N-acylhomoserine lactones. *Proceedings of the National Academy of Sciences of the United States of America,* 102(2)**,** 309-314.

Kendall, M. & Sperandio, V. (2016) What a Dinner Party! Mechanisms and Functions of Interkingdom Signaling in Host-Pathogen Associations. *mBio,* 7(2)**,** e01748.

Kennedy, A., Sundström, L., Geschwinder, A., Poon, E., Jiang, Y., Chen, R., Cooke, R., Johnstone, S., Madin, A., Lim, J., Liu, Q., Lohman, R., Nordqvist, A., Fridén-Saxin, M., Yang, W., Brown, D., Fairlie, D. & Dekker, N. (2020) Protease-activated receptor-2 ligands reveal orthosteric and allosteric mechanisms of receptor inhibition. *Communications Biology* 3(1)**,** 782.

Khambati, I., Han, S., Pijnenburg, D., Jang, H. & Forsythe, P. (2017) The bacterial quorum-sensing molecule, *N*-3-oxo-dodecanoyl-L-homoserine lactone, inhibits mediator release and chemotaxis of murine mast cells. *Inflammation Research,* 66**,** 259–268.

Khan, N. A. & Siddiqui, R. (2015) Is there evidence of sexual reproduction (meiosis) in *Acanthamoeba? Pathogens and Global Health,* 109(4)**,** 193-195.

King, S. & Hyams, J. (1982) Synchronisation of mitosis in a cell division cycle mutant of *Schizosaccharomyces pombe* released from temperature arrest. *Canadian Journal of Microbiology,* 28(2)**,** 261-264.

Kobilka, B. K. (2007) G Protein Coupled Receptor Structure and Activation. *Biochimica et biophysica acta,* 1768(4)**,** 794–807.

Koley, D. & Bard A. J. (2010) Triton X-100 concentration effects on membrane permeability of a single HeLa cell by scanning electrochemical microscopy (SECM). PNAS 107 (39) 16783–16787

Korn, E. & Wright, P. (1973) Macromolecular Composition of an *Amoeba* Plasma Membrane. *The Journal of Biological Chemistry,* 248(2), 439-447.

Kosakivska, I., Babenko, L., Romanenko, K. & Futorna, O. (2020) Effects of exogenous bacterial quorum sensing signal molecule (messenger) N-hexanoyl-L-homoserine lactone (C6-HSL) on morphological and physiological responses of winter wheat under simulated acid rain. *Dopovidi Nacional ' noï akademiï nauk Ukraïni,* 8**,** 92-100.

Kostetsky, E., Chopenko, N., Barkina, M., Velansky, P. & Sanina, N. (2018) Fatty Acid Composition and Thermotropic Behavior of Glycolipids and Other Membrane Lipids

of *Ulva lactuca* (Chlorophyta) Inhabiting Different Climatic Zones. *Marine drugs,* 16(12)**,** 494.
Kostetsky, E., Goncharova, S., Sanina, N. & Shnyrov, V. (2004) Season influence on lipid composition of marine macrophytes. *Botanica Marina,* 47**,** 134-139.
Kostiou, V., Theodoropoulou, M. & Hamodrakas, S. (2016) GprotPRED: Annotation of Gα, Gβ and Gγ subunits of G-proteins using profile Hidden Markov Models (pHMMs) and application to proteomes. *Biochimica et biophysica acta,* 1864(5)**,** 435-440.
Koutsogiannis, Z., Macleod, E. & Maciver, S. (2019) G418 induces programmed cell death in *Acanthamoeba* through the elevation of intracellular calcium and cytochrome c translocation. *Parasitology research,* 118(2)**,** 641-651.
Kreinest, T., Volkmer, I. & Staege, M. (2020) Melittin Increases Cisplatin Sensitivity and Kills KM-H2 and L-428 Hodgkin Lymphoma Cells. *International journal of molecular sciences,* 22(1)**,** 343.
Krishna Murti, C. & Shukla, O. (1984) Differentiation of pathogenic amoebae: encystation and excystation of *Acanthamoeba culbertsoni* — A model. *Journal of Biosciences,* 6(4)**,** 475-489.
Kumar, S. R., Bryan, J. N., Eaton, A. M., Robinson, K. L. & Gajagowni, S. (2018) Differential Modulation of Transcription Factors and Cytoskeletal Proteins in Prostate Carcinoma Cells by a Bacterial Lactone. *Biomed Research International* 2018**,** 6430504.
Kung, A., Zetterberg, A., Sherwood, S. & Schimke, R. (1990) Cytotoxic effects of cell cycle phase specific agents: result of cell cycle perturbation. *Cancer research,* 50(22)**,** 7307-7317.
Lamin, A., Kaksonen, A., Cole, I. & Chen, X. (2022) Quorum sensing inhibitors applications: A new prospect for mitigation of microbiologically influenced corrosion. *Bioelectrochemistry,* 145**,** 108050.
Lancaster, C. E., Fountain, A., Dayam, R. M., Somerville, E., Sheth, J., Jacobelli, V., Somerville, A., Terebiznik, M. R. & Botelho, R. J. (2021) Phagosome resolution regenerates lysosomes and maintains the degradative capacity in phagocytes. *The Journal of cell biology,* 220(9)**,** e202005072.
Lee, G., Elwood, F., Mcnally, J., Weiszmann, J., Lindstrom, M., Amaral, K., Nakamura, M., Miao, S., Cao, P., Learned, R., Chen, J. & Li, Y. (2002a) T0070907, a selective ligand for peroxisome proliferator-activated receptor gamma, functions as an antagonist of biochemical and cellular activities. *The Journal of biological chemistry,* 277(22)**,** 19649–19657.
Lee, J. & Zhang, L. (2015) The hierarchy quorum sensing network in *Pseudomonas aeruginosa*. *Protein & cell,* 6(1)**,** 26-41.
Lee, N., Bertholet, S., Debrabant, A., Muller, J., Duncan, R. & Nakhasi, H. (2002b) Programmed cell death in the unicellular protozoan parasite *Leishmania*. *Cell death and differentiation,* 9(1)**,** 53-64.
Lee, N., Gannavaram, S., Selvapandiyan, A. & Debrabant, A. (2007) Characterization of metacaspases with trypsin-like activity and their putative role in programmed cell death in the protozoan parasite *Leishmania*. *Eukaryotic cell,* 6(10)**,** 1745-1757.
Lee, R., Chen, B., Redding, K., Margolskee, R. & Cohen, N. (2014) Mouse nasal epithelial innate immune responses to *Pseudomonas aeruginosa* quorum-sensing molecules require taste signalling components. *Innate immunity,* 20(6)**,** 606-617.
Leesnitzer, L., Parks, D., Bledsoe, R., Cobb, J., Collins, J., Consler, T., Davis, R., Hull-Ryde, E., Lenhard, J., Patel, L., Plunket, K., Shenk, J., Stimmel, J., Therapontos, C., Willson, T. & Blanchard, S. (2002) Functional consequences of cysteine modification

in the ligand binding sites of peroxisome proliferator activated receptors by GW9662. *Biochemistry,* 41(21)**,** 6640–6650.
Lehmann, D., Seneviratne, A. & Smrcka, A. (2008) Small molecule disruption of G protein beta gamma subunit signalling inhibits neutrophil chemotaxis and inflammation. *Molecular pharmacology,* 73(2)**,** 410–418.
Leonhardt, I., Spielberg, S., Weber, M., Albrecht-Eckardt, D., Bläss, M., Claus, R., Barz, D., Scherlach, K., Hertweck, C., Löffler, J., Hünniger, K. & Kurzai, O. (2015) The fungal quorum-sensing molecule farnesol activates innate immune cells but suppresses cellular adaptive immunity. *mBio,* 6(2)**,** e00143.
Levin, R., Grinstein, S. & Canton, J. (2016) The life cycle of phagosomes: formation, maturation, and resolution. *Immunological reviews,* 273(1)**,** 156-179.
Li, H., Wang, L., Ye, L., Mao, Y., Xie, X., Xia, C., Chen, J., Lu, Z. & Song, J. (2009) Influence of *Pseudomonas aeruginosa* quorum sensing signal molecule *N*-(3-oxododecanoyl) homoserine lactone on mast cells. *Medical microbiology and immunology,* 198(2)**,** 113-121.
Li, L., Hooi, D., Chhabra, S., Pritchard, D. & Shaw, P. (2004) Bacterial N-acylhomoserine lactone-induced apoptosis in breast carcinoma cells correlated with down-modulation of STAT3. *Oncogene,* 23(28)**,** 4894-4902.
Li, P., Snyder, G. & Vanover, K. (2016) Dopamine Targeting Drugs for the Treatment of Schizophrenia: Past, Present and Future. *Current topics in medicinal chemistry,* 16(29)**,** 3385–3403.
Li, Z. & Nair, S. (2012) Quorum sensing: how bacteria can coordinate activity and synchronize their response to external signals? *Protein Science,* 21(10)**,** 1403-1417.
Liu, F., Bian, Z., Jia, Z., Zhao, Q. & Song, S. (2012) The GCR1 and GPA1 participate in promotion of *Arabidopsis* primary root elongation induced by *N*-acyl-homoserine lactones, the bacterial quorum-sensing signals. *Molecular plant-microbe interactions,* 25(5)**,** 677-683.
Liu, J., Fu, K., Wu, C., Qin, K., Li, F. & Zhou, L. (2018) "In-Group" Communication in Marine *Vibrio*: A Review of *N*-Acyl Homoserine Lactones-Driven Quorum Sensing. *Frontiers in cellular and infection microbiology,* 8**,** 139.
Liu, Y., Wang, X., Dong, D., Guo, L., Dong, X., Leng, J., Zhao, B., Guo, Y. & Zhang, N. (2021) Research Advances in Heterotrimeric G-Protein α Subunits and Uncanonical G-Protein Coupled Receptors in Plants. *International Journal of Molecular Sciences,* 22(16)**,** 8678.
Lloyd, D., John, L., Edwards, C. & Chagla, A. (1975) Synchronous Cultures of Micro-organisms: Large-scale Preparation by Continuous-flow Size Selection. *Microbiology,* 88(1).
Lohia, A. (2003) The cell cycle of *Entamoeba histolytica*. *Molecular and cellular biochemistry,* 253(1-2)**,** 217–222.
Lomovatskaya, L., Romanenko, A., Filinova, N. & Salyaev, R. (2011) Influence of exopolysaccharides of the ring rot pathogen on the kinetic parameters of adenylate cyclases in potato plants. *Doklady Biological Sciences,* 441**,** 404-407.
Lou, L., Urbani, J., Ribeiro-Neto, F. & Altschuler, D. (2002) cAMP inhibition of Akt is mediated by activated and phosphorylated Rap1b. *The Journal of biological chemistry,* 277(36)**,** 32799–32806.
Lu, Q., Lin, Y., Yang, X., Liu, W., Zhang, X., Huang, D. & Zhong, H. (2012) Regulation on expression of toll-like receptors on monocytes after stimulation with the 3-o-C12-HSL molecule from *Pseudomonas aeruginosa*. *Current microbiology,* 65(4)**,** 384-389.

Ludewig-Klingner, A., Michael, V., Jarek, M., Brinkmann, H. & Petersen, J. (2018) Distribution and Evolution of Peroxisomes in Alveolates (Apicomplexa, Dinoflagellates, Ciliates). *Genome biology and evolution,* 10(1)**,** 1-13.

Luquet, S., Gaudel, C., Holst, D., Lopez-Soriano, J., Jehl-Pietri, C., Fredenrich, A. & Grimaldi, P. A. (2005) Roles of PPAR delta in lipid absorption and metabolism: a new target for the treatment of type 2 diabetes. *Biochimica et Biophysia Acta (BBA) - Molecular Basis of Disease,* 1740(2)**,** 313-317.

Ma, H., Yanofsky, M. & Meyerowitz, E. (1990) Molecular cloning and characterization of GPA1, a G protein alpha subunit gene from *Arabidopsis thaliana*. *Proceedings of the National Academy of Sciences of the United States of America,* 87(10)**,** 3821-3825.

Maciver, S. K., Koutsogiannis, Z. & De Obeso Fernández Del Valle, A. (2019) Meiotic genes are constitutively expressed in an asexual amoeba and are not necessarily involved in sexual reproduction. *Biology letters,* 15(3)**,** 20180871.

Maeda, Y. (1986) A New Method for Inducing Synchronous Growth of *Dictyostelium discoideum* Cells Using Temperature Shifts. *Journal of General Microbiology,* 132**,** 1189-1196.

Malumbres, M. (2011) Physiological relevance of cell cycle kinases. *Physiological reviews,* 91(3)**,** 973-1007.

Manefield, M., De Nys, R., Naresh, K., Roger, R., Givskov, M., Peter, S. & Kjelleberg, S. (1999) Evidence that halogenated furanones from *Delisea pulchra* inhibit acylated homoserine lactone (AHL)-mediated gene expression by displacing the AHL signal from its receptor protein. *Microbiology,* 145(2)**,** 283–291.

Mangmool, S. & Kurose, H. (2011) G(i/o) protein-dependent and -independent actions of Pertussis Toxin (PTX). *Toxins,* 3(7)**,** 884–899.

Maton, A., Lahart, D., Hopkins, J., Warner, M., Johnson, S. & Wright, J. (1997) *Cells: Building Blocks of Life.* New Jersey: Prentice Hall.

Maurer, S., Wabnitz, G., Kahle, N., Stegmaier, S., Prior, B., Giese, T., Gaida, M., Samstag, Y. & Hänsch, G. (2015) Tasting *Pseudomonas aeruginosa* Biofilms: Human Neutrophils Express the Bitter Receptor T2R38 as Sensor for the Quorum Sensing Molecule *N*-(3-Oxododecanoyl)-l-Homoserine Lactone. *Frontiers in immunology,* 6**,** 369.

Mcalester, G., O'gara, F. & Morrissey, J. P. (2008) Signal-mediated interactions between *Pseudomonas aeruginosa* and *Candida albicans*. *Journal of Medical Microbiology,* 57**,** 563-569.

Mcclean, D. & Zimmerman, A. (1976) Action of delta 9-tetrahydrocannabinol on cell division and macromolecular synthesis in division-synchronized protozoa. *Pharmacology,* 14(4)**,** 307-321.

Mcknight, S., Iglewski, B. & Pesci, E. (2000) The *Pseudomonas* quinolone signal regulates rhl quorum sensing in *Pseudomonas aeruginosa*. *Journal of bacteriology,* 182(10)**,** 2702-2708.

Mebratu, Y. & Tesfaigzi, Y. (2009) How ERK1/2 activation controls cell proliferation and cell death: Is subcellular localization the answer? *Cell cycle,* 8(8)**,** 1168-1175.

Medina, G., Flores-Martin, S., Fonseca, B., Otth, C. & Fernandez, H. (2014) Mechanisms associated with phagocytosis of *Arcobacter butzleri* by *Acanthamoeba castellanii*. *Parasitology Research,* 113**,** 1933–1942.

Mengue, L., Régnacq, M., Aucher, W., Portier, E., Héchard, Y. & Samba-Louaka, A. (2016) *Legionella pneumophila* prevents proliferation of its natural host *Acanthamoeba castellanii*. *Scientific reports,* 6**,** 36448.

Meslin, B., Barnadas, C., Boni, V., Latour, C., De Monbrison, F., Kaiser, K. & Picot, S. (2007) Features of apoptosis in *Plasmodium falciparum* erythrocytic stage through a

putative role of PfMCA1 metacaspase-like protein. *The Journal of infectious diseases,* 195(12)**,** 1852-1859.
Miller, M. & Bassler, B. (2001) Quorum sensing in bacteria. *Annual Review of Microbiology,* 55**,** 165-199.
Milligan, G. & Kostenis, E. (2006) Heterotrimeric G-proteins: a short history. *British journal of pharmacology,* 147**,** S46–S55.
Mort, R., Ford, M., Sakaue-Sawano, A., Lindstrom, N., Casadio, A., Douglas, A., Keighren, M., Hohenstein, P., Miyawaki, A. & Jackson, I. (2014) Fucci2a: a bicistronic cell cycle reporter that allows Cre mediated tissue specific expression in mice. *Cell cycle,* 13(17)**,** 2681-2696.
Murad, H., Hawat, M., Ekhtiar, A., Aljapawe, A., Abbas, A., Darwish, H., Sbenati, O. & Ghannam, A. (2016) Induction of G1-phase cell cycle arrest and apoptosis pathway in MDA-MB-231 human breast cancer cells by sulfated polysaccharide extracted from *Laurencia papillosa*. *Cancer cell international,* 16**,** 39.
Mühl, H., Nitsch, D., Sandau, K., Brüne, B., Varga, Z. & Pfeilschifter, J. (1996) Apoptosis is triggered by the cyclic AMP signalling pathway in renal mesangial cells. *FEBS letters,* 382(3)**,** 271-275.
Nasser, W. & Reverchon, S. (2007) New insights into the regulatory mechanisms of the LuxR family of quorum sensing regulators. *Analytical and bioanalytical chemistry,* 387(2)**,** 381-390.
Nealson, K. H., Platt, T. & Hastings, J. W. (1970) Cellular Control of the Synthesis and Activity of the Bacterial Luminescent System. *Journal of Bacteriology,* 104(1)**,** 313-322.
Nguewa, P., Fuertes, M., Valladares, B., Alonso, C. & Pérez, J. (2004) Programmed cell death in trypanosomatids: a way to maximize their biological fitness? *Trends in parasitology,* 20(8)**,** 375-380.
Nyholm, T. & Slotte, J. P. (2001) Comparison of Triton X-100 Penetration into Phosphatidylcholine and Sphingomyelin Mono- and Bilayers. Langmuir, 17 (16), 4724-4730.
Olie, R., Durrieu, F., Cornillon, S., Loughran, G., Gross, J., Earnshaw, W. & Golstein, P. (1998) Apparent caspase independence of programmed cell death in *Dictyostelium*. *Current biology,* 8(17)**,** 955-958.
Pacheco, A. R. & Sperandio, V. (2009) Inter-kingdom signaling: chemical language between bacteria and host. *Current Opinion in Microbiology,* 12(2)**,** 192-198.
Palkar, P., Borland, M., Naruhn, S., Ferry, C., Lee, C., Sk, U., Sharma, A., Amin, S., Murray, I., Anderson, C., Perdew, G., Gonzalez, F., Müller, R. & Peters, J. (2010) Cellular and pharmacological selectivity of the peroxisome proliferator-activated receptor-beta/delta antagonist GSK3787. *Molecular pharmacology,* 78(3)**,** 419–430.
Pan, M., Xu, X., Chen, Y. & Jin, T. (2016) Identification of a Chemoattractant G-Protein-Coupled Receptor for Folic Acid that Controls Both Chemotaxis and Phagocytosis. *Developmental cell,* 36(4)**,** 428–439.
Pan, P., Hall, E. & Bonner, J. (1972) Folic acid as second chemotactic substance in the cellular slime moulds. *Nature: New biology,* 237(75)**,** 181–182.
Papenfort, K. & Bassler, B. (2016) Quorum sensing signal-response systems in Gram-negative bacteria. *Nature Reviews; Microbiology,* 14(9)**,** 576–588.
Patzelt, D., Wang, H., Buchholz, I., Rohde, M., Gröbe, L., Pradella, S., Neumann, A., Schulz, S., Heyber, S., Münch, K., Münch, R., Jahn, D., Wagner-Döbler, I. & Tomasch, J. (2013) You are what you talk: quorum sensing induces individual morphologies and cell division modes in *Dinoroseobacter shibae*. *The ISME journal,* 7(12)**,** 2274-2286.

Pauwels, A. M., Trost, M., Beyaert, R. & Hoffmann, E. (2017) Patterns, Receptors, and Signals: Regulation of Phagosome Maturation. *Trends in immunology,* 38(6)**,** 407-422.

Pearson, G., Robinson, F., Beers Gibson, T., Xu, B., Karandikar, M., Berman, K. & Cobb, M. (2001) Mitogen-activated protein (MAP) kinase pathways: regulation and physiological functions. *Endocrine reviews,* 22(2)**,** 153-183.

Pereira, C., Thompson, J. & Xavier, K. (2013) AI-2-mediated signalling in bacteria. *FEMS microbiology reviews,* 37(5)**,** 156–181.

Pernin, P., Ataya, A. & Cariou, M. L. (1992) Genetic structure of natural populations of the free-living amoeba, *Naegleria lovaniensis.* Evidence for sexual reproduction. *Heredity,* 68**,** 173–181.

Pesci, E., Milbank, J., Pearson, J., Mcknight, S., Kende, A., Greenberg, E. & Iglewski, B. (1999) Quinolone signaling in the cell-to-cell communication system of *Pseudomonas aeruginosa*. *Proceedings of the National Academy of Sciences of the United States of America,* 96(20)**,** 11229–11234.

Peters, B., Jabra-Rizk, M., O'may, G., Costerton, J. & Shirtliff, M. (2012) Polymicrobial interactions: impact on pathogenesis and human disease. *Clinical microbiology reviews,* 25(1)**,** 193–213.

Pickup, Z., Pickup, R. & Parry, J. (2007) A comparison of the growth and starvation responses of *Acanthamoeba castellanii* and *Hartmannella vermiformis* in the presence of suspended and attached *Escherichia coli* K12. *FEMS microbiology ecology,* 59(3)**,** 556–563.

Pierce, K., Premont, R. & Lefkowitz, R. (2002) Seven-transmembrane receptors. *Nature reviews. Molecular cell biology,* 3(9)**,** 639-650.

Pines, J. (1995) Cyclins and cyclin-dependent kinases: a biochemical view. *The Biochemical journal,* 308**,** 697-711.

Plouffe, B. & Tiberi, M. (2013) Functional analysis of human D1 and D5 dopaminergic G protein-coupled receptors: lessons from mutagenesis of a conserved serine residue in the cytosolic end of transmembrane region 6. *Methods in molecular biology,* 964**,** 141-180.

Podlipaeva, Y., Demin, S. & Goodkov, A. (2013) New method for cell cycle synchronization in *Amoeba proteus* culture. *Protistology,* 8(1)**,** 3-7.

Polke, M., Leonhardt, I., Kurzai, O. & Jacobsen, I. (2018) Farnesol signalling in *Candida albicans* - more than just communication. *Critical reviews in microbiology,* 44(2)**,** 230-243.

Prescott, R. & Decho, A. (2020) Flexibility and Adaptability of Quorum Sensing in Nature. *Trends in microbiology,* 28(6)**,** 436–444.

Pringle, H., Bradley, S. & Harris, L. (1979) Susceptibility of *Naegleria fowleri t*o delta 9-tetrahydrocannabinol. *Antimicrobial agents and chemotherapy,* 16(5)**,** 674-679.

Proskuryakov, S., Konoplyannikov, A. & Gabai, V. (2003) Necrosis: a specific form of programmed cell death? *Experimental cell research,* 283(1)**,** 1-16.

Pupillo, M., Insall, R., Pitt, G. & Devreotes, P. (1992) Multiple cyclic AMP receptors are linked to adenylyl cyclase in *Dictyostelium*. *Molecular biology of the cell,* 3(11)**,** 1229-1234.

Pupillo, M., Kumagai, A., Pitt, G., Firtel, R. & Devreotes, P. (1989) Multiple alpha subunits of guanine nucleotide-binding proteins in *Dictyostelium*. *Proceedings of the National Academy of Sciences of the United States of America,* 86(13)**,** 4892–4896.

Pérez-Posada, A., Dudin, O., Ocaña-Pallarès, E., Ruiz-Trillo, I. & Ondracka, A. (2020) Cell cycle transcriptomics of *Capsaspora* provides insights into the evolution of cyclin-CDK machinery. *PLoS genetics,* 16(3)**,** e1008584.

Qazi, B. S., Tang, K. & Qazi, A. (2011) Recent Advances in Underlying Pathologies Provide Insight into Interleukin-8 Expression-Mediated Inflammation and Angiogenesis. *International Journal of Inflammation,* 2011**,** 908468.

Quinn, P., Chapman, D. & Keith, A. (1980) The Dynamics Of Membrane Structure. *CRC Critical Reviews in Biochemistry,* 8(1)**,** 1-117.

Radhakrishnan, K., Halász, Á., Vlachos, D. & Edwards, J. S. (2010) Quantitative understanding of cell signaling: the importance of membrane organization. *Current opinion in biotechnology,* 21(5)**,** 677-682.

Raistrick, H. (2022) N-dodecanoyl Homoserine Lactones Reduce Population Growth of *Naegleria gruberi* Via Binding of G Protein-Coupled Receptors Containing the Gαs subunit. Lancaster University.

Ramage, G., Saville, S. P., Wickes, B. L. & López-Ribot, J. L. (2002) Inhibition of *Candida albicans* biofilm formation by farnesol, a quorum-sensing molecule. *Applied and Environmental Microbiology,* 68(11)**,** 5459–5463.

Rasmussen, T., Manefield, M., Andersen, J., Eberl, L., Anthoni, U., Christophersen, C., Steinberg, P., Kjelleberg, S. & Givskov, M. (2000) How *Delisea pulchra* furanones affect quorum sensing and swarming motility in *Serratia liquefaciens* MG1. *Microbiology,* 146(12)**,** 3237–3244.

Reuter, K., Steinbach, A. & Helms, V. (2016) Interfering with Bacterial Quorum Sensing. *Perspectives in medicinal chemistry,* 8**,** 1–15.

Roberts, P. & Der, C. (2007) Targeting the Raf-MEK-ERK mitogen-activated protein kinase cascade for the treatment of cancer. *Oncogene,* 26(22)**,** 3291-3310.

Rosa, I., Atella, G. & Benchimol, M. (2014) T*ritrichomonas foetus* displays classical detergent-resistant membrane microdomains on its cell surface. *Protist,* 165(3)**,** 293-304.

Rosenbaum, D. M., Rasmussen, S. G. & Kobilka, B. K. (2009) The structure and function of G-protein-coupled receptors. *Nature,* 459(7245)**,** 356-363.

Rutherford, S. T. & Bassler, B. L. (2012) Bacterial quorum sensing: its role in virulence and possibilities for its control. *Cold Spring Harbor perspectives in medicine,* 2(11)**,** a012427.

Sadana, R. & Dessauer, C. (2009) Physiological roles for G protein-regulated adenylyl cyclase isoforms: insights from knockout and overexpression studies. *Neurosignals,* 17**,** 5-22.

Saheb, E., Trzyna, W. & Bush, J. (2014) Caspase-like proteins: *Acanthamoeba castellanii* metacaspase and *Dictyostelium discoideum* paracaspase, what are their functions? *Journal of biosciences,* 39(5)**,** 909-916.

Sakaue-Sawano, A., Kurokawa, H., Morimura, T., Hanyu, A., Hama, H., Osawa, H., Kashiwagi, S., Fukami, K., Miyata, T., Miyoshi, H., Imamura, T., Ogawa, M., Masai, H. & Miyawaki, A. (2008) Visualizing spatiotemporal dynamics of multicellular cell-cycle progression. *Cell,* 132(3)**,** 487–498.

Sanders, R. (2021) Protists: Flagellates and Amoebae☆ , ***. *Reference Module in Earth Systems and Environmental Sciences.* Elsevier.

Schuster, M. & Greenberg, E. (2006) A network of networks: quorum-sensing gene regulation in *Pseudomonas aeruginosa*. *International journal of medical microbiology,* 296(2-3)**,** 73-81.

Sebolt-Leopold, J., Dudley, D., Herrera, R., Van Becelaere, K., Wiland, A., Gowan, R., Tecle, H., Barrett, S., Bridges, A., Przybranowski, S., Leopold, W. & Saltiel, A. (1999) Blockade of the MAP kinase pathway suppresses growth of colon tumors in vivo. *Nature medicine,* 5(7)**,** 810-816.

Sebolt-Leopold, J. & Herrera, R. (2004) Targeting the mitogen-activated protein kinase cascade to treat cancer. *Nature reviews Cancer,* 4(12)**,** 937-947.
See-Too, W., Convey, P., Pearce, D. & Chan, K. (2018) Characterization of a novel N-acylhomoserine lactonase, AidP, from Antarctic P*lanococcus sp. Microbial cell factories,* 17(1)**,** 179.
Senoo, H., Sesaki, H. & Iijima, M. (2016) A GPCR Handles Bacterial Sensing in Chemotaxis and Phagocytosis. *Developmental Cell,* 36(4)**,** 354-356.
Servant, G., Weiner, O., Herzmark, P., Balla, T., Sedat, J. & Bourne, H. (2000) Polarization of chemoattractant receptor signalling during neutrophil chemotaxis. *Science,* 287(5455)**,** 1037-1040.
Shimizu, H., Baba, N., Nose, T., Taguchi, R., Tanaka, S., Joe, G., Maseda, H., Nomura, N., Hagio, M., Lee, J., Fukiya, S., Yokota, A., Ishizuka, S. & Miyazaki, H. (2015) Activity of ERK regulates mucin 3 expression and is involved in undifferentiated Caco-2 cell death induced by 3-oxo-C12-homoserine lactone. *Bioscience, biotechnology, and biochemistry,* 79(6)**,** 937-942.
Shiner, E., Rumbaugh, K. & Williams, S. (2005) Inter-kingdom signaling: deciphering the language of acyl homoserine lactones. *FEMS microbiology reviews,* 29(5)**,** 935–947.
Shiner, E. K., Terentyev, D., Bryan, A., Sennoune, S., Martinez-Zaguilan, R., Li, G., Gyorke, S., Williams, S. C. & Rumbaugh, K. P. (2006) *Pseudomonas aeruginosa* autoinducer modulates host cell responses through calcium signalling. *Cellular Microbiology,* 8(10)**,** 1601-1610.
Shrestha, A. & Schikora, A. (2020) AHL-priming for enhanced resistance as a tool in sustainable agriculture. *FEMS microbiology ecology,* 96(12)**,** fiaa226.
Silvestro, S., Schepici, G., Bramanti, P. & Mazzon, E. (2020) Molecular Targets of Cannabidiol in Experimental Models of Neurological Disease. *Molecules,* 25(21)**,** 5186.
Simpson, A. (2003) Cytoskeletal organization, phylogenetic affinities and systematics in the contentious taxon Excavata (Eukaryota). *International Journal of Systematic and Evolutionary Microbiology,* 53(6)**,** 1759–1777.
Singh, P. K., Schaefer, A. L., Parsek, M. R., Moninger, T. O., Welsh, M. J. & Greenberg, E. P. (2000) Quorum-sensing signals indicate that cystic fibrosis lungs are infected with bacterial biofilms. *Nature,* 407(6805)**,** 762-764.
Singh, R., Baghel, R., Reddy, C. & Jha, B. (2015) Effect of quorum sensing signals produced by seaweed-associated bacteria on carpospore liberation from *Gracilaria dura*. *Frontiers in plant science,* 6**,** 117.
Smirnov, A. (2002) Re-description of *Vannella mira* Schaffer 1926 (Gymnamoebia, Vannellidae), an often mentioned but poorly known amoebae species *Protistology,* 2(3)**,** 178-184.
Smirnov, A. (2008) Amoebas, Lobose. *Encyclopedia of Microbiology.* 1st ed.: Oxford : Elsevier.
Smirnov, A. (2012) Chapter 14: Amoebas, Lobose. *Eukaryotic microbes.* Elsevier.
Smirnov, A. & Brown, S. (2004) Guide to the methods of study and identification of soil gymnamoebae. *Protistology,* 3(3)**,** 148-190.
Smirnov, A., Chao, E., Nassonova, E. & Cavalier-Smith, T. (2011) A revised classification of naked lobose amoebae (Amoebozoa: lobosa). *Protist,* 162(4)**,** 545–570.
Smirnova, T. & Segall, J. (2007) Amoeboid chemotaxis: future challenges and opportunities. *Cell adhesion & migration,* 1(4)**,** 165-170.
Sommer, A., Fries, A., Cornelsen, I., Speck, N., Koch-Nolte, F., Gimpl, G., Andrä, J., Bhakdi, S. & Reiss, K. (2012) Melittin modulates keratinocyte function through P2

receptor-dependent ADAM activation. *The Journal of biological chemistry,* 287(28)**,** 23678–23689.

Song, D., Meng, J., Cheng, J., Fan, Z., Chen, P., Ruan, H., Tu, Z., Kang, N., Li, N., Xu, Y., Wang, X., Shu, F., Mu, L., Li, T., Ren, W., Lin, X., Zhu, J., Fang, X., Amrein, M., Wu, W., Yan, L., Lü, J., Xia, T. & Shi, Y. (2019) *Pseudomonas aeruginosa* quorum-sensing metabolite induces host immune cell death through cell surface lipid domain dissolution. *Nature microbiology,* 4(1)**,** 97-111.

Song, S., Jia, Z., Xu, J., Zhang, Z. & Bian, Z. (2011) N-butyryl-homoserine lactone, a bacterial quorum-sensing signaling molecule, induces intracellular calcium elevation in *Arabidopsis* root cells. *Biochemical and biophysical research communications,* 414(2)**,** 355–360.

Soto, M., Calatrava-Morales, N. & López-Lara, I. (2019) Functional Roles of Non-membrane Lipids in Bacterial Signaling. In: Geiger, O. (ed.) *Biogenesis of Fatty Acids, Lipids and Membranes.* First ed.: Springer.

Stöhr, M., Bommert, K., Schulze, I. & Jantzen, H. (1987) The cell cycle and itsrelationship to development in *Acanthamoeba castellanii*. *Journal of Cell Science,* 88**,** 579-589.

Sullivan, A. M. (2017) Neuronal Signalling: an introduction. *Neuronal Signalling,* 1(1)**,** NS20160025.

Sunahara, R. & Taussig, R. (2002) Isoforms of mammalian adenylyl cyclase: multiplicities of signaling. *Molecular interventions,* 2(3)**,** 168-184.

Szallies, A., Kubata, B. & Duszenko, M. (2002) A metacaspase of *Trypanosoma brucei* causes loss of respiration competence and clonal death in the yeast *Saccharomyces cerevisiae*. *FEBS letters,* 517(1-3)**,** 144-150.

Szczepański, K., Kwapiszewska, K. & Hołyst, R. (2019) Stability of cytoplasmic nanoviscosity during cell cycle of HeLa cells synchronized with Aphidicolin. *Scientific reports , 9 (1), 16486.* , 9(1)**,** 16486.

Taguchi, R., Tanaka, S., Joe, G. H., Maseda, H., Nomura, N., Ohnishi, J., Ishizuka, S., Shimizu, H. & Miyazaki, H. (2014) Mucin 3 is involved in intestinal epithelial cell apoptosis via *N*-(3-oxododecanoyl)-L-homoserine lactone-induced suppression of Akt phosphorylation. *American Journal of Physiology; Cell Physiology,* 307(2)**,** C162-168.

Tait, K. & Havenhand, J. (2013) Investigating a possible role for the bacterial signal molecules *N*-acylhomoserine lactones in *Balanus improvisus* cyprid settlement. *Molecular Ecology,* 22(9)**,** 2588–2602.

Tait, K., Joint, I., Daykin, M., Milton, D., Williams, P. & Cámara, M. (2005) Disruption of quorum sensing in seawater abolishes attraction of zoospores of the green alga *Ulva* to bacterial biofilms. *Environmental Microbiology,* 7(2)**,** 229-240.

Tanase, C. P., Ogreseanu, T. & Badiu, C. (2012) Signal Transduction; G protein Coupled Receptors. *Molecular Pathology of Pituitary Adenomas.* 1st ed.: Elsevier Insights.

Tao, S., Xiong, Y., Han, D., Pi, Y., Zhang, H. & Wang, J. (2021) N-(3-oxododecanoyl)-l-homoserine lactone disrupts intestinal epithelial barrier through triggering apoptosis and collapsing extracellular matrix and tight junction. *Journal of cellular physiology,* 236(8)**,** 5771-5784.

Tariqul Islam, A., Yue, H., Scavello, M., Haldeman, P., Rappel, W. & Charest, P. (2018) The cAMP-induced G protein subunits dissociation monitored in live *Dictyostelium* cells by BRET reveals two activation rates, a positive effect of caffeine and potential role of microtubules. *Cellular signalling,* 48**,** 25-37.

Tateda, K., Ishii, Y., Horikawa, M., Matsumoto, T., Miyairi, S., Pechere, J. C., Standiford, T. J., Ishiguro, M. & Yamaguchi, K. (2003) The *Pseudomonas aeruginosa* autoinducer

N-3-oxododecanoyl homoserine lactone accelerates apoptosis in macrophages and neutrophils. *Infection and Immunity,* 71(10)**,** 5785-5793.
Tilley, D. (2011) G protein-dependent and G protein-independent signalling pathways and their impact on cardiac function. *Circulation Research,* 109(2)**,** 217-230.
Tims, N. (2021) *An Investigation into the Molecular Targets Mediating Cannabidiol Action in the Free-living Ciliate Tetrahymena pyriformis.* MSc by Research Lancaster University.
Tizzano, M., Gulbransen, B., Vandenbeuch, A., Clapp, T., Herman, J., Sibhatu, H., Churchill, M., Silver, W., Kinnamon, S. & Finger, T. (2010) Nasal chemosensory cells use bitter taste signalling to detect irritants and bacterial signals. *Proceedings of the National Academy of Sciences of the United States of America,* 107(7)**,** 3210-3215.
Tobita, N., Tsuneto, K., Ito, S. & Yamamoto, T. (2022) Human TRPV1 and TRPA1 are receptors for bacterial quorum sensing molecules. *Journal of biochemistry,* 170(6)**,** 775–785.
Tocris (2019) *Product Datasheet; Melittin*. Available at: https://www.tocris.com/products/melittin_1193 [Accessed 14th December 2021].
Tocris (2021) *Product Datasheet; Pertussis Toxin*. Available at: https://www.tocris.com/products/pertussis-toxin_3097 [Accessed 14th December 2021].
Toki, S., Donati, R. J., & Rasenick, M. M. (1999). Treatment of C6 glioma cells and rats with antidepressant drugs increases the detergent extractionof Gsα from plasma membrane. Journal of Neurochemostry, 73, 1114 – 1120.
Topf, P. & Stockem, W. (1996) Protein and lipid composition of the cell surface complex from *Amoeba proteus* (Rhizopoda: Amoebida). *European Journal of Protistology,* 32**,** 156-170.
Trzyna, W., Legras, X. & Cordingley, J. (2008) A type-1 metacaspase from *Acanthamoeba castellanii*. *Microbiological research,* 163(4)**,** 414-423.
Turkina, M. & Vikström, E. (2019) Bacteria-Host Crosstalk: Sensing of the Quorum in the Context of *Pseudomonas aeruginosa* Infections. *Journal of innate immunity,* 11(3)**,** 263–279.
Tyagi, S., Gupta, P., Saini, A. S., Kaushal, C. & Sharma, S. (2011) The peroxisome proliferator-activated receptor: A family of nuclear receptors role in various diseases. *Journal of advanced pharmaceutical technology & research,* 2(4)**,** 236-240.
Ulsamer, A., Wright, P., Wetzel, M. & Korn, E. (1971) Plasma and phagosome membranes of *Acanthamoeba castellanii*. *The Journal of cell biology,* 51(1)**,** 193-215.
Umemoto, T. & Fujiki, Y. (2012) Ligand-dependent nucleo-cytoplasmic shuttling of peroxisome proliferator-activated receptors, PPARα and PPARγ. *Genes to cells:devoted to molecular & cellular mechanisms,* 17(7)**,** 576-596.
Unsworth, A., Flora, G. & Gibbins, J. (2018) Non-genomic effects of nuclear receptors: insights from the anucleate platelet. *Cardiovascular research,* 114(5)**,** 645–655.
Uren, A., O'rourke, K., Aravind, L., Pisabarro, M., Seshagiri, S., Koonin, E. & Dixit, V. (2000) Identification of paracaspases and metacaspases: two ancient families of caspase-like proteins, one of which plays a key role in MALT lymphoma. *Molecular cell,* 6(4)**,** 961-967.
Uroz, S., Chhabra, S., Cámara, M., Williams, P., Oger, P. & Dessaux, Y. (2005) *N*-Acylhomoserine lactone quorum-sensing molecules are modified and degraded by *Rhodococcus erythropolis* W2 by both amidolytic and novel oxidoreductase activities. *Microbiology,* 151(10)**,** 3313-3322.

Van Vliet, H., Spies, F., Linnemans, W., Klepke, A., Op Den Kamp, J. & Van Deenen, L. (1976) Isolation and characterization of subcellular membranes of *Entamoeba invadens*. *The Journal of cell biology,* 71(2)**,** 357–369.
Vesty, E., Whitbread, A., Needs, S., Tanko, W., Jones, K., Halliday, N., Ghaderiardakani, F., Liu, X., Cámara, M. & Coates, J. (2020) Cross-kingdom signalling regulates spore germination in the moss *Physcomitrella patens*. *Scientific reports,* 10(1)**,** 2614.
Vikström, E., Tafazoli, F. & Magnusson, K. (2006) *Pseudomonas aeruginosa* quorum sensing molecule N-(3 oxododecanoyl)-l-homoserine lactone disrupts epithelial barrier integrity of Caco-2 cells. *FEBS letters,* 580(30)**,** 6921-6928.
Villalba, J., Gómez, C., Medel, O., Sánchez, V., Carrero, J., Shibayama, M. & Ishiwara, D. (2007) Programmed cell death in *Entamoeba histolytica* induced by the aminoglycoside G418. *Microbiology,* 153**,** 3852-3863.
Von Rad, U., Klein, I., Dobrev, P., Kottova, J., Zazimalova, E., Fekete, A., Hartmann, A., Schmitt-Kopplin, P. & Durner, J. (2008) Response of *Arabidopsis thaliana* to *N*-hexanoyl-DL-homoserine-lactone, a bacterial quorum sensing molecule produced in the rhizosphere. *Planta,* 229(1)**,** 73-85.
Wang, L., Zhu, L., Meister, J., Bone, D., Pydi, S., Rossi, M. & Wess, J. (2021) Use of DREADD Technology to Identify Novel Targets for Antidiabetic Drugs. *Annual review of pharmacology and toxicology,* 61**,** 421-440.
Wang, Y., Ji, P., Liu, J., Broaddus, R., Xue, F. & Zhang, W. (2009) Centrosome-associated regulators of the G2/M checkpoint as targets for cancer therapy. *Molecular cancer,* 8**,** 8.
Wanlahbeh, N. (2020) *An investigation into the targets for cannabinoid action in the ciliate Tetrahymena pyriformis.* MSc by Research Lancaster University.
Watts, V. & Neve, K. (2005) Sensitization of adenylate cyclase by Galpha i/o-coupled receptors. *Pharmacology & therapeutics,* 106(3)**,** 405-421.
Weeks, G. & Herring, F. (1980) The lipid composition and membrane fluidity of *Dictyostelium discoideum* plasma membranes at various stages during differentiation. *Journal of Lipid Research,* 21(6)**,** 681-686.
Wehbe, N., Slika, H., Mesmar, J., Nasser, S., Pintus, G., Baydoun, S., Badran, A., Kobeissy, F., Eid, A. & Baydoun, E. (2020) The Role of Epac in Cancer Progression. *International journal of molecular sciences,* 21(18)**,** 6489.
Weisman, R. & Moore, M. (1969) Bead uptake as a tool for studying differentiation in *Acanthamoeba*. *Experimental cell research,* 54(1)**,** 17–22.
Wheeler, G., Tait, K., Taylor, A., Brownlee, C. & Joint, I. (2006) Acyl-homoserine lactones modulate the settlement rate of zoospores of the marine alga *Ulva intestinalis* via a novel chemokinetic mechanism. *Plant, cell & environment,* 29(4)**,** 608–618.
Williams, P. (2007) Quorum sensing, communication and cross-kingdom signalling in the bacterial world. *Microbiology,* 153(12)**,** 3923-3938.
Williams, P., Winzer, K., Chan, W. C. & Cámara, M. (2007) Look who's talking: communication and quorum sensing in the bacterial world. *Philosophical Transactions of the Royal Society B Biological Sciences,* 362(1483)**,** 1119-1134.
Willson, T. M., Brown, P. J., Sternbach, D. D. & Henke, B. R. (2000) The PPARs: From Orphan Receptors to Drug Discovery. *Journal of Medicinal Chemistry,* 43(4)**,** 527-550.
Wong, C., Koh, C., Sam, C., Chen, J., Chong, Y., Yin, W. & Chan, K. (2013) Degradation of bacterial quorum sensing signaling molecules by the microscopic yeast *Trichosporon loubieri* isolated from tropical wetland waters. *Sensors,* 13(10)**,** 12943–12957.
Wymann, M. & Schneiter, R. (2008) Lipid signalling in disease. *Nature Reviews Molecular Cell Biology,* 9(2)**,** 162–176.

Xavier, K. & Bassler, B. (2005) Interference with AI-2-mediated bacterial cell-cell communication. *Nature,* 437(7059)**,** 750-753.
Yan, L., Herrmann, V., Hofer, J. & Insel, P. (2000) beta-adrenergic receptor/cAMP-mediated signaling and apoptosis of S49 lymphoma cells. *American journal of physiology: Cell physiology,* 279(5)**,** C1665–C1674.
Yarbro, J. (1992) Mechanism of action of hydroxyurea. *Seminars in oncology,* 19(3)**,** 1-10.
Yates, E., Philipp, B., Buckley, C., Atkinson, S., Chhabra, S., Sockett, R., Goldner, M., Dessaux, Y., Cámara, M., Smith, H. & Williams, P. (2002) *N*-acylhomoserine lactones undergo lactonolysis in a pH-, temperature-, and acyl chain length-dependent manner during growth of *Yersinia pseudotuberculosis* and *Pseudomonas aeruginosa*. *Infection and immunity,* 70(10)**,** 5635-5646.
York-Andersen, A., Hu, Q., Wood, B., Wolfner, M. & Weil, T. (2020) A calcium-mediated actin redistribution at egg activation in *Drosophila*. *Molecular reproduction and development,* 87(2)**,** 293-304.
Zada-Hames, I. & Ashworth, J. (1978) The cell cycle and its relationship to development in *Dictyostelium discoideum*. *Developmental biology,* 63(2)**,** 307-320.
Zaugg, M., Xu, W., Lucchinetti, E., Shafiq, S., Jamali, N. & Siddiqui, M. (2000) Beta-adrenergic receptor subtypes differentially affect apoptosis in adult rat ventricular myocytes. *Circulation,* 102(3)**,** 344-350.
Zeiss, C. (2003) The apoptosis-necrosis continuum: insights from genetically altered mice. *Veterinary pathology,* 40(5)**,** 481-495.
Zeouk, I., Sifaoui, I., Rizo-Liendo, A., Arberas-Jiménez, I., Reyes-Batlle, M., L Bazzocchi, I., Bekhti, K., E Piñero, J., Jiménez, I. & Lorenzo-Morales, J. (2021) Exploring the Anti-Infective Value of Inuloxin A Isolated from *Inula viscosa* against the Brain-Eating Amoeba (*Naegleria fowleri*) by Activation of Programmed Cell Death. *ACS chemical neuroscience,* 12(1)**,** 195-202.
Zhang, J., Gong, F., Li, L., Zhao, M. & Song, J. (2014) *Pseudomonas aeruginosa* quorum-sensing molecule *N*-(3-oxododecanoyl) homoserine lactone attenuates lipopolysaccharide-induced inflammation by activating the unfolded protein response. *Biomedical reports,* 2(2)**,** 233-238.
Zhao, P., Lieu, T., Barlow, N., Sostegni, S., Haerteis, S., Korbmacher, C., Liedtke, W., Jimenez-Vargas, N., Vanner, S. & Bunnett, N. (2015a) Neutrophil Elastase Activates Protease-activated Receptor-2 (PAR2) and Transient Receptor Potential Vanilloid 4 (TRPV4) to Cause Inflammation and Pain. *The Journal of biological chemistry,* 290(22)**,** 13875–13887.
Zhao, Q., Li, M., Jia, Z., Liu, F., Ma, H., Huang, Y. & Song, S. (2016) AtMYB44 Positively Regulates the Enhanced Elongation of Primary Roots Induced by N-3-Oxo-Hexanoyl-Homoserine Lactone in *Arabidopsis thaliana*. *Molecular plant-microbe interactions,* 29(10)**,** 774–785.
Zhao, Q., Yang, X., Li, Y., Liu, F., Cao, X., Jia, Z. & Song, S. (2020) *N*-3-oxo-hexanoyl-homoserine lactone, a bacterial quorum sensing signal, enhances salt tolerance in *Arabidopsis* and wheat. *Botanical studies,* 61(1)**,** 8.
Zhao, Q., Zhang, C., Jia, Z., Huang, Y., Li, H. & Song, S. (2015b) Involvement of calmodulin in regulation of primary root elongation by *N*-3-oxo-hexanoyl homoserine lactone in *Arabidopsis thaliana*. *Frontiers in plant science,* 5**,** 807.
Zhu, W., Zheng, M., Koch, W., Lefkowitz, R., Kobilka, B. & Xiao, R. (2001) Dual modulation of cell survival and cell death by beta(2)-adrenergic signaling in adult mouse cardiac myocytes. *Proceedings of the National Academy of Sciences of the United States of America,* 98(4)**,** 1607-1612.

Zielke, N. & Edgar, B. (2015) FUCCI sensors: powerful new tools for analysis of cell proliferation. *Wiley interdisciplinary reviews; Developmental biology*, 4(5)**,** 469-487.
Zimmerman, S., Zimmerman, A. & Laurence, H. (1981) Effect of delta 9-tetrahydrocannabinol on cyclic nucleotides in synchronously dividing T*etrahymena*. *Canadian journal of biochemistry*, 59(7)**,** 489-493.
Zoete, V., Grosdidier, A. & Michielin, O. (2007) Peroxisome proliferator-activated receptor structures: Ligand specificity, molecular switch and interactions with regulators. *Biochimica et Biophysica Acta (BBA)- Molecular and Cell Biology of Lipids*, 1771(8)**,** 915-925.

Appendix I

Stock formulations

Amoeba saline solution 1 (AS1)

- 0.142 g Na_2HPO_4
- 0.136 g KH_2PO_4

Add to 500 mL Distilled water. Autoclave at 121 °C for 15 minutes, cool to 47 °C before use.

Amoeba saline solution 2 (AS2)

- 4.0 mg $MgSO_4 \cdot 7H_2O$
- 4.0 mg $CaCl_2 \cdot 2H_2O$
- 0.120 g NaCl

Add to 500 mL Distilled water. Autoclave at 121 °C for 15 minutes, cool to 47 °C before use.

Amoeba Saline (AS)

- 0.5 mL AS1
- 0.5 mL AS2

Add to 100 mL Distilled Water. Autoclave at 121 °C for 15 minutes, cool to 47 °C before use.

Media formulations

Non-nutrient agar (NNA)

- 5 mL AS1
- 5 mL AS2
- 15 g agar

Add to 1 L distilled water. Autoclave at 121 °C for 15 minutes, cool to 47 °C before pouring aseptically.

Non-nutrient agarose (NNAg)

- 5 mL AS1
- 5 mL AS2

-15 g Agarose

Add to 1 L distilled water. Autoclave at 121 °C for 15 minutes, cool to 47 °C before pouring aseptically.

Diagnostic sensitivity testing agar

- 37.5 g DST

Add to 1 L distilled water. Autoclave at 121 °C for 15 minutes, cool to 47 °C before pouring aseptically.

When required, add 1 mL of filter sterilised antibiotic stock to agar broth once cooled to 47 °C, before aseptically pouring;

- 1 mL Chloramphenicol stock (30 mg/mL) to give 30 μg/mL in 1 L DST

Receptor antagonist flow chart

Table A. The initial 5 'general' Blockers (bold), and their targets, with additional blockers (bold) available for further testing.

Blocker	Initial Test	Further testing
GW9662	All PPARs	Test with blockers for individual isoforms; α, β/δ and γ, (**GW6471, GSK3787** and **T0070907**, respectively)
Haloperidol hydrochloride	Dopamine & Serotonin	Test D2 and 5-HT1A (**Pertussis Toxin**), D1 (**SCH23390 hydrochloride**), 5-HT2A (**EMD281014 hydrochloride**)
Capsazepine	TRPV1	No further tests available
ZM241385	Adenosine A2	No further tests available
Gallein	All GPCRs	**Mellitin** (Gs-GPCRs) – no further tests available **Pertussis toxin** (Gi/o and Gt-GPCRs) – further test on the following; - D2 receptor – **Halo** but can also confirm with **Remoxipride hydrochloride** - 5-HT1A receptor– **Halo**, but can also confirm with **S-WAY 100135**

Appendix II

DMSO CONTROLS

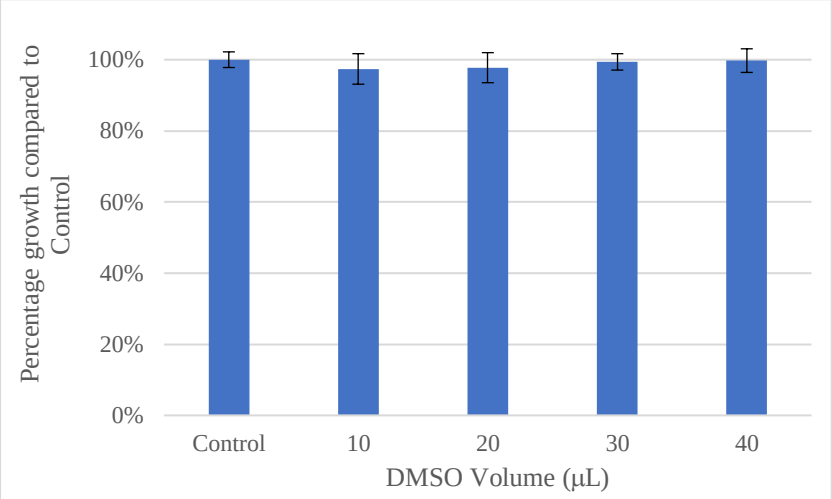

Figure A. Percentage population growth of *Vermamoeba vermiformis* (7A) in the presence of different DMSO volumes. Dose response experiments were carried out in which *V. vermiformis* (7A) cells, (15 amoeba/cm^2) were fed with *Escherichia coli* (5 x 10^6 cells/cm^2) in the absence (Control) and presence of DMSO (10-40 µL). Amoeba cell counts were conducted after 3 population divisions and the percentage population growth (compared to Control) was calculated. Data are presented as Average ± SEM, n=15. Statistical analysis by One-way ANOVA, **P = 0.9734.**

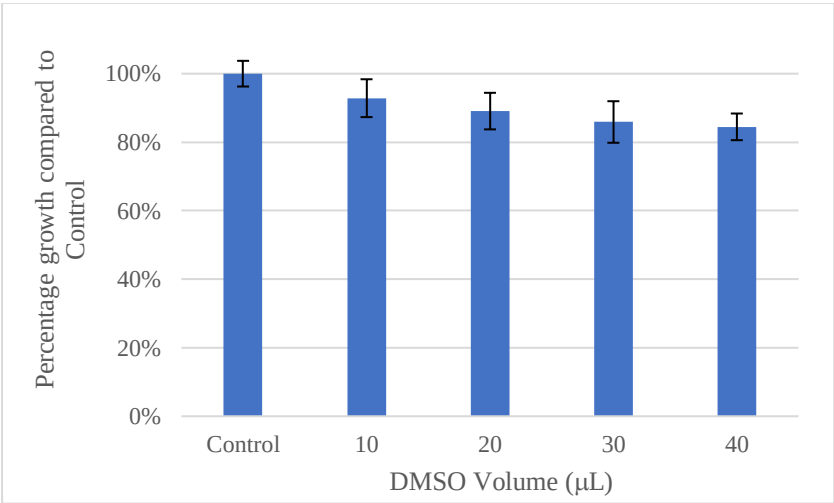

Figure B. Percentage population growth of *Vermamoeba vermiformis* (14) in the presence of different DMSO volumes. Dose response experiments were carried out in which *V. vermiformis* (14) cells, (15 amoeba/cm^2) were fed with *Escherichia coli* (5 x 10^6 cells/cm^2) in the absence (Control) and presence of DMSO (10-40 µL). Amoeba cell counts were conducted after 3 population divisions and the percentage population growth (compared to Control) was calculated. Data are presented as Average ± SEM, n=10. Statistical analysis by One-way ANOVA, **P = 0.2035.**

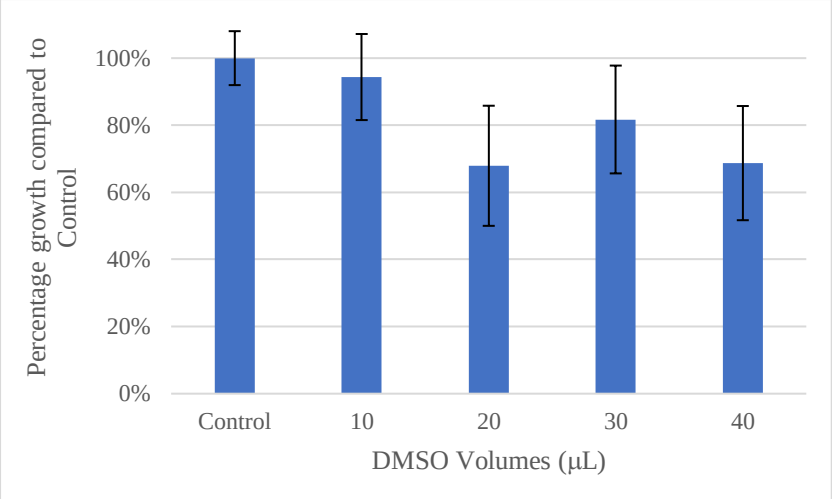

Figure C. Percentage population growth of *Flamella arnhemensis* in the presence of different DMSO volumes. Dose response experiments were carried out in which *F. arnhemensis* cells (15 amoeba/cm^2) were fed with *Escherichia coli* (5 x 10^6 cells/cm^2) in the absence (Control) and presence of DMSO (10-40 µL). Amoeba cell counts were conducted after 3 population divisions and the percentage population growth (compared to Control) was calculated. Data are presented as Average ± SEM, n=10. Statistical analysis by One-way ANOVA, **P = 0.4339.**

Growth rate P values

Table B. The P values of Post-hoc tukey analysis of the population growth of *V. vermiformis* (14) across 9 days in C12 concentrations (100-400 µM), compared to Control, **BOLD (*/**)** = significantly different to Control, (* = P<0.05, ** = P<0.01).

day	100	200	300	400
0	0.2720	**0.0010****	**0.0010****	**0.0010****
1	0.0549	**0.0010****	**0.0013****	**0.0010****
2	0.1354	**0.0012****	**0.0027****	**0.0012****
3	**0.0189***	**0.0010****	**0.0010****	**0.0010****
4	**0.0036****	**0.0010****	**0.0010****	**0.0010****
5	**0.0074****	**0.0010****	**0.0010****	**0.0010****
6	**0.0133***	**0.0010****	**0.0010****	**0.0010****
7	**0.0084****	**0.0010****	**0.0010****	**0.0010****
8	**0.0056****	**0.0010****	**0.0010****	**0.0010****
9	**0.0139***	**0.0010****	**0.0010****	**0.0010****